MS – thesis December 2010

Landscape scale measurements of wind erosion of volcanic materials in the Hekla area

Elín Fjóla Þórarinsdóttir

Faculty of Environmental Sciences

MS – thesis December 2010

Landscape scale measurements of wind erosion of volcanic materials in the Hekla area

Elín Fjóla Þórarinsdóttir

Supervisor: Ólafur Arnalds, Agricultural University of Iceland
Co-supervisor: Ingibjörg Jónsdóttir, University of Iceland

Agricultural University of Iceland
Faculty of Environmental Sciences

Yfirlýsing höfundar

Hér með lýsi ég því yfir að ég samdi þessa ritgerð og vann að gagnasöfnun og úrvinnslu gagna sjálf með aðstoð leiðbeinenda. Ritgerðin hefur hvorki að hluta til né í heild verið lögð fram áður til hærri prófgráðu.

Gunnarsholti, 9. desember 2010

_____

Elín Fjóla Þórarinsdóttir

Abstract

Wind erosion is one of the principal factors responsible for desertification. Due to volcanic activity, harsh climate and unsustainable land use, Iceland has extensive desert areas where wind erosion in common. The objectives of the present study were to i) measure aeolian sand transport on a landscape scale, ii) to estimate the effect of environmental factors on sand transport and iii) estimate the effect of reclamation efforts on wind erosion.

The research area, north of Hekla in South Iceland, extends approximately 110 km^2 of barren or sparsely vegetated land, with sandy lava fields and sand and pumice fields dominating the surface. Wind erosion was studied for two summers, 2008-2009, on a landscape scale, by measuring the actual aeolian sand transport during erosion events with dust traps at 32 locations. Electronic sensors, meteorological data, field mapping, remote sensing and GIS analysis were also used to measure sand transport and estimate the effect of reclamation efforts and environmental factors on wind erosion.

The aeolian sand transport ranged from negligible to approximately 150 kg m^{-1} hr^{-1} at locations with the most intensive erosion. At some of the most active aeolian transport sites the mass sand transport was >1 t m^{-1} per summer and at one location it was almost 3 t m^{-1} during the summer of 2008. There are interactions between aeolian and fluvial processes within the research area. The most active erosion areas are in the northeast, fed by aeolian sediment sources, but an active pathway for aeolian sand movement runs through the research area from the north-eastern part, along the hillsides of Valafell and then into the Þjórsá river, mostly along a major seasonally active waterway. Therefore, both aeolian and fluvial sediment sources affect the erosion intensity.

Environmental factors considerably affect the wind erosion and my conclusion is that field mapping of surface characteristic can be used to estimate erosion susceptibility. Image classification and spatial analysis based on field mapping were used to transform data on sand movement from dust traps onto landscape scale measurements. A better correlation with the aeolian sand transport was gained by using spatial analysis based on field mapping attributes, with r^2 of 0.70, compared to r^2 as 0.65 using the image classification where reference sites were chosen based on knowledge from field mapping. The surface characteristics that mostly affect the erosion susceptibility are: amount of loose materials on surface, vegetation cover, grain size and rock outcrop.

Measurements on the effect of reclamation efforts on wind erosion show that vegetation cover in reclamation areas has detrimental effect on the sand transport, and wind erosion is greater by an order of magnitude outside reclamation areas compared to wind erosion within them.

Ágrip

Vindrof er einn af megin orsakavöldum eyðimerkurmyndunar. Auðnir eru algengar á Íslandi m.a. vegna eldvirkni, óblíðrar veðráttu og ósjálfbærrar landnýtingar og vindrof á auðnasvæðum er mikið. Markmið þessarar rannsóknar var að mæla vindrof á landslagsskala, að meta áhrif umhverfisþátta á sandflutning og að meta áhrif uppgræðsluaðgerða á vindrof.

Rannsóknarsvæðið er norðan Heklu og nær yfir um 110 km^2 svæði. Það er að mestu gróðurvana og ríkjandi yfirborðsgerðir eru sendin hraun, sandar og vikrar. Sumurin 2008-2009 var vindrof á landslagsskala rannsakað með því að mæla sandflutning með sandgildrum á 32 stöðum innan rannsóknarsvæðisins, þegar rof átti sér stað. Til að mæla sandflutninginn og meta áhrif umhverfisþátta á vindrof voru auk sandgildranna, notaðir Sensit nemar, sjálfvirk veðurstöð og kortlagning á vettvangi, en einnig voru landfræðileg upplýsingakerfi og fjarkönnun var notuð.

Sandflutningur innan rannsóknarsvæðisins reyndist vera frá vart merkjanlegu rofi upp í það að vera um 150 kg m^{-1} $klst^{-1}$ á svæðum þar sem mest rof átti sér stað. Á virkustu rofsvæðunum var sandflutningurinn >1 t m^{-1} á sumri og á einum stað reyndist það vera nálægt 3 t m^{-1} sumarið 2008. Bæði vindrof og vatnsrof á sér stað á rannsóknarsvæðinu. Virkustu vindrofsvæðin eru á norðausturhluta svæðisins en mikið af sandi berst með vindi frá aðliggjandi sandsvæðum í norðaustri. Virk sandleið liggur svo niður með hlíðum Valafells og út í Þjórsá. Hluti sandleiðarinnar fylgir leysingavatnsfarvegum og því ljóst að vatnsrof á sinn þátt í að bera efnið út í Þjórsá.

Umhverfisþættir hafa mikil áhrif á vindrofið og með vettvangskortlagningu yfirborðs-eiginleika má meta hversu líklegt er að viðkomandi svæði verði fyrir áhrifum vindrofs. Landupplýsingakerfi og fjarkönnun voru notuð til að yfirfæra upplýsingar byggðar á mælingum með sandgildrum yfir á landslagsskala. Betri fylgni við hámarks fok fékkst með því að nota staðbundna greiningu byggða á vettvangskortlagningu (r^2 = 0,7) heldur en með því að nota stýrða flokkun gervitunglamynda (r^2 = 0,65). Þeir yfirborðseiginleikar sem mest áhrif hafa á vindrof eru magn lausra efna á yfirborði, gróðurþekja, kornastærð og hlutfall grjóts á yfirborði.

Mælingar á áhrifum uppgræðsluaðgerða á vindrof sýna að gróðurþekjan í uppgræðslum dregur mjög mikil úr sandflutningi þannig að rofið er af annarri stærðargráðu utan uppgræðslna heldur en innan þeirra.

Acknowledgements

I want to thank my supervisor Ólafur Arnalds for his help and good advise throughout the research process and for all his encouragement and support. I also want to thank my co-supervisor Ingibjörg Jónsdóttir for her helpful advise especially regarding remote sensing and GIS analysis.

I want to thank the Soil Conservation Service for financial support and for making this study possible by providing measuring equipment and other facilities. I would also like to thank Sveinn Runólfsson director of the SCS especially, for his encouragement and support.

My thanks also to the numerous SCS employees that have contributed to this research by helping me and giving me advise, especially Óðinn Burki Helgason for his help with programming the data loggers and installing the measuring equipment in the field, Guðmundur Halldórsson for his advise on the outlines of the research project and Jóhann Þórsson and Anne Bau for various advise and helpful comments on the text. Thanks also to Reynir Þorsteinsson, Garðar Þorfinnsson and Árni Einarsson for their help in the field.

I would like to thank Ása Aradóttir at the AUI for her help with statistical analysis. I also want to thank my family for their support and patience throughout the research and for their help with the field work.

Orkurannsóknarsjóður Landsvirkjunar supported this research with a grant and I want to express my gratitude for that.

Table of Contents

List of Tables

List of Figures

1. Introduction

Degradation of land, including vegetation, soils, landforms and water, occurs in all climatic environments. Land degradation is considered to be caused or exacerbated by human actions, and is thereby distinguished from natural hazards (Conacher, 2009). Soil degradation is one form of land degradation and can cause accelerated soil erosion. Erosion can be a natural phenomenon but it is widely recognized that accelerated soil erosion is a serious global problem and wind erosion is one of the principal factors responsible for desertification (Lal, 1994). Iceland has extensive desert areas where wind erosion is common.

1.1 Land degradation and soil erosion in Iceland

Iceland is a volcanic island on the Mid-Atlantic Ridge and is one of the most volcanic active countries in the world. With its location in the North Atlantic Ocean, between 63° and 66° northern latitudes, Iceland has mostly maritime climate with mild and moist winters but cool summers (Einarsson, 1984). The climate is cold-temperate in the lowlands, but in the highlands and in some parts of the lowlands in northern Iceland it is classified as low arctic (Einarsson, 1976). Rainfall generally varies between 600 and 2000 mm $year^{-1}$.

The cold maritime climate with intensive cryogenic processes, frequent volcanic activity and extremely active soil erosion by wind, water, and gravity are the three factors that predominantly influence the Icelandic soil environment (Arnalds and Kimble, 2001). The combination of frequent small tephra deposition events and a steady transport of volcanic aeolian materials may be unique and has a major influence on soil formation (Arnalds, 2004; Arnalds, 2008). A new soil map of Iceland (Arnalds and Óskarsson, 2009) divides Icelandic Andosols into andic soils under vegetation and vitric soils in desert areas. The vitric Andosols are subdivided further as Cambic-, Gravelly-, Arenic- and Pumice Vitrisols based on environmental factors such as geology and grain size. Icelandic desert soils are coarse grained, with low organic matter and contain large amounts of volcanic glass. Clay content (allophane) is limited compared to other Icelandic soils (Arnalds and Kimble, 2001).

Icelandic ecosystems have undergone dramatic changes since the Settlement during Viking times. Iceland is believed to have been largely covered with dwarf shrubs and birch woodlands when the first settlers came about 1100 years ago (see *Landnámabók*, 1968) and it has been

estimated that about 65% of the area of Iceland was vegetated at the time of settlement (Thorsteinsson et al., 1971). Livestock grazing and wood cutting in conjunction with highly erodible volcanic soils and a harsh climate have caused extensive vegetation degradation and soil erosion (Arnalds, 1987). There are many indicators that these problems became more severe in the late 17th century and for example during the 19th century when sand encroachment from the highlands into the lowlands in southern Iceland became a severe problem (Árnason, 1958).

Erosion is widespread in Iceland. According to a national soil erosion survey, > 40% of the country is classified with considerable to very severe erosion (Arnalds et al., 1997). Much of this severe erosion occurs within deserts. The deserts cover about 42% of Iceland and have been divided into several surface types or landforms, with sandy deserts covering about 21% (Arnalds et al., 1997). The presence of deserts in Iceland is noteworthy in light of the humid climate. The sand fields are widespread, extending from costal sand-fields to highland deserts. The parent material of the sand is mainly basaltic volcanic glass together with porous tephra and basaltic crystalline materials (Arnalds et al., 2001). These extensive barren desert areas comprise the largest sandy tephra areas on Earth (Arnalds, 2008).

In the national survey of soil erosion (Arnalds et al., 1997) sandy areas were divided into tree morphological classes; sand-fields, sandy lava and sandy lag gravel. These classes have been described in more detail by Arnalds et al. (2001). The sand fields have two main origins: glacio-fluvial deposits and volcanic ash (Arnalds et al., 2001). The erosion processes are often a collaboration of aeolian and fluvial processes as is common in most deserts which are neither very wet nor very dry (Cooke et al., 1993).

From a global perspective, aeolian processes, including dust pollution is a global problem. Dust storms from Iceland are known to be carried hundreds of kilometres out over the ocean from Iceland (Arnalds and Metúsalemsson, 2004). Research has also shown (Ovadnevaite et al., 2009) that volcanogenic emissions and aeolian dust from deserts in Iceland can be potentially significant regional sources of aerosols over the North Atlantic and should therefore be considered in regional and global climate models.

1.2 Wind erosion

There are three basic phases in the erosion process; detachment, transportation and deposition (Fig. 1). Wind erosion is the detachment of soil particles caused by wind effect. It is the turbulence of surface winds, together with velocity, that is responsible for starting the movement of soil in the wind-erosion process (Stallings, 1957).

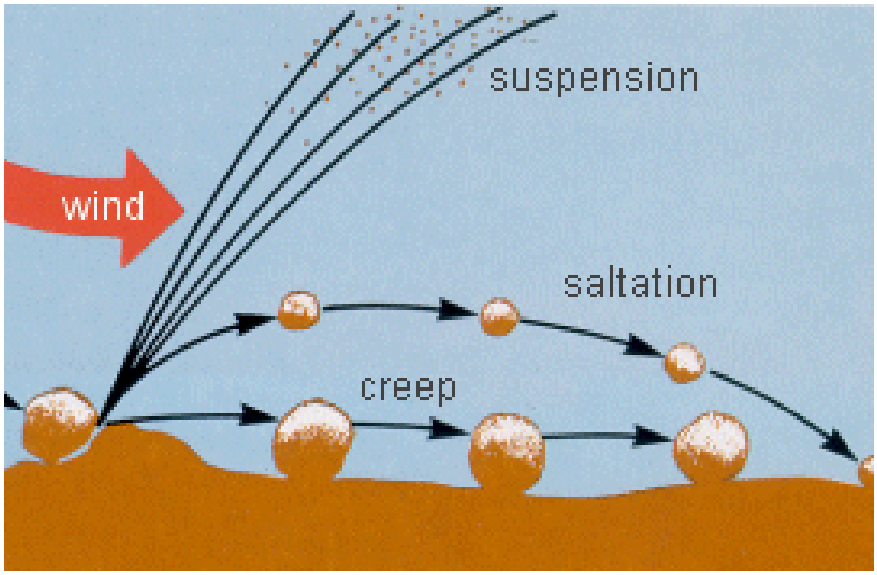

Figure 1. Three forms of transport by wind.

Current understanding of wind erosion and aeolian transport processes is largely based on the quantitative theories developed by Bagnold (1941). The transport of soil and sand particles by wind takes place in surface creep, saltation and suspension and these different forms of transport and their interactions have been described by many e.g. Stallings (1957), Hudson (1981) and Morgan (1986). Surface creep is the rolling of coarse grains along the ground surface. Suspension describes the movement of fine particles, usually fine silt and clay, high in the air and over long distances. Saltation is the process of grains movement in a series of jumps and is caused by the direct pressure of the wind on the soil particles and their collision with other particles. The bouncing movement of saltating grains starts with a particle rising into the airstream, after rising to a peak it starts to fall, but continues to accelerate laterally under the force of the wind, returning to the soil in a long flat glide path. Once any particle has gone into saltation it returns to the ground with sufficient energy picked up from the wind to bounce many more particles into the air, because the collision of particles detaches other particles, thus accelerating the erosion process. This high energy impact of saltating particles

is also a powerful force on the large grains rolling along the surface as part of the creep process. Soils composed of fine dust particles are resistant to erosion by wind due to their cohesiveness. Movement of fine dust in an air current is mainly the result of saltation which has detached the finer grains (Stallings, 1957). More soil is moved by saltation than either of the other two, and also neither creep nor suspension occurs without there being saltation (Hudson, 1981). Saltation can therefore be considered the major component of wind erosion. The saltation layer does not have a clearly defined upper limit but its maximum height is approximately ten times the mean saltation height (Pye and Zoar, 1990). The saltation process becomes more significant as particle size and wind strength increase, thus increasing the saltation height (Dong et al., 2002). The surface also affects the saltation height as grains of any given size bounce higher on hard desert surfaces, such as rock pavements and gravel fans, than on loose sand (Bagnold, 1941).

Wind blowing across a sandy surface exerts fluid forces upon that surface. There is a shallow layer above the surface where the wind velocity is zero and the thickness of this layer is known as the roughness height, z_0 (Cooke et al., 1993). The roughness height is affected by soil, stones, vegetation and other obstacles on the surface. Above the roughness height the wind speed increases exponentially with height so the velocity values plot as a straight line on a graph against the logarithmic values of the height (Morgan, 1986). The critical point when wind speed has increased enough to cause the individual grains at the surface to move, is called the threshold for aeolian transport (Stout, 2004). The entrainment of soil particles by wind is also affected by the bombardment of the soil by grains already in motion. Bagnold (1937) identified two threshold velocities required to initiate grain movement, the static or fluid threshold which applies to the direct action of the wind and the dynamic or impact threshold which allows for the bombarding effect of moving particles.

Threshold velocity is one measure of erodibility and the size of the soil grains is the greatest single factor influencing the threshold velocity. The threshold velocity is lowest for grains 0.1-0.15 mm in diameter but increases with either an increase or decrease in the size of grains from these diameters (Chepil, 1945; Stallings, 1957; Hudson, 1981). The resistance of the finer particles is due to their cohesiveness and the protection afforded by surrounding coarse grains but of the larger particles the resistance results from their weight (Morgan, 1986).

Chepil (1945) found that saltation accounts for the greatest part of soil movement, from 55-72% of the total, while 3-38% moved in suspension and 7-25% by surface creep. A majority of total soil movement occurs within 1 m of the soil surface but the mode of particle transport changes continuously as wind speed fluctuates and soil surface roughness changes (Fryrear, 1986).

The size range of particles which may move in saltation is mainly sand and coarse silt. Chepil (1950) determined relative erodibility of soils reasonably free from organic residues from wind tunnel tests. Since then, the nonerodible soil fraction > 0.84 mm has been widely used to indicate the upper limit of erodible soil materials by wind (Skidmore, 1994). This definition is subject to wind speed and the shape and density of soil grains. Conditions in Iceland are in many ways unique and research in Iceland has shown that this definition for nonerodible soil fraction is not valid in Iceland, because grains >2 mm are transported in saltation, especially tephra (Arnalds, 1990; Arnalds and Gísladóttir, 2009).

Wind speed is the driving factor for wind erosion but the threshold velocity is not significantly influenced by wind speed in the surrounding area (Stout, 2004) but describes the surface erodibility condition. The wind erosion is modified by many other factors than wind speed such as texture, structure, stoniness, landscape, vegetation cover and climatic factors which affect surface soil moisture and wind speed (Rose, 1998). The soil texture affects the soil erodibility as, for example, sandy soils have lower run-off rates, and are more easily detached, but less easily transported than silty soils (Lal and Elliot, 1994). The surface roughness is important because it affects the wind profile and soil erodibility (Zobeck et al., 2003). Stout (2007) concluded in his research of aeolian activity between sites, that it is more likely that fundamental differences in the inherent erodibility of the surfaces contributed to the difference in measured saltation activity, rather than climatic factors.

The nature of the eroding surface is modified as wind erosion proceeds. The different aeolian transport method of soil grains causes grain size sorting (Shao et al., 1996). The fine particles (<60 μm) carried in suspension can be dispersed away from the surface by atmospheric turbulence and transported over large distances. The grains transported by saltation are moved further from its source than coarse grains transported by creep. The amount of erodible material also affects the transport capacity (Zobeck et al., 2003). If no new material is added to

the area the surface generally tends to become less erodible as more erodible components are preferentially removed and the availability of erodible source material becomes limiting (Rose, 1998; Shao et al., 1993). Aeolian entrainment and transport are most effective where sediment has been pre-sorted and the majority of sediment of the aeolian system is made available through the sorting action of fluvial channel transport or pre-worked aeolian deposits (Bullard and Livingstone, 2002). In Iceland the volcanic eruptions, the glaciers and glacial rivers are active sources of erodible material.

Interactions between aeolian and fluvial processes

In erosion the two main processes are aeolian and fluvial. There are critical differences between these two processes including the density of the transport fluid (water vs. air), directionality of sediment and dust transport, spatial scales of the impact (from localized to global) and temporal scales of the erosion events. At large spatial and temporal scales aeolian transport is expected to be dominant because it is not confined to watersheds as the fluvial processes (Field et al., 2009). But aeolian and fluvial processes are not considered to be mutually exclusive, rather that one becomes dominant under certain conditions and if conditions change, another process may dominate (Bullard and Livingstone, 2002). Interactions between these two processes can have a large influence on the transport and deposition of fine sediment and sand sized material in dry land environments (Field et al., 2009). Bullard and Livingstone (2002) identified four possible sediment stores in arid environments for sand-sized material; aeolian-, fluvial-, lacustrine- and marine sediment stores and emphasized the importance of sediment transfer from one type of sediment store to another.

Fluvial processes are important in sandy deserts in Iceland, transporting material in snow-melt floods to lower positions which create new source areas for aeolian transport (Arnalds et al., 2001). At the research site there are interactions of aeolian and fluvial processes but there are seasonal variations determining which process is dominant. Fluvial processes are most common during thawing in early spring but they can also occur during freeze-thaw cycles in winter. Aeolian processes are dominant during the summer but they can also occur during winter because when the surface remains snow-free, many freeze-thaw cycles occur each winter causing intense cryoturbation that influences the erodibility of the soil (Arnalds, 2004).

Because of the interactions between these two processes it is important to know the extent and dispersion of waterways. Therefore the main flow channels in the research area were mapped using field work and remote sensing.

The effect of vegetation on wind erosion

Vegetation plays an important role in controlling wind erosion because it affects the roughness height and thereby the wind speed. The roughness height is affected by four characteristics of the vegetation; the height of plants, vegetative characteristics, density of plant cover and plant litter (Cooke et al., 1993). Scientists realized early the value of crop residue for controlling wind erosion and reported quantitative relationships (Skidmore, 1994). Whisenant (1999) defined five ways in which plant affect wind erosion i) plant foliage reduces wind speed by exerting a drag on airflows ii) the foliage traps moving sediment iii) vegetative cover protects the soil surface iv) plant root systems increase the resistance of the soil to erosional processes v) vegetation influences soil moisture through uptake, transpiration and micro environmental modifications (Whisenant, 1999).

In sandy areas in Iceland, such as the research area, reclamation work in the form of seeding of grass species is common. Lyme-grass (*Leymus arenarius*) has been used extensively in Iceland to stabilize drifting sand and to halt erosion (e.g. Runólfsson, 1986; Greipsson and Davy, 1997). Its main distribution is in northern Europe and it grows predominantly on the coast where it forms sand dunes, but it is also found away from the coast, especially in Iceland. Lyme-grass has been sown in many sites in the research area and one of them was used to measure the effect of vegetation on aeolian transport.

1.3 Studies of wind erosion in Iceland

Research on wind erosion is relatively young in Iceland. Thorarinsson (1961) published pioneering research in using tephrochronology to show increased wind erosion after the settlement in Iceland. Sigurbjarnarson (1969) studied wind erosion at Haukadalsheiði in South Iceland, showing rapid aeolian deposition within the research area and suggesting that most of the aeolian materials were volcanic ash. A team of scientists at the Agricultural Research Institute, now the Agricultural University of Iceland (AUI), has in recent years gathered

experience and knowledge on equipment and methods for wind erosion research in order to increase the understanding of the nature of wind erosion in Iceland. Numerous researches have been conducted, e.g. of the extent of sandy areas in Iceland, as part of a national survey on soil erosion in Iceland (Arnalds et al., 1997). Ólafur Arnalds and other scientists at AUI measured wind erosion in sandy areas in various locations in Iceland (Sigurjónsson et al., 1999) and measurements were also made as part of two master theses (Gísladóttir, 2000; Sigurjónsson, 2002). A few articles on wind erosion have been published in recent years e.g. an overview of sandy deserts in Iceland (Arnalds et al., 2001), an article on the effect of landscape and retreating glaciers on wind erosion in south Iceland (Gísladóttir et al., 2005), measurements on wind erosion of sandy soils in northeast Iceland (Arnalds and Gísladóttir, 2009) and shoreline erosion and aeolian deposition along a recently formed hydro-electric reservoir (Vilmundardóttir et al., 2010).

A number of models have been developed to estimate wind erosion e.g. the USDA Wind Erosion Equation (Skidmore et al., 1994), WEAM Wind Erosion Assessment Model (Shao et al., 1996) WEELS Wind Erosion on European Light Soils (Böhner et al., 2003) and TEAM Texas Tech Erosion Analysis Model (Singh et al., 1997; Gregory et al., 2004). In Iceland an Australian model (Saho et al., 1996) has been adapted for Icelandic conditions by Hjalti Sigurjónsson and Vatnaskil Consulting Engineers and appears to work successfully (Sigurjónsson, 2002; Kjaran et al., 2006).

In this research, methods developed by scientist at AUI were used. They consist mainly of two measuring methods in the field. One is to use field samplers or so called dust traps of BSNE type (Fryrear, 1986), which have been used successfully for wind erosion measurements (e.g. Shao et al., 1993; Gossens and Offer, 2000) and have also been effective in research in Iceland (e.g. Arnalds et al., 2001; Gisladottir et al., 2005). The other method is to use Sensit automated sensors which are devices that produce an electrical pulse signal when they are impacted by saltating grains. The sensors are important for understanding the context between wind speed and sand flux (kg m^{-1} hr^{-1}) at a given location (Arnalds and Gísladóttir, 2009).

1.4 Objectives of the study

Reliable and direct measurements of sand transport are necessary to assess the intensity of aeolian processes in a given environment. Field measurements on wind erosion have proven to be complicated (e.g. Stout, 1998; Zobeck et al., 2003) and not many field measurements have been carried out on a landscape scale. One of the complications is that researchers have found high spatial variability in sediment discharge in their experimental fields (Sterk, 1997; van Donk and Skidmore, 2001). Other causes often mentioned in connection with the difficulty to determine the magnitude of erosion are: temporal variation, the paucity of accurate erosion measurements and the problem of extrapolating data from small plots to higher scales (Stroosnijder, 2005). A new method *single dust trap method* is used in this research to measure the aeolian transport on a landscape scale.

Quantitative knowledge as to the rate and extent of erosion is essential but it is still rather limited relative to the scope of the erosion problems in Iceland. Gísladóttir (2000) did large scale measurements on aeolian transport but other than that this is the first landscape scale measurement on aeolian transport conducted in Iceland. The purpose of this research is to gain knowledge and understanding of the erosion processes, especially wind erosion, in a big heterogeneous area and to understand how other factors in the environment such as water erosion, surface roughness and difference in grain size affect the wind erosion. Reclamation is commonly used in Iceland to halt erosion but this is the first research on the effect of reclamation work on aeolian transport in Iceland. This research will add to current knowledge and understanding on wind erosion in Iceland because the research area is different from other areas in Iceland where wind erosion has been studied because of the amount of tephra and pumice on surface.

The objectives of this research can be categorized as follows, and the first is the main objective.

i) To establish knowledge of the magnitude and nature of aeolian transport in the research area by empirical measurements.

ii) To estimate the effect of reclamation work on aeolian transport by empirical measurements.

iii) To estimate the extent of water erosion by field mapping and remote sensing and to investigate the relationship between wind and water erosion in the area.

iv) To establish relationships between environmental factors such as grain size, surface roughness, rock outcrop and vegetation cover, and aeolian transport based on field mapping, spatial analysis, remote sensing and empirical measurements.

2. Experimental site and layout

The research area is located in the southern part of Iceland near Hekla (Fig. 2), extending across approximately 110 km^2. The area stretches from the lowlands up into the Icelandic highlands as the elevation varies from 210 m in the south-western part to 420 m in the north-eastern part.

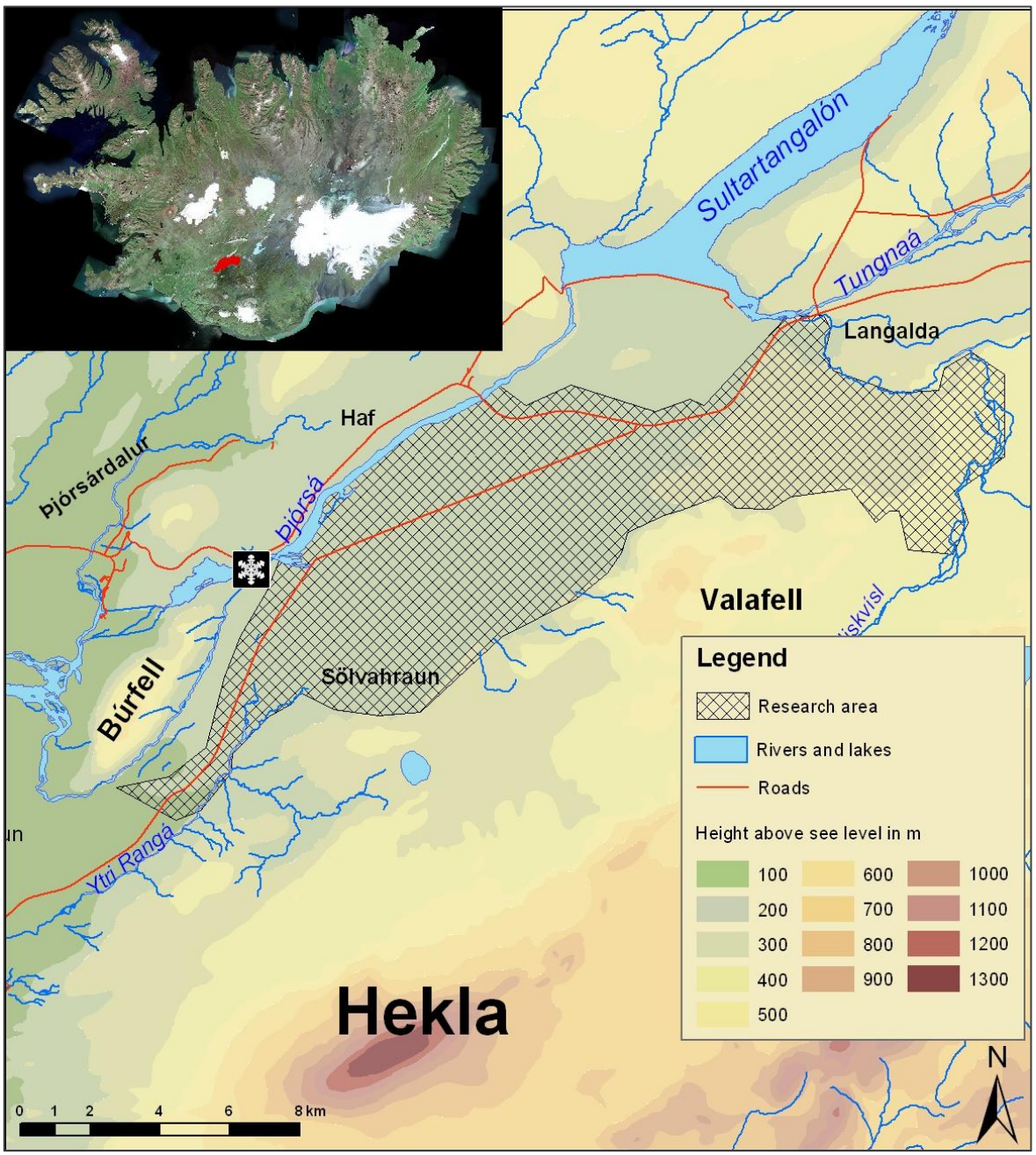

Figure 2. A map of the research area (cross hatched) and its surroundings. A meteorological station at Búrfell is marked with a star.

The reason for choosing the location near Hekla to conduct this research is twofold; i) the amount of tephra (pumice and volcanic ash) on surface makes this area different from other areas where wind erosion has been measured in Iceland and also unique in a global prospective; ii) the area falls within an area where a large scale restoration project called Hekla forest or "Hekluskógar" was initiated in 2005. The main objective of the Hekla forest project is to restore woodlands of native birch woodlands and willows to reduce the potential damage caused by tephra or ash from eruptions in Hekla (Aradóttir, 2005).

Volcanic eruptions from Hekla have played an important role in the development of the area. Since the end of the last glacial period, or during the last 11 000 years or so, Hekla has produced more tephra than any other Icelandic volcano, or about 32.4 km^3 calculated as freshly fallen tephra (Hjartarson, 1995). Since the settlement in the late 9^{th} century AD eighteen eruptions are recorded in Hekla (Hjartarson, 1995; Höskuldsson et al., 2007). The plinian eruptions in the Hekla volcano appear to have produced mainly acid and intermediate tephra (Gudmundsson et al., 1992) which is light in color. In some eruptions basaltic tephra, described by Thórarinsson and Sigvaldason (1972) as "*black highly vesicular pumice fragments ranging in size from large frothy blocks near the craters to a sand or dust fraction in the farthest parts of the tephra sector"* has been dispersed from the volcano.

Tephra, especially pumice is very erodible due to its light density. Tephra dispersed from Hekla has damaged low vegetation, created large pumice and sand fields in the vicinity of the mountain and caused extensive soil erosion. There are various written sources about land degradation and erosion in the vicinity of Hekla e.g. Arnalds (1988) and a number of articles in „Sandgræðslan 50 ára" (Sigurjónsson, 1958).

2.1. Soil and soil erosion

According to a new soil map of Iceland (Arnalds and Óskarsson, 2009) the soil in the research area is classified as Pumice Vitrisol (desert soil characterized by pumice). The texture, composition and structure of the surface vary considerably within the research area. There are two dominant surface types, i) sandy lava which is rough lava fields mostly filled with sand and pumice and ii) sand-fields which make extensive flat areas covered with sand and pumice.

The surface is unstable and erosion is widespread in the research area. In a survey of soil erosion in Iceland conducted in the scale 1:100 000 (Arnalds et al., 1997), the majority of the research area is classified with severe or very severe erosion. The most dominant erosion forms are sandy lava ~73%, sand-fields ~3% and sandy lag gravel ~21%. The soil erosion was mapped in more detail in the field (1: 15 000) as part of this research (see chapter 4.5).

The erodible materials in the area originate from various sources which can be difficult to identify with full certainty, except the source of tephra and pumice which is the frequent volcanic eruptions in Hekla. The source of sand can partly be the huge highland deserts northeast of the research area where soil erosion is very severe (Arnalds et al., 1997), fed by glacial rivers and aeolian processes. Other sources that may contribute to the erodible material, especially to the finest material transferred by plumes (suspension), can by far away from the research area. Arnalds (2010) has identified major source areas for plumes in Iceland, based on wind erosion research, soil erosion maps and satellite imagery.

The surface in the research area has high infiltration rates and the bedrock is permeable. Rain water infiltrates quickly and enters the ground water except in intensive rain events and when the ground is frozen in winter. Open, sparsely vegetated areas as within the research area, have tendency to develop deep, infiltration-retarding soil frost in winter (Orradóttir et al., 2008) and are therefore more prone to water erosion. The number of dry waterways in the area show evidence of fluvial processes and their size indicates that the surface flow can be extensive during spring thaw and also during freeze-thaw cycles in winter when the ground is frozen (Fig. 3).

Figure 3. Waterway through a revegetated area, dry in summer (left) but filled with water in winter thaw (right).

Interactions between fluvial and aeolian processes are changeable because during summertime the aeolian processes are dominant as the area is mostly dry with very little surface water.

Bullard and Livingstone (2002) defined four kinds of sediment stores, two types can be identified in the research area, aeolian sediment store and fluvial sediment store. Because of the seasonal variation in aeolian and fluvial processes, sediment is transferred from one sediment store to another, providing an active source of erosion material (Fig. 4).

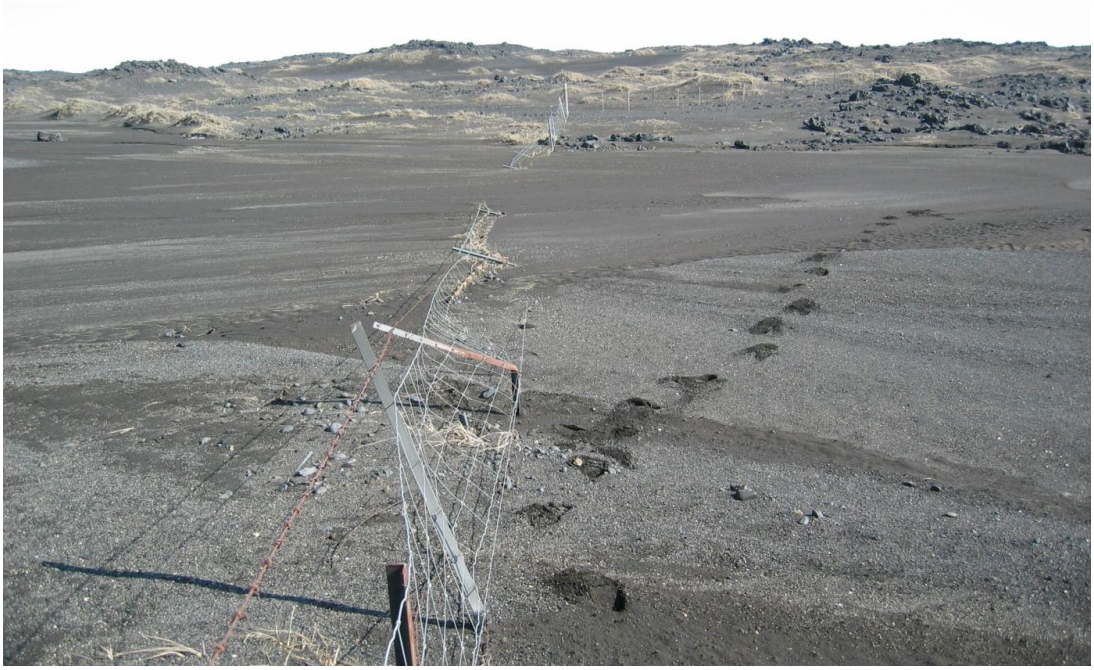

Figure 4. A fence buried in sediment in a dry waterway. This fluvial sediment store provides an active source for aeolian erosion.

2.2 Vegetation

A generalized vegetation map of Iceland (Guðjónsson and Gíslason, 1998) in a scale 1:500 000 classifies this area as sand, lava, gravel and other sparsely vegetated land with vegetation cover < 50%. There are some written sources that, at least, the southern part of the research area used to be densely vegetated and partly covered with birch woodland (Kjartansson, 1945; Árnason, 1958; Hjartarson, 1995). Wood cutting and grazing have contributed to the degradation of the area, as well as eruptions in Hekla (Árnason, 1958). The last volcanic eruption in Hekla that had considerable effect on vegetation was in 1980, when part of the area was covered in tephra and pumice (Hjartarson, 1995).

In 1970 most of the research area was fenced off and protected from grazing. Since then the Soil Conservation Service in Iceland has been working on reclamation in parts of the area (Ágústdóttir and Thórarinsdóttir, 2000). Fertilization and planting of birch has also been carried out under the Hekla forest project. Apart from the revegetated sites the research area is sparsely vegetated with Lyme grass (*Leymus arenarius*) as the dominant species. Biological soil crust is forming in some areas decreasing the erodibility of those areas. The vegetation cover was mapped in the field in a scale 1: 15 000 as part of this research (see chapter 4.5).

2.3 Weather conditions

An automatic meteorological station has been operating since 1993 at Búrfell. It´s location is just outside of the research area (64°07.010'N, 19°44.691'W, elevation 249 m).

Based on measurements from 1993-2009, the mean wind speed at Búrfell, measured at 10 m height, was 7.06 m s^{-1} and north-easterly winds were dominant as shown in Fig. 5 (http://gagnavefsja.vatn.is:81/vindatlas/6430/).

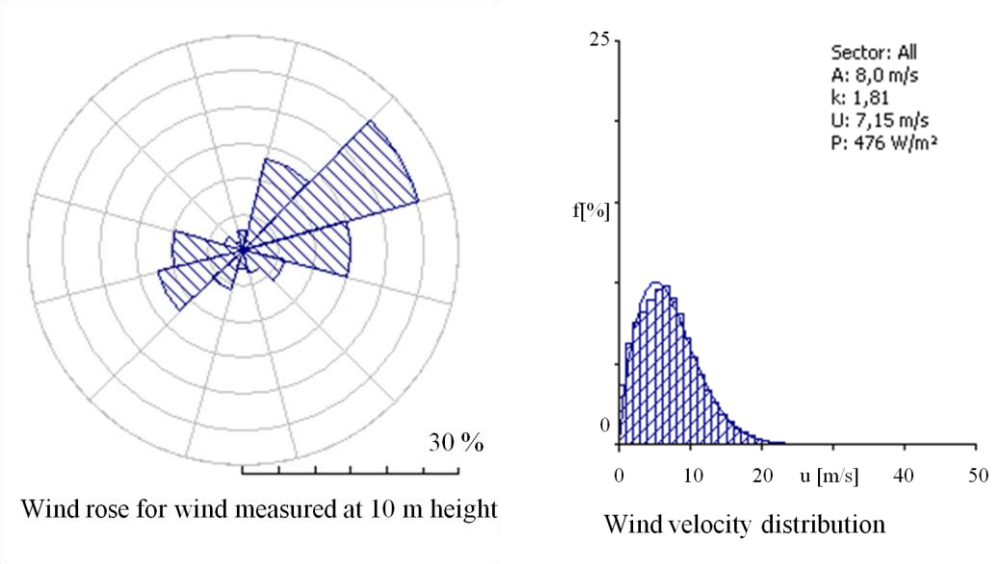

Figure 5. Wind rose (left), showing wind directions frequency and mean wind speed, wind is measured at 10 meters height. Frequency distribution (right) shows wind speed frequency.

Based on data from 2002-2009, the mean annual temperature ranges from 2.9° C to 4.1° C with mean July temperatures about 11° C. The annual precipitation during the same time period ranges from 828 mm to 1459 mm (Icelandic Met Office, 2009).

The average wind speed, air temperature, air moisture and precipitation for June, July and August 2002-2009 are shown in Table 1.

Table 1. The average weather conditions at Búrfell during June, July and August 2002-2009.

	2002	2003	2004	2005	2006	2007	2008	2009
Wind speed	5.8	5.2	5.2	5.6	5.7	5.6	6.1	5.6
Air humidity	77.9	77.5	71.9	75.7	78.0	73.0	73.7	73.8
Air temperature	9.8	11.4	10.2	9.9	9.9	10.6	10.7	10.1
Precipitation	183	181	137	211	166	211	112	169

According to a yearly weather overview from the Icelandic Met Office the weather during the measurement period in 2008 and 2009 were unusually warm and dry in the research area (http://en.vedur.is/weather/articles/nr/1802; http://www.vedur.is/vedur/frodleikur/greinar/nr/1433). However erosion events were rare and the weather was unusually calm, especially during June 2009.

3 Materials and methods

Wind erosion was studied for two summers, from June to August 2008 and from May to August 2009. The type of sampling methods and equipment used in aeolian field studies depend upon the specific objectives of the study. In this research the main purpose was to gather information on wind erosion on a landscape scale and the measuring equipment consisted of BSNE field samplers, Sensit electronic sensors and meteorological equipment. Various environmental factors which affect wind erosion were looked at as well to be able to transfer information on aeolian transport from measured point data to the landscape scale.

3.1 Measuring equipment

BSNE field samplers

The big spring number eight (or BSNE) sampler developed by D.W. Fryrear in 1986 was used to collect airborne material at 32 different locations within the experimental area. The BSNE field sampler or dust trap was originally designed to collect airborne dust, but is now also frequently used to collect soil and sand (Goossens and Offer, 2000). This sampler is a passive device, reliant on ambient wind conditions, to measure horizontal sand movement. The sampler is placed on a pole and turns to orientate into erosive winds (Fig. 6).

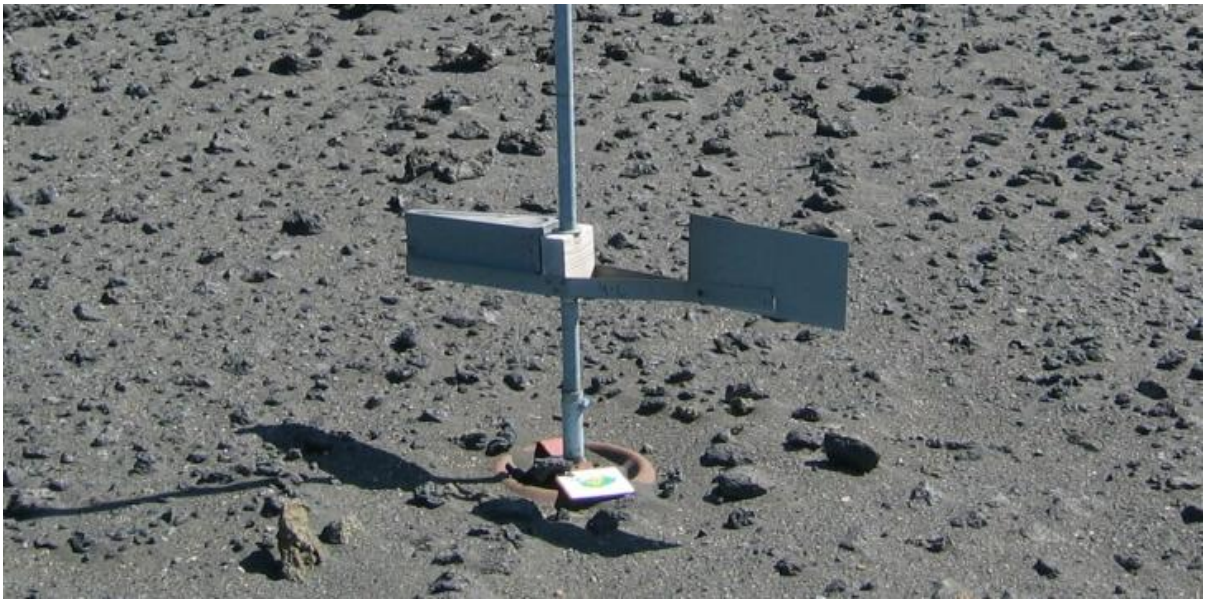

Figure 6. BSNE dust sampler mounted at 30 cm height on an iron pole. Sampler and collecting pan (left) and tail (right).

Dust-laden air passes through the sampler opening which is approximately 9 cm^2 and once inside the sampler, air speed is reduced and the dust settles out in a collection pan. The BSNE field sampler has been described in more detail by Fryrear (1986), Stout and Fryrear (1989) and Shao et al. (1993).

The overall efficiency of the BSNE for sand has been tested by Fryrear (1986), Stout and Fryrear (1989) and Shao et al. (1993) and it varies between 86 and 96%. According to Fryrear (1986) the sampler will retain 95 to 98% of the material entering the sample slot. Gossens and Offer (2000) compared the efficiency of six different dust samplers and concluded that the BSNE was the most recommendable sampler for field measurements because its efficiency varied only very slightly with wind speed.

Sensit electronic sensors and meteorological data

In 2008 a sampling system capable of measuring a continuous meteorological record as well as collecting information about aeolian activity (Fig. 7) was installed near the center of the research area, at location no 21 (Fig. 8).

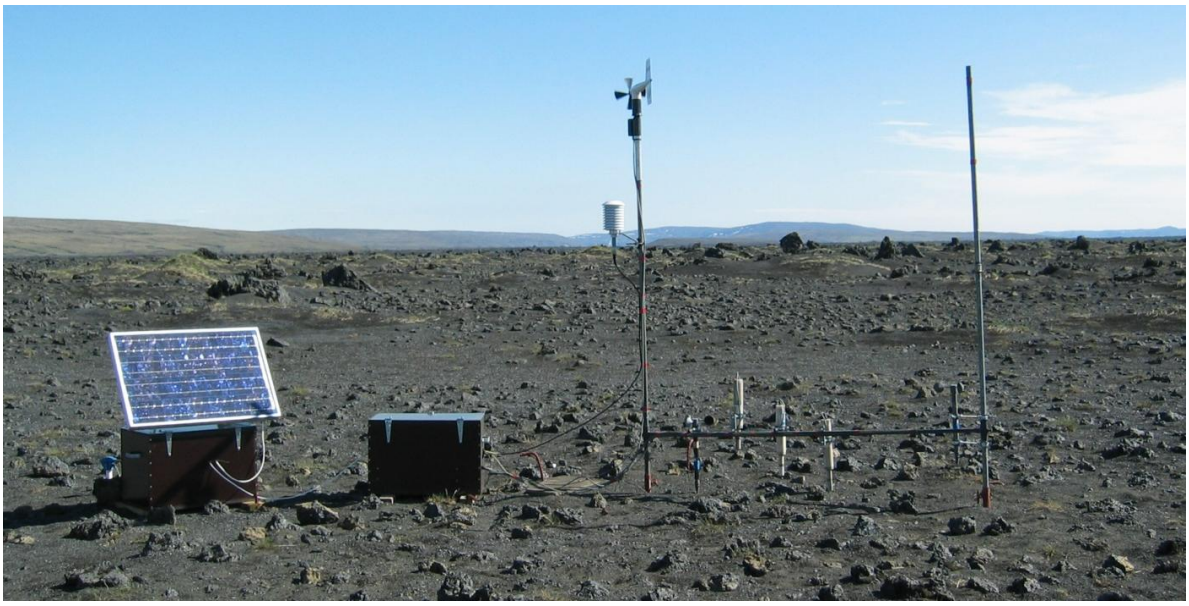

Figure 7. Equipment to measure aeolian transport including three Sensit sensors, meteorological devices, solar panel and data logger and battery contained in boxes.

Three piezoelectric saltation sensors (Sensit) were used to measure aeolian transport. The Sensit sensor is a device that produces an electrical pulse signal when it is impacted by

saltating grains. The center of the piezoelectric sensing element was mounted at a height of 7.5 cm, 15 and 30 cm. The Sensit sensor counts particle impacts at a fixed height near the surface.

Simultaneous to the measurements by the Sensit sensors and BSNE dust traps, the following meteorological data were recorded:

- Wind speed at 40 and 60 cm height (MetOne 014A anemometers)
- Wind speed and wind direction at 220 cm height (Young Wind monitor Model 05103)
- Air humidity and air temperature at 150 cm height (Vaisala HMP45C)
- Soil temperature (CAMP 107-L temperature probe)

This allows for the determination of the duration and direction of wind erosion to be monitored (Skidmore et al., 1994).

Aeolian transport was measured with this equipment from June 3rd to August 30th 2008 and from May 19th to August 28th 2009. During that time, data was gathered during six erosion events: June 4th, July 1st and August 28th 2008 and May 24th-29th, July 27th and August 21st-24th 2009.

In 2009 an additional sampling system was added to gather information in another part of the experimental area, at location no 11 (Fig. 8). That sampling system consisted of one Sensit sensor mounted at 15 cm height, meteorological equipment measuring wind speed and wind direction at 220 cm height (Young Wind monitor Model 05103) and air humidity and air temperature at 150 cm height (Vaisala HMP45C).

All the data from the Sensit sensors and the meteorological stations were gathered by Campell CR3000 data loggers, each one connected to a battery powered by a solar panel. The loggers were programmed to sample all variables every 10 sec and to summarize them every 10 minutes. In erosion events, when the Sensit sensors were impacted by saltating grains, the variables were also summarized every one minute.

Failures and technical problems in measurements of meteorological data and with the Sensit sensors are more likely to happen than failures in measurements with dust traps. These failures can for example be due to equipment failure, programming mistakes or flies and raindrops impacting the Sensit sensors.

Location of BSNE field samplers

Dust traps were located in 32 different locations within the research area (Fig. 8) where most of them remained throughout the research period.

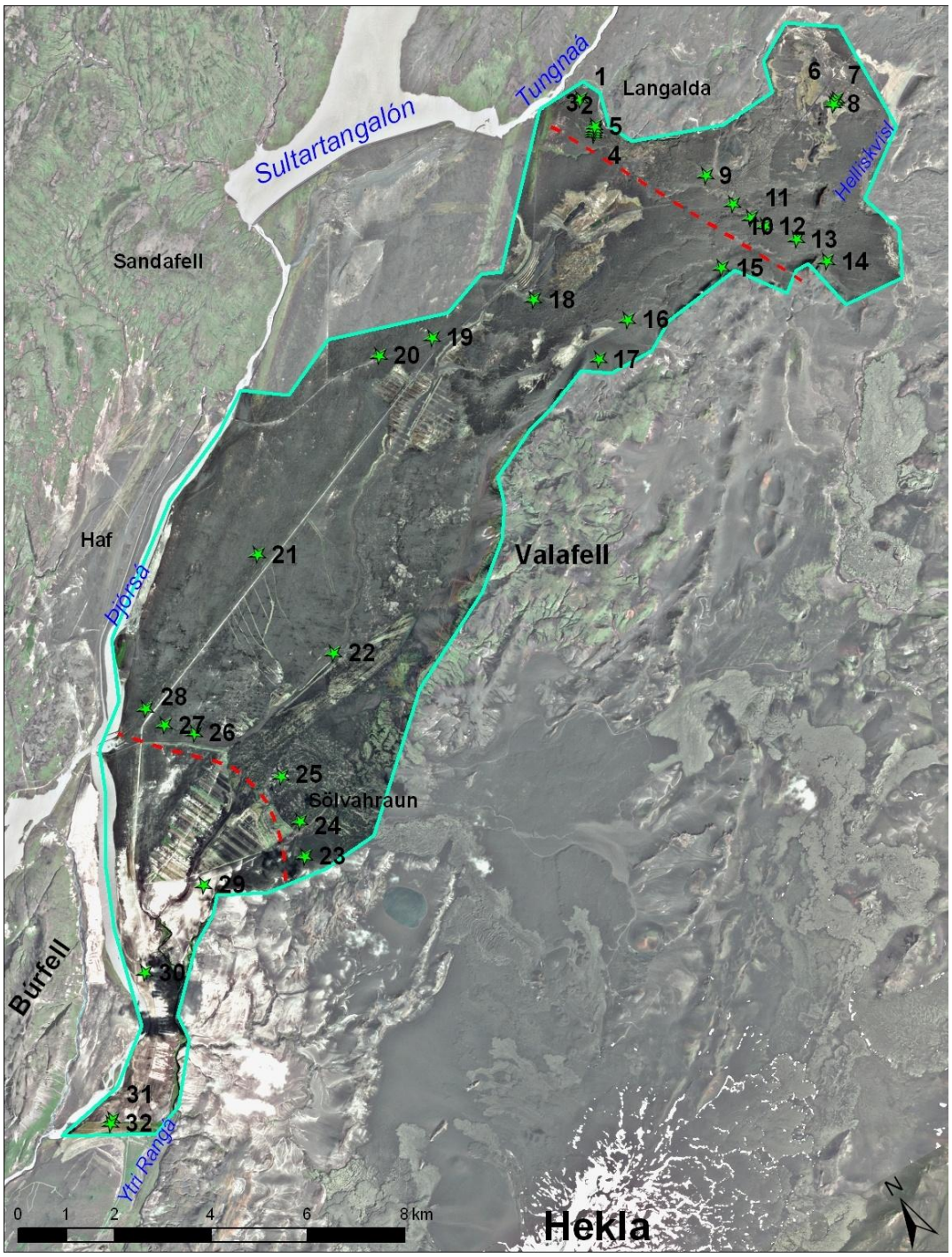

Figure 8. A map of the research area showing the dust traps locations. Red dotted lines show cross-sectional profiles perpendicular to the main, dry wind direction

The dust traps were distributed systematically to gain a comprehensive overview of sand transport in the area. Three main objectives when choosing the locations for the dust traps were: i) locations that were representative for large areas within the research area ii) locations reflected the spatial variability of the area and ii) locations that formed cross-sectional profiles perpendicular to the main wind direction. A few locations were also chosen to determine the effect of reclamation on aeolian transport.

A set of four BSNE samplers on a pole were placed at four different locations within the research area during the research (Fig. 9). The samplers were mounted at 15, 30, 60 and 100 cm height on the pole to gain information on the height distribution of the aeolian transport. Samplers rarely need to exceed 1 m in height for studies of saltation movement as a majority of total soil movement occurs within 1 m of the soil surface (Fryrear, 1986).

Figure 9. A set of four BSNE samplers mounted at 15, 30, 60 and 100 cm height.

One of the sets of four dust traps on a pole was placed at the same location (no 21) during the whole measurement period but the other three sets were moved between locations to gather information on the ratio of aeolian transport by height. At all other locations, one BSNE dust

trap was placed on a pole at the height of 30 cm but some of them had to be raised up to 60 cm height because they filled repeatedly during sandstorms. The height of field samplers at various locations is shown in Table 2.

Table 2. Height of the BSNE field samplers used in each location during the six sampling periods, which included erosion events in 2008 and 2009.

Nr of location	Sampling periods 2008			Sampling periods 2009		
	June 3rd - 7th	June 20th- July 5th	July 5th- August 30th	May 16th- June 30th	July 24th- July 30th	July 30th- August 24th
1	30	30	30	30	30	30
2	30	30	30	30	30	30
3	-	-	30	30	30	30
4	-	-	30	30	30	30
5	-	-	30	30	30	30
6	30	15/30/60/100	15/30/60/100	15/30/60/101	30	30
7	30	30	30	30	30	30
8	30	30	30	30	30	30
9	30	30	30	30	30	30
10	15/30/60/100	30	60	60	60	60
11	30	30	60	15/30/60/100	15/30/60/100	15/30/60/100
12	-	-	60	60	60	60
13	30	15/30/60/100	15/30/60/100	15/30/60/100	30	30
14	-	-	60	60	60	60
15	-	-	-	60	60	60
16	30	30	60	60	60	60
17	30	30	60	60	15/30/60/100	15/30/60/100
18	30	30	30	30	30	30
19	30	30	30	30	30	30
20	30	30	30	30	30	30
21	15/30/60/100	15/30/60/100	15/30/60/100	15/30/60/101	15/30/60/100	15/30/60/100
22	-	-	-	60	15/30/60/100	15/30/60/100
23	30	30	30	30	30	30
24	30	30	30	30	30	30
25	30	30	30	30	30	30
26	30	30	30	30	30	30
27	15/30/60/100	30	30	30	30	30
28	30	30	30	30	30	30
29	30	15/30/60/100	15/30/60/100	30	30	30
30	30	30	30	30	30	30
31	30	30	30	-	-	-
32	30	30	30	-	-	-

Pictures were taken at all the dust traps locations (see Appendix 1), one picture showing the dust traps and its surrounding and another one showing the surface type. Pictures from locations no 9 and 13 are shown in Fig. 10 as examples.

Figure 10. Pictures from sampling sites; location no 9, overview (a) and surface (b) and location no 13, overview (c) and surface (d).

Single dust trap method

The method of using only one BSNE sampler at each location is a new method called *single dust trap method.* It is based on research by Arnalds and Gísladóttir (2009) where their result showed that the ratio of materials that are caught in a set of dust traps of certain height is similar at the same location for all storms. By gathering information on the aeolian transport ratio between dust traps at different heights at a given location, during one erosion event, it is possible to estimate the mass transport at that same location during another erosion event from

only one dust trap. The four sampler sets were moved between locations to gather comparable information in other locations within the research area. This method provides the possibility to gather information from a large area using much fewer dust traps then placing four at each location.

The length of the sampling periods varied from four days to almost two months but after every erosion event, all dust traps were emptied and the content dried and weighted.

Grain size analysis

To gather information on grain size, samples were taken at eleven chosen locations which were believed to be representative to larger areas (Fig. 11). An iron frame, 10 x 10 cm wide and 5 cm high, was used to take one sample at each location. The frame was pushed into the ground and the top 2.5 cm of soil within the frame was removed and placed in a sample bag. All nonerodible material like stones and pebbles were excluded from the samples, but big grains of pumice were included as they can be transported by wind. The soil samples were dried, weighted and sieved using classification based on Udden-Wentworth grain size classification scheme (Wentworth, 1922), see Table 3.

Table 3. Size range used for sieving soil samples

Size range	Wentworth size class
> 8 mm	medium gravel
5–8 mm	fine gravel
4–5 mm	fine gravel
2–4 mm	very fine gravel
1–2 mm	very coarse sand
0.5–1 mm	coarse sand
0.25–0.5 mm	medium sand
125–250 µm	fine sand
63–125 µm	very fine sand
40–63 µm	silt
< 40 µm	fine silt - clay

Grain size parameters were calculated with the Gradistat 5.0 program using the method of moments statistics (Blott and Pye, 2001). The parameters used are the average size, the sorting

that describes the spread of the sizes around the average and the skewness which describes the symmetry or preferential spread to one side of the average.

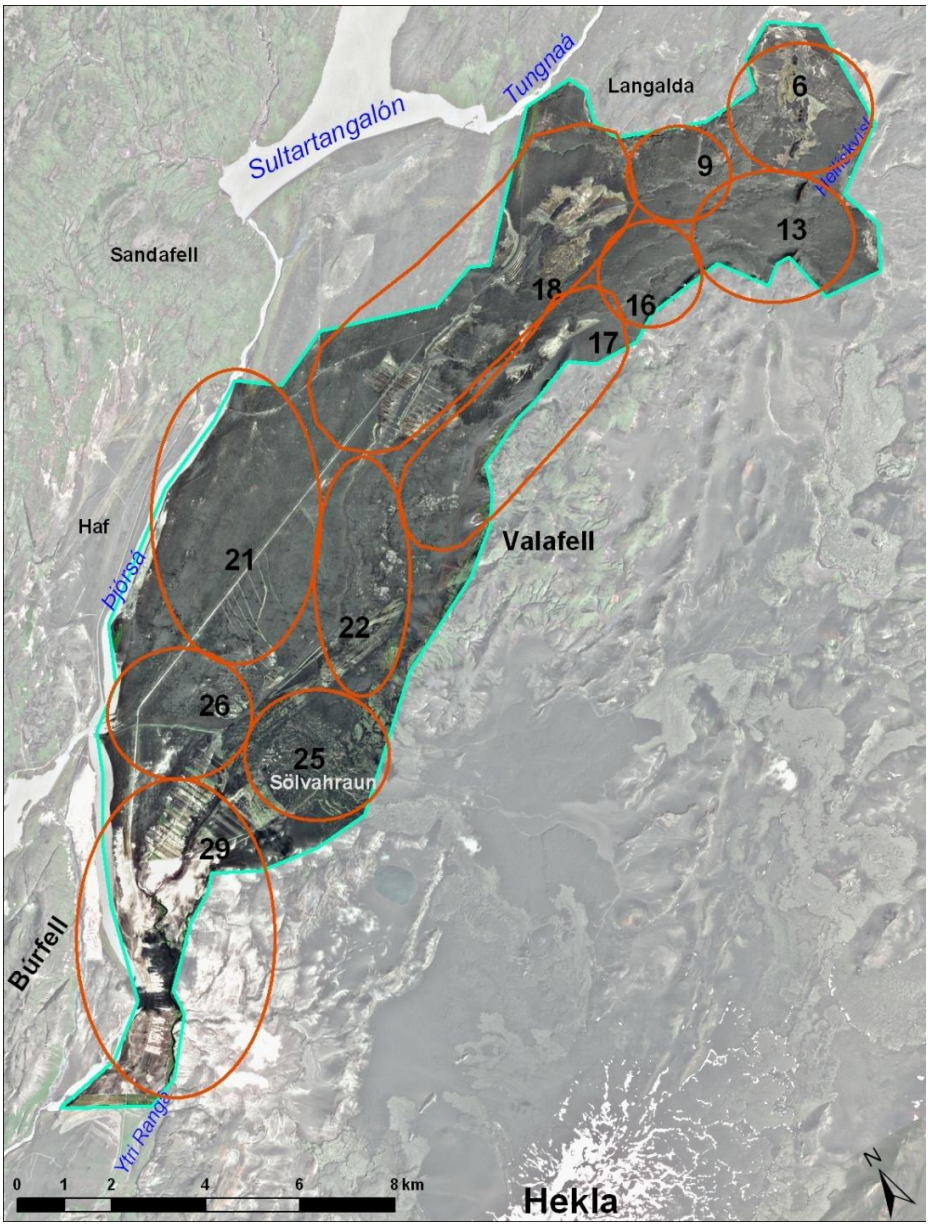

Figure 11. Locations where surface grain size samples were obtained are marked with numbers. Circles show the area which each sample is believed to represent.

3.2 Effect of reclamation work on aeolian transport

Seeding of grass species, especially Lyme grass (*Leymus arenarius*) and Lupine (*Lupinus nootkatensis*) has been used in the research area to stabilize the surface and to reclaim vegetation cover. To measure what effect reclamation work has on aeolian transport, BSNE

field samplers were placed outside of a reclamation area and also at 50 m intervals into the reclamation area, in the direction of the prevailing wind erosion direction. This method was used to gain information on the changes in mass transport into vegetated areas and to see if there are changes in grain size combination.

The effect of reclamation work on aeolian transport was measured in two different areas. One area was in the north-eastern part of the research area, near Helliskvísl, where the surface type is sand field but with some pumice (Fig. 12). In 2005 Lyme grass and other grass species were seeded in the reclamation area and it was refertilized in 2006 and 2007. One field sampler was placed at an unvegetated site outside the reclamation area (location no 6) and two dust trap (locations no 7 and 8) were placed 50 and 100 m, respectively, into a revegetated area (Fig. 13).

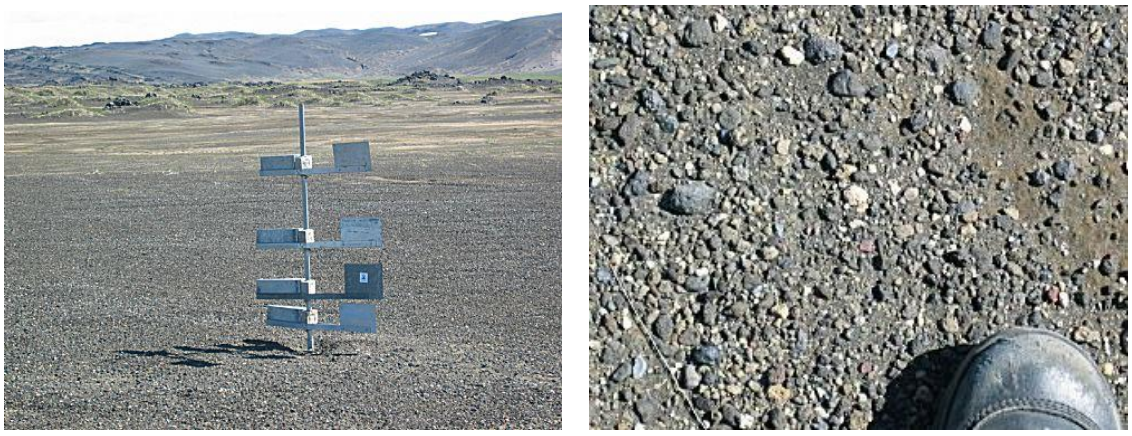

Figure 12. Overview (left) and surface (right) of an unvegetated sandy area at location no 6.

Figure 13. Overview of field samplers 50 m (left) and 100 m (right) inside a revegetated area at locations no 7 and 8, respectively.

The other area was in the south-western part of the research area, near Búrfell, where the surface type is white pumice (Fig. 14). In 1998 Lyme grass was seeded in the area but Lupine and other grass species were added to the reclamation area in the years 2001-2004. One dust trap (location no 31) was placed in an unvegetated area outside the reclamation area (Fig. 14) and another dust trap (location no 32) was placed 50 m into the revegetaded area (Fig. 15).

Figure 14. Overview and surface of unvegetated pumice field at location no 31.

Figure 15. Overview and surface of revegetated pumice field at location no 32.

3.3 Land assessment based on field work and remote sensing

Measurements on aeolian transport obtained by single BSNE dust trap is point samples that give an idea of the "big picture". Knowledge of spatial and temporal variation in different erosion processes and surface field conditions is necessary to understand aeolian processes. Field surface characteristics that may affect aeolian processes include for example surface

roughness and nonerodible surface cover (Zobeck et al., 2003). Knowledge of these factors is also necessary to be able to transfer the information gained from point measurements to a landscape scale. Therefore the research area was mapped using field assessment and remote sensing.

The field mapping is based on visual assessment and estimates, but not quantitative measurements but SPOT 5 satellite images in a scale 1:15 000 were used for interpretation and to draw polygon boundaries. The field mapping system used in this research was based on a classification system used by the Soil Conservation Service of Iceland (SCS), for land assessment prior to reclamation work. The SCS mapping system was developed to accumulate information on initial condition in an area before reclamation work is started and is also used to evaluate the potentials for reclamation work, to evaluate what methods are possible based on physical factors and how much intervention is needed (Thórarinsdóttir, 2009). The SCS mapping system was simplified and adjusted to this project (see field mapping system in Appendix 2). The field mapping included information on soil erosion, surface roughness, rock outcrop, vegetation cover and the proportion of sand and other loose material on surface. The main waterways and flow channels were also mapped using the same methods.

Soil erosion

The soil erosion was mapped in the field using the same classification system that was used in the national soil erosion survey (Arnalds et al., 1997) where erosion forms are classified as well as the erosion severity. Sandy areas are divided into three different classes as shown in Fig. 16. The classes are: i) sandy lava - where sand has drifted over lava fields, where large amount of tephra is deposited on lava surfaces in volcanic eruptions or where floods leave sediments in lavas ii) sand fields - which represent areas with sand, tephra or pumice on surface and iii) sandy lag gravel – where sand drifts over lag gravel surfaces and accumulates at the surface. The amount of loose material, sand or pumice, on surface was also estimated.

Figure 16. Different erosion classes; sandy lava (left), sand fields (middle) and sandy lag gravel (right).

Surface roughness

Wind is characterized by its speed and its direction. The wind pattern over the surface depends on various factors including topographic conditions. The topographic surface roughness in an area affects the wind profile. The surface roughness referred to in this research is the relief that refers to meso-scale surface features such as stones, rocks and lava formations. The surface roughness was estimated using a 15 m radius from any chosen spot. In the field mapping, visual assessment was used to define the area into four surface roughness classes, from smooth to very rough (Fig. 17).

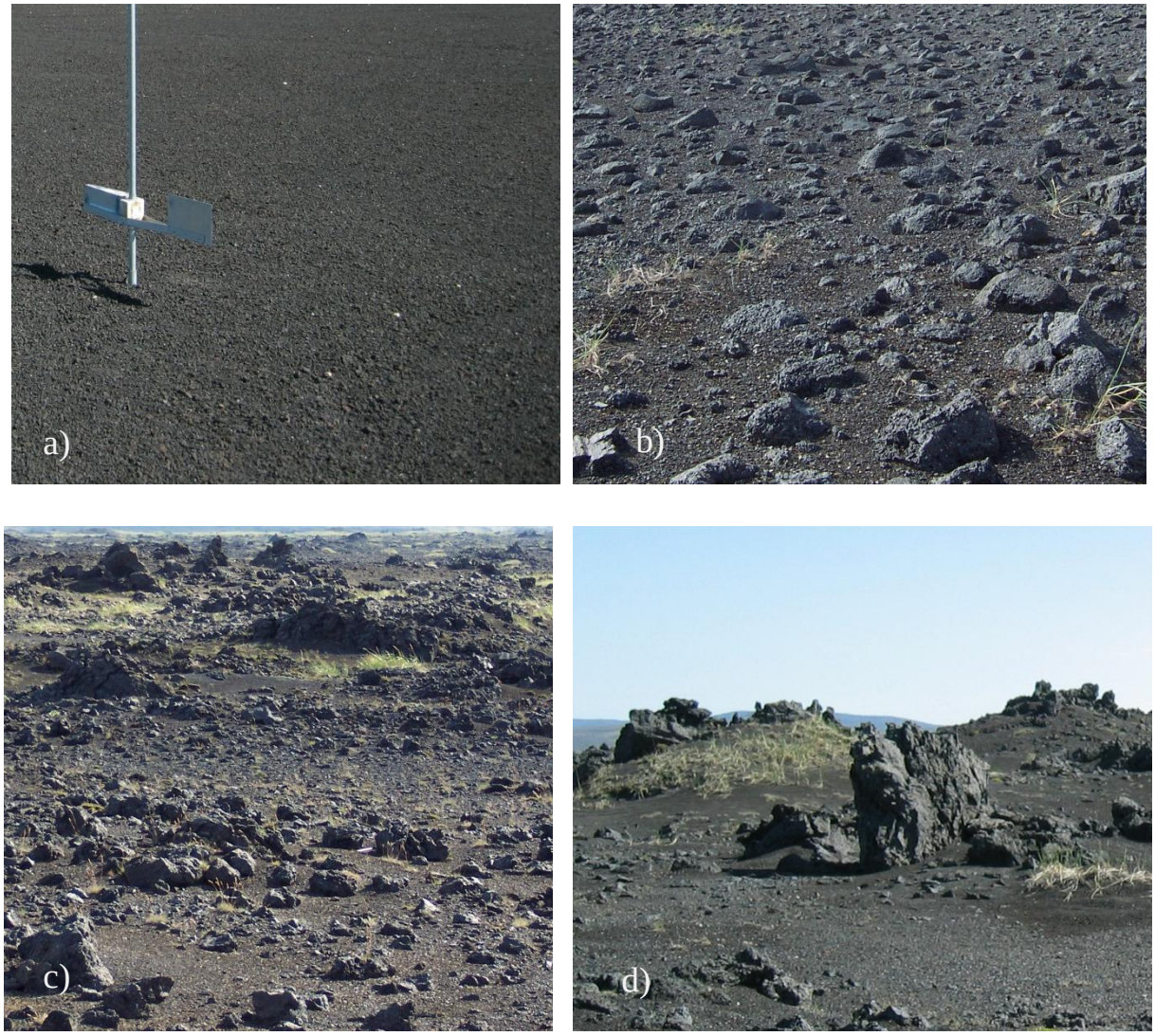

Figure 17. Surface roughness classes: a) smooth, <5cm roughness; b) rather smooth, 5-50 cm roughness; c) rough, 50-150 cm roughness; d) very rough, >150 cm roughness.

Surface roughness was also estimated by obtaining wind profiles at sites that represent each surface roughness class. For that purpose wind speed was measured at three different heights, 40, 60 and 220 cm. These wind profiles were used to verify the classification based on visual assessment.

Rock outcrop and vegetation cover

Nonerodible surface cover includes any material protecting the soil surface from the force of wind and impact of saltating grains. To estimate the amount of nonerodible surface cover, vegetation cover and rock outcrop was estimated by visual assessment. The rock outcrop is

defined as stones or rocks > 10 cm in diameter and four classes were used to assess their cover, from no rock outcrop to extensive rock outcrop (Fig. 18).

Figure 18. Rock outcrop classes: a) no rock outcrop b) 1-20% cover c) 21-40% cover d) 41-60% cover.

Vegetation cover can also affect the erodibility of the surface and to estimate that effect the vegetation cover was mapped using field mapping and image interpretation. The % vegetation cover was estimated at the soil surface using classes with 20% interval. As most of the research area has very little vegetation cover, or < 20%, it was decided to divide this class into four subclasses with 5% intervals (Fig. 19).

Figure 19. Vegetation cover; 0-5% (left), 21-40% (middle) and 41-60% (right)

Biological soil crust was also mapped as it is an important indicator of the stability of the surface.

Water erosion

One of the challenges of transferring the mass transport to a landscape scale is to be able to identify the factors that influence the wind erosion. As mentioned earlier fluvial and aeolian processes interact in the area and to be able to estimate the water erosion on a landscape scale all major waterways (Fig. 20) were mapped using remote sensing and field work. All waterways were dry at the time of mapping.

Figure 20. One of the major waterways in the research area, in May 2009, recently dried after spring thaw.

3.4 Spatial analysis and image classification

Geographical information systems GIS, are able to capture, model, store, retrieve, share, manipulate, analyse and present geographically referenced date (Worboys and Duckham, 2004). All data acquired from field mapping was stored and analysed in a GIS system, using the ArcGIS software from ESRI.

The emphasis of spatial analysis is to measure properties and relationships, based on the spatial locations of the phenomenon under study. It includes the techniques which study entities using their topological, geometric or geographic properties. In erosion cause-effect studies, like in this research, one looks for relationships between erosion processes and variables. Spatial analysis was used to translate patterns such as vegetation cover and rock outcrop, obtained by field mapping, into objective and measurable considerations. The digitized data layers were rasterized into 10x10 m cells. All the new raster data layers were reclassified based on attribute values given in the field mapping e.g. erosion severity and vegetation cover.

Principal components analysis was made using the Canoco 4.5 software (ter Braak and Smilauer, 2002) to estimate which surface characteristics used in the spatial analysis effect wind erosion the most.

The SPOT 5 satellite has a sensor that detects radiances of various surfaces of the Earth through different spectral channels (pan 480-710nm, green 500-590nm, red 610-680nm, near IR 780-890 nm and shortwave IR 1580-1750nm). ERDAS Imagine 9.3 software was used to classify a SPOT image of the research area. Image classification attempts to associate each pixel in an image to a thematic group describing a real world object, on the basis of its spectral characteristics (Lillesand and Kiefer, 2000). A supervised classification compares multidimensional spectral response values for a single ground sample unit (a pixel) to a control area (training area) of known landscape conditions for subsequent classification, whereas the unsupervised approach generates spectral clusters on the landscape though iterative cluster building achieved without a priori knowledge of the landscape. A supervised approach was chosen because a good knowledge about the research area had been gained, based on the field mapping. A SPOT 5 image from August 2009 was used for the supervised classification to produce a thematic map showing distribution of identified surface types, using 10x10 m cells.

4. Results

The research approach consisted mainly of three steps, determination of *i)* the mass sand transport in the area *ii)* the effect of reclamation work on sand transport and *iii)* the effect of environmental factors such as water erosion, different surface roughness and particle size on sand transport dynamics.

4.1 Material collected in dust traps

During the two summers that the research was conducted, six erosion events occurred. The dust traps were emptied as soon after each erosion event as possible. The sampling periods, that included these erosion events (called sampling periods A, B, C, D, E and F), lasted from four days to almost two months (Table 4).

Table 4. Sampling periods and erosion events dates during the research period.

Sampling period	Dates	Erosion event
A	June 3rd - June 7th 2008	June 4th 2008
B	June 20th - July 5th 2008	July 1st 2008
C	July 5th - August 30th 2008	August 29th 2008
D	May 16th - June 30th 2009	May 28th 2009
E	July 24th - July 30th 2009	July 27th 2009
F	July 30th - August 24th 2009	August 24th 2009

There was a considerable variation in the total amount of material collected in dust traps between locations (see Appendix 3). There were < 10 g collected in dust traps at 30 cm height during each of the erosion events at ten of the locations. Most of these low sand collection locations are in the north-western part of the research area. The maximum transport was measured in the north-eastern part, especially at locations no 15, 16 and 17. The highest value for collected material in a dust trap at 30 cm height was >1485 g, from sampling period A at location no 17. At five locations, dust traps at 30 cm height filled up during erosion events, some of them repeatedly. At locations with traps mounted at 60 cm height, sand contents ranged from negligible at locations with limited aeolian activity in the measured storms to >600 g. Dust traps placed at 100 cm height received up to 182 g during the most intensive storms.

The lowest dust traps at 15 cm height are placed within the active part of the saltation layer, which is often considered to be the bottom 10-30 cm (e.g. Zhang et al., 2007; Pye and Zoar, 1990). The amount of material collected in dust traps placed higher, for example during the last erosion event, where ≥100 g was collected in two dust traps at 100 cm height, indicates that the upper limit of the saltation layer is possibly well above 1 m height in the Hekla area, while some of the 100 cm material is also suspended (dust). This will be given more consideration in relation to the grain size analysis.

Measured erosion varied considerably between sampling periods. The most intense erosion event at locations no 21 and 26 occurred during the third sampling period (C), while at location no 28 the second sampling period (B) was most intense. At locations no 9 and 13 it was in the last sampling period (F). This indicates that local differences influence overall wind speeds and erosion susceptibility of the surface at any given time.

Grain size analysis

Grain size distribution obtained for surface samples from eleven locations within the research area are shown in Fig. 21.

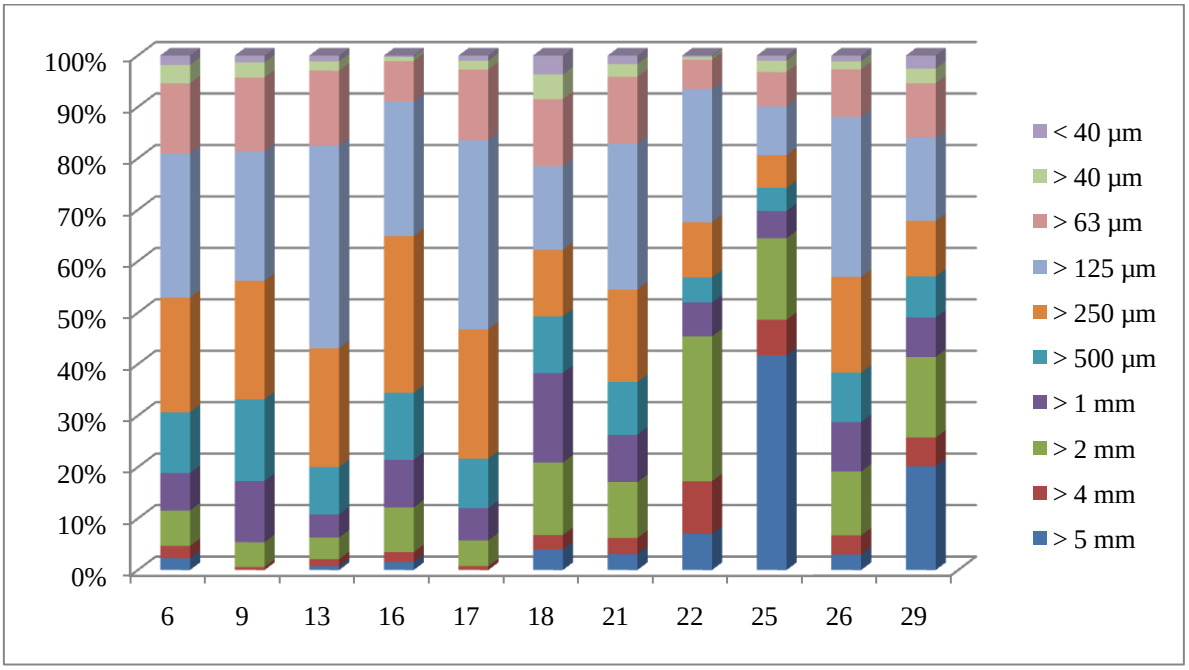

Figure 21. Grain size distribution of surface samples at eleven locations.

The grain size analysis shows that the proportion of coarse grains (>1 mm) increases from northeast to the southwest of the research area, with the highest proportion in the areas closest to Hekla, at locations no 25 and 29 (about 65% and 45% respectively). The only exception to this is at location no 18, where the proportion of coarse grains is >35%, compared to <20% of coarse grains in all other locations in the north-eastern part of the research area.

As explained earlier, grains are transported by wind in three different ways, surface creep, saltation and suspension. The majority of grains are transported by saltation, but the upper limit of the saltation layer is often considered to be about 30 cm although it can exceed 3 m on hard surfaces such as rock pavements and gravel fans (Pye and Tsoar, 1990). The proportion of grains carried by saltation decreases with height, while the proportion of grains carried by suspension increases with height. Saltating grains are usually considered to be grains <0.84 mm in diameter (Skidmore, 1994). The particle fraction >84 mm has been termed the nonerodible soil fraction and it has been used as such for example in soil loss equations and for estimation on soil erodibility (Skidmore, 1994; Zobeck et al,. 2003).

To gain information on the difference in grains size distribution by height, samples collected in a set of four dust traps at location no 22 were weighted and sieved (Fig. 22a and Fig. 22b). Two sampling periods, E and F (see Table 4) were used to obtain a comparison between two different events. The mean wind speed during the erosion event in sampling period E was 13.9 compared to 15.4 for the erosion event during sampling period F. The amount of material collected in the dust traps in sampling period E was approximately one third of what was collected in sampling period F.

The grain size distribution by height (Fig. 22a and Fig. 22b) shows that the proportion of the coarsest grains (>4 mm) decreases with height, from 12.1% at 15 cm height to 4% at 100 cm height (sampling period E) and from 11.5% at 15 cm height to 5.6% at 100 cm height (sampling period F). The proportion of the finest grains (<63 µm) increases from 27.6% to 33.3% from 15 to 100 cm height during sampling period E and from 28.0% to 30.9% during sampling period F. The grain size distribution by height also shows that in all the samples, >35% of collected material is >1 mm, regardless of height. This indicates that the upper limit of the saltation layer in the Hekla area is well above 1 m.

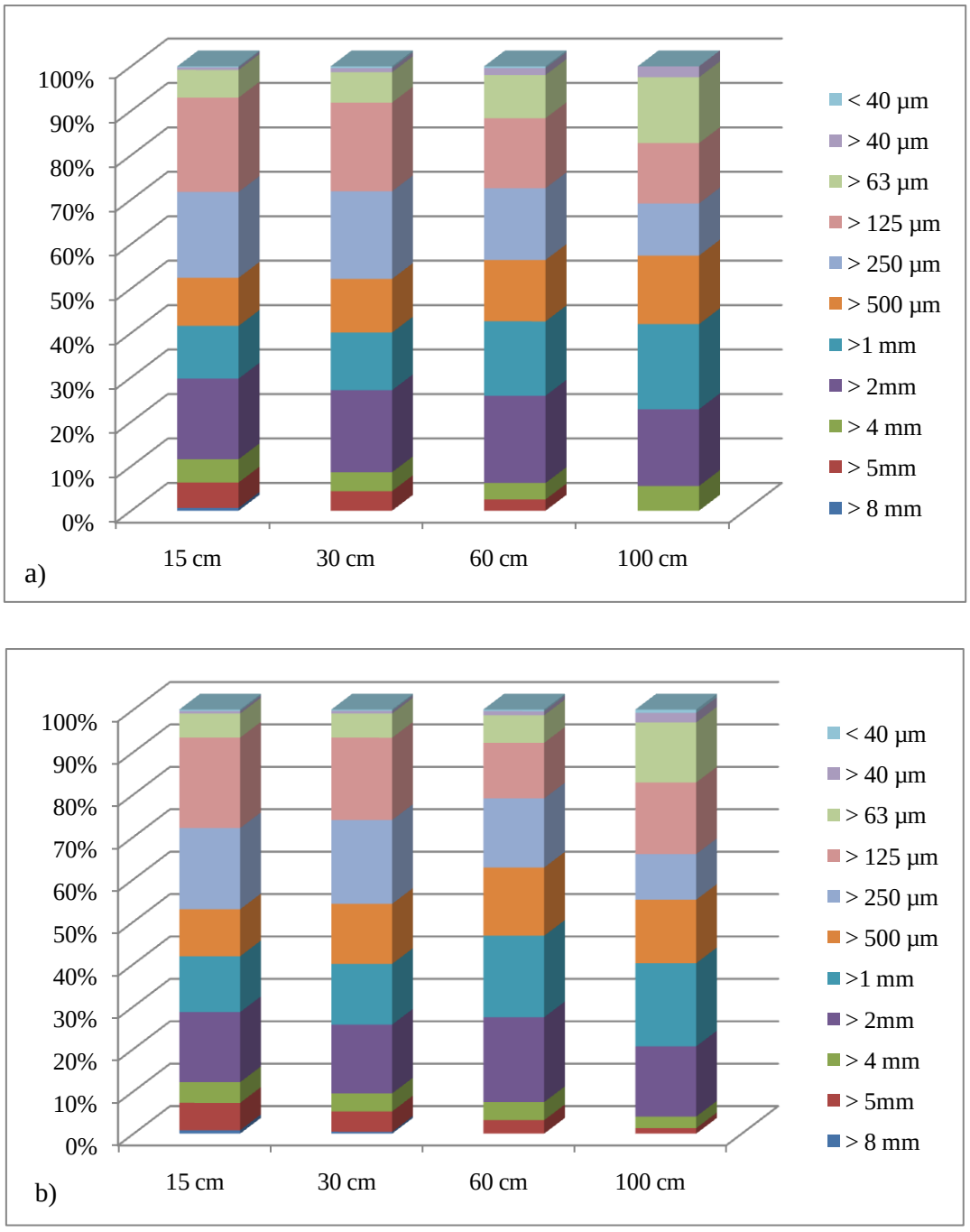

Figure 22. a) Grain size distribution at different heights, for samples collected at location no 22 during sampling period E, from July 24th to 30th 2009. b) Grain size distribution for samples obtained at different height, from samples collected in a set of four dust traps at location no 22 during sampling period F, from July 30th to August 24th 2009.

The average difference between the two erosion events, when comparing the proportions of material in each grain size class based on height distribution, was low, or 0.8%. The largest difference was 3.3% in grain size class 63-125 µm at 100 cm height.

4.2 Calculation of sand transport

The quantity of material collected in dust traps in erosion events was used to calculate the mass sand transport over a 1 m wide transect (kg m^{-1}). The method used to calculate the mass sand transport was developed by Arnalds and Gísladóttir (2009). This method is based on the ratio of eroding material between different heights being rather constant between erosion events at a given location.

Samples collected in a set of four dust traps, were used to calculate the height distribution of the materials. Small samples, <10 g collected at 30 cm height, were excluded as well as samples where dust traps filled up during erosion events, because they did not give valid height distribution. The amount collected in traps at 15 cm height was given the value 1 and other values used as ratio of that, to calculate the average height distribution (Table 5).

Table 5. The average distribution of sediment by height, collected in sets of four dust traps. Sediment in the lowest dust trap (15 cm) is given the value of 1 and other heights are shown as a ratio of that.

Dust trap	Location														
height	6	6	11	13	13	17	21	21	21	21	22	22	27	29	
cm	proportional values relative to the 15 cm trap														**Average**
15	1	1	1	1	1	1	1	1	1	1	1	1	1	1	**1**
30	0.56	0.56	0.47	0.47	0.41	0.43	0.60	0.51	0.68	0.48	0.73	0.72	0.54	0.65	**0.56**
60	0.26	0.23	0.12	0.17	0.17	0.12	0.18	0.18	0.27	0.17	0.29	0.28	0.30	0.27	**0.21**
100	0.13	0.09	0.05	0.09	0.08	0.03	0.07	0.07	0.11	0.10	0.10	0.13	0.11	0.12	**0.09**

In locations where more than one sample was collected the distribution of sediment by height is very similar between sampling periods, except in location no 21 which shows a little more variability. This result supports the credibility of the single dust trap method.

All valid measurements from sets of four dust traps were plotted on curves showing the height distribution of eroding material, see Fig. 23.

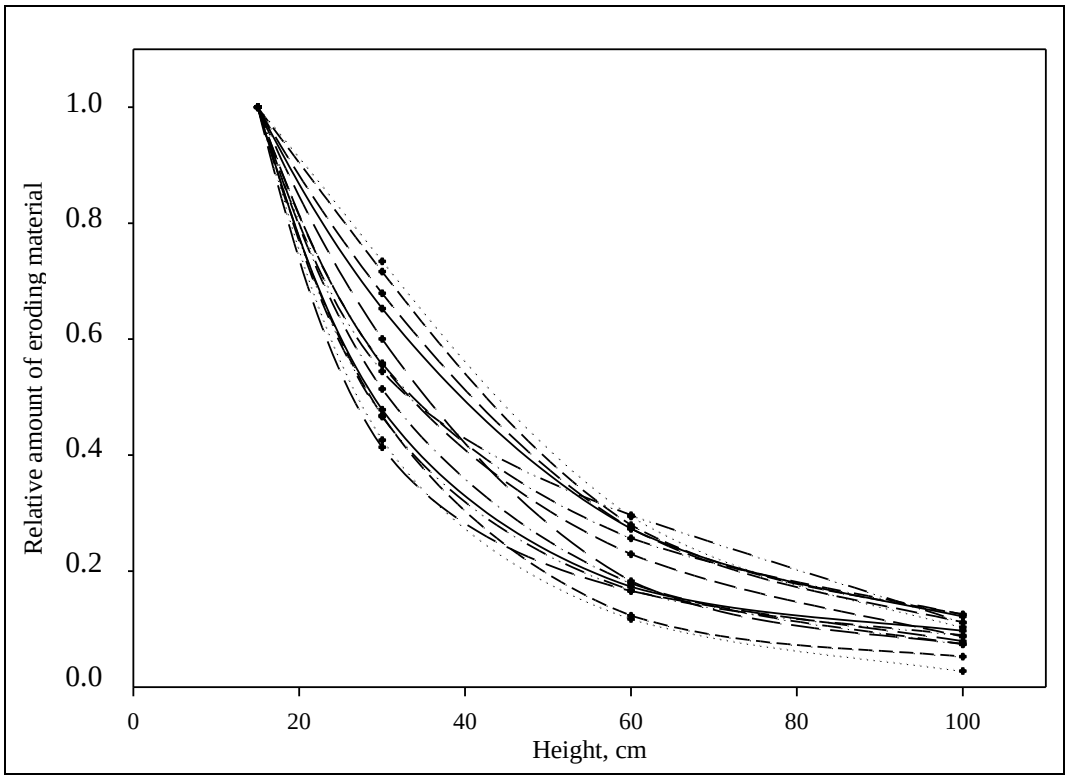

Figure 23. All valid curves for height distribution of material collected in sets of four dust traps, normalized for 15 cm height. The amount collected in the lowest trap (15 cm) is given the value of 1, and the remainder values (30, 60 and 100 cm) are proportional amount compared to the lowest trap.

The height distribution curves (Fig. 23) showed some variation between locations within the research area. Physical properties of individual particles, such as shape, size and density, play an important role in their interactions in the erosion process (Shao, 2000). To test if this variability was due to grain size distribution and the amount of pumice on surface, the material collected in all dust traps in one sampling period were sieved and the results reported using the Udden-Wentworth grain size classification scheme. Samples from dust traps at 30 cm height were used for the grain size analysis except at locations no 10, 12, 14, 15 and 16, where samples from dust traps at 60 cm height were used. It was established earlier (Fig. 22a and Fig. 22b) that the grain size distribution is not markedly different between 30 and 60 cm height.

The grain size parameters of the collected material are shown in Table 6, for all locations except locations no 3 and 4 where the samples were < 1g. The distribution between different

grain size classes from 20 locations is shown in Fig. 24, but samples < 8 g were excluded as they were believed to be too small to give reliable information.

Table 6. Grain size parameters of material collected in dust traps at 30 locations (mean, sorting and skewness, μm). The method of moments was used to calculate statistics.

Site	Textural group	Mean (x) μm	Sorting (σ) μm	Skewness μm	Gravel (%)	Sand (%)	Silt (%)
Location 1 *	Sand	299	278	2.6	0.0	97.1	2.9
Location 2 *	Slightly Gravelly Sand	433	568	3.1	3.0	94.1	2.9
Location 5 *	Sand	635	511	0.8	0.0	100.0	0.0
Location 6	Gravelly Sand	917	947	2.6	9.4	90.1	0.5
Location 7	Sand	215	204	3.4	0.0	92.9	7.1
Location 8 *	Muddy Sand	140	113	3.8	0.0	86.6	13.4
Location 9	Slightly Gravelly Sand	570	686	3.6	3.0	95.7	1.4
Location 10	Slightly Gravelly Sand	363	367	3.2	0.5	97.6	1.8
Location 11	Slightly Gravelly Sand	406	380	4.3	0.7	98.9	0.4
Location 12	Slightly Gravelly Sand	353	332	3.1	0.3	98.8	0.8
Location 13	Slightly Gravelly Sand	348	317	4.6	0.3	98.7	1.0
Location 14	Slightly Gravelly Sand	282	356	9.0	0.5	96.4	3.1
Location 15	Slightly Gravelly Sand	542	576	3.0	2.2	96.0	1.8
Location 16	Slightly Gravelly Sand	421	408	4.4	0.7	98.4	0.8
Location 17	Slightly Gravelly Sand	567	620	4.1	2.4	97.1	0.5
Location 18 *	Gravelly Sand	1062	1538	2.1	17.0	80,1	2.9
Location 19 *	Sand	270	274	2.8	0.0	97.3	2.7
Location 20 *	Gravelly Sand	1063	1381	2. 2	16.1	83.9	0.0
Location 21	Slightly Gravelly Sand	399	598	4.8	2.6	95.1	2.2
Location 22	Gravelly Sand	1593	1962	2.1	27.2	72.1	0.7
Location 23	Sandy Gravel	5723	3883	0.6	79.9	20.1	0.0
Location 24 *	Gravelly Muddy Sand	1216	1756	1.8	18.2	73.0	8.8
Location 25	Muddy Sandy Gravel	4005	4355	0.9	52.1	42.8	5.1
Location 26	Gravelly Sand	1332	1851	2.7	20.8	78.3	0.9
Location 27	Gravelly Sand	796	1354	3.1	11.1	87.8	1.2
Location 28	Gravelly Sand	1032	1275	2.1	15.9	83.3	0.9
Location 29	Sandy Gravel	3970	3356	1.2	68.6	30.0	1.4
Location 30	Sandy Gravel	3028	2686	1.5	50.8	49.2	0.0
Location 31	Sandy Gravel	3431	3811	1.2	47.4	50.7	1.9
Location 32 *	Muddy Sand	86	17	-1.5	0.0	80.4	19.6

* samples < 8g which might be too small to give reliable information

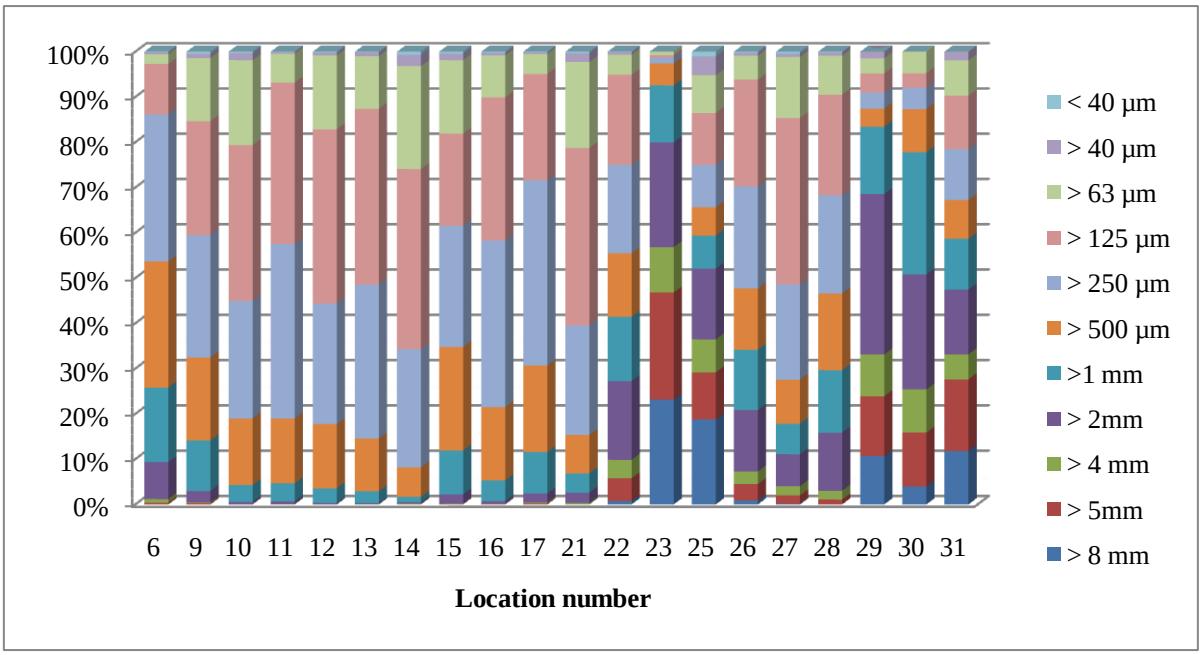

Figure 24. Grain size distribution for samples collected in dust traps at 30 or 60 cm height, at 20 locations, during one sampling period in August 2009.

The grain size analysis shows that many locations had a high proportion of coarse grains collected in the traps. At five locations (no 23, 25, 29, 30 and 31), the mean grain size was >3 mm and grains > 1 mm were over 50% of the sample. Based on grain size analysis the research area could be roughly divided into two parts; the north-eastern part, with a low percentage of coarse grains; and the south-western part, with a high percentage of coarse grains. There is one exception to this and that is location no 6 in the north-eastern part of the research area, which is different from other locations in that part because it has a higher proportion of coarse grains with over 20% of the grains > 1mm. This is probably due to the fact that a small seasonally active creek, Helliskvísl, runs through that area and causes periodic deposition of tephra and pumice within this site.

Based on the grain size analysis, the locations were divided into three sections as shown in Fig. 25, i) **northeast**; the textural group is slightly gravelly sand, with the mean grain size ranging from 282-570µm and grains >2 mm in diameter < 5% of the sample, ii) **southwest**; areas with high proportion of pumice on the surface and the textural group is gravelly sand or sandy gravel. The mean grain size was 796-5723µm and grains >2 mm in diameter > 10% of the sample and iii) **Helliskvísl**; the area near the creek were pumice is transported by water

into a sandy area, resulting in the textural group being gravelly sand, with the mean grain size 917µm and grains >2 mm 5-10% of the sample.

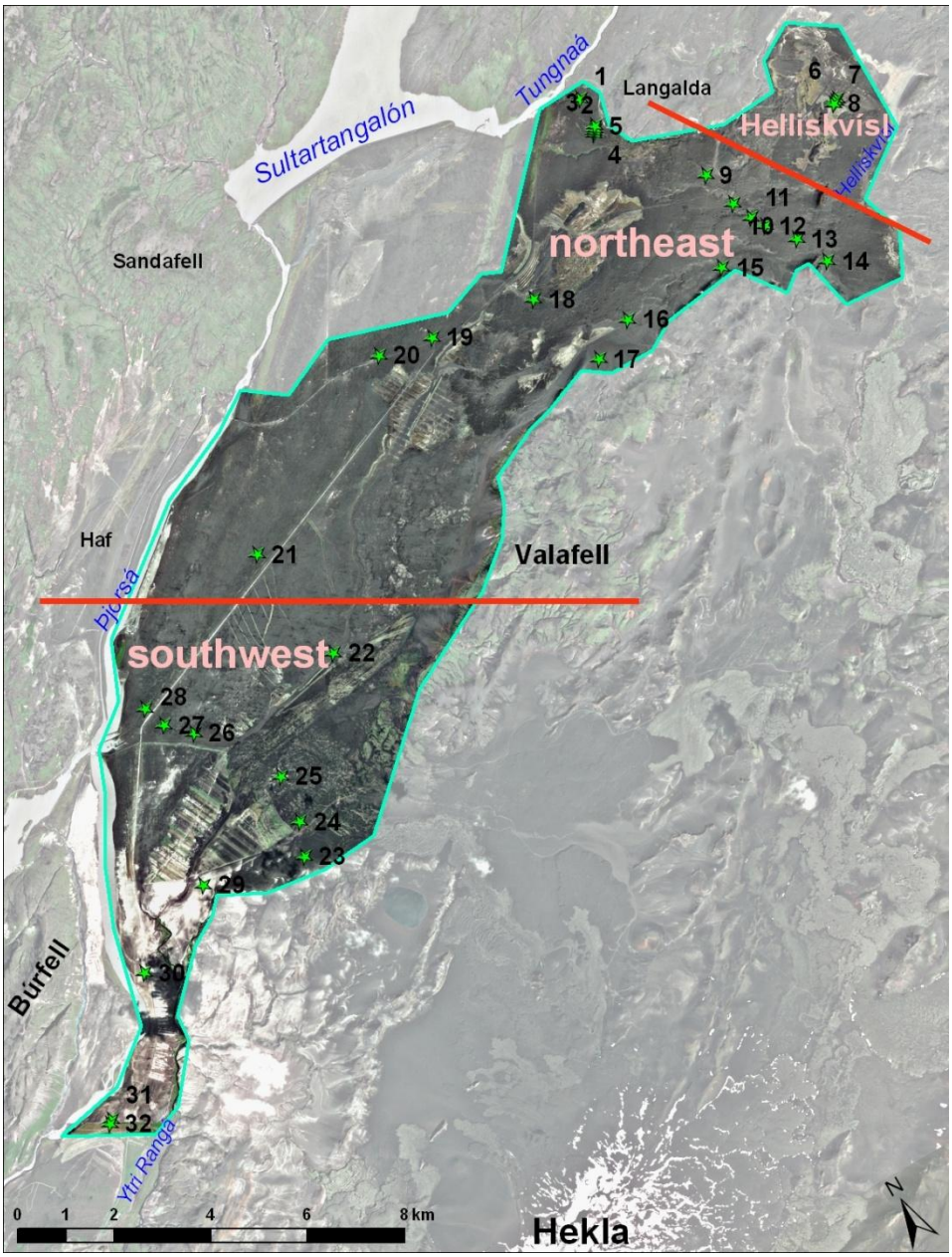

Figure 25. The research area divided into three sections based on grain size analysis from samples collected in dust traps. At Helliskvísl 5-10% of the material was >2 mm, in the north-eastern area it was <5% but >10% in the south-western area.

Locations were divided into three groups based on these sections and the groups were subsequently used to calculate three different curves for the average normalized height distribution of sand transport for all locations within each group, see Fig. 26.

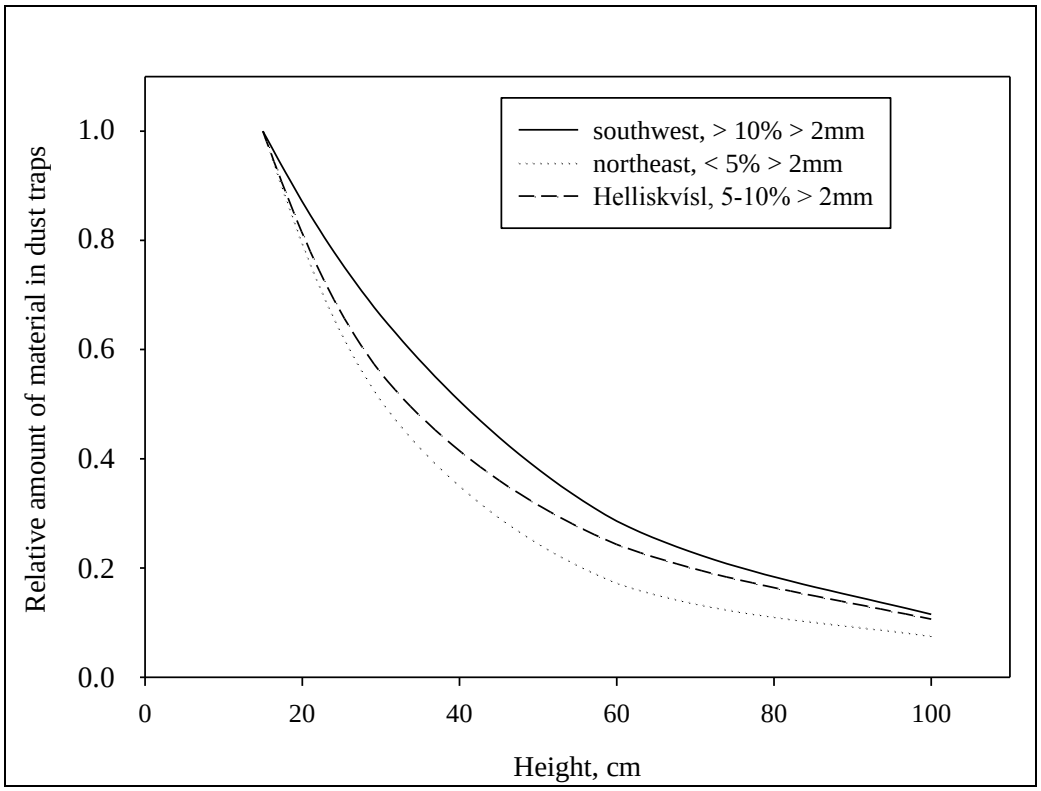

Figure 26. Height distribution of aeolian transport for sites within three sections which are classified based on size distribution. The distribution is shown relative to the amount collected in the lowest trap, which is given the value 1.

The curves in Fig. 26 are based on measurements from dust traps placed at 15 – 100 cm height. A t-test was used to assess whether the curves are statistically different from each other. The t-test showed that there is a significant difference ($p < 0.01$) between the average curves from the south-western and the north-eastern parts, based on the height distribution. The average proportion at 30 cm height in the south-western part is 0.66 and 0.51 in the north-eastern part, at 60 cm height it is 0.29 and 0.17 respectively, and at 100 cm height it is 0.12 and 0.08 respectively. The curve from Helliskvísl is based on averages from only two measurements and could therefore not be compared to the other two using a t-test.

The average curves (Fig. 26) were used to find a coefficient for calculating aeolian transport for each 10 cm interval (10 cm * 100 cm, using the median) up to 60 cm height, then 20 cm increments up to 100 cm height. One 40 cm interval was also added to calculate the sand transport from 100 to 140 cm. Data from Sensit sensors mounted at 7.5 cm and 15 cm height at location no 21 (see chapter 4.3), was used to estimate the sediment transport below 10 cm

height, relative to the 10-20 cm interval. Based on that data, the same amount of sediment was assumed to be at the lowest interval, from 0-10 cm (5 cm median) as for the second lowest interval from 10-20 cm (15 cm median). This methodology is in accordance with a research done by Arnalds and Gísladóttir (2009) where they estimated that the maximum sand transport is at approximately 10 cm height, based on data from Sensit sensors in 4, 8 and 28 cm height.

The coefficients obtained from these curves were used to calculate sand mass transport in kg of material, which is transported over a 1 m wide transect, up to 140 cm height. Most of the single dust traps were mounted at 30 cm height or 60 cm height and the curves and coefficients were adjusted to the dust traps height, so that dust traps in 30 cm height have the coefficient 1 at 30 cm and dust traps in 60 cm height have coefficient 1 at 60 cm.

An example of the calculation from a sample collected at 30 cm height at location no 13 is shown in Table 7. The amount collected in a dust trap (e.g. 125 g in the first sampling period in 2008 at location no 13) is multiplied by the coefficient for each height range (e.g. 2.03 for 0-10 cm) and divided by 1000 to change the amount into kg. To transfer the amount calculated for each height range into sand transport over a 1 m wide transect, the opening slot size of the samplers is multiplied by a factor to represent 1 m transect.

Table 7. Calculated mass aeolian sand transport (kg m^{-1}) for each 10 cm interval and total, at location no 13, for six sampling periods.

Sampling period		A	B	C	D	E	F
Height range cm	Coefficient relative to 30 cm	----------			kg m^{-1}	----------	
0 - 10	2.03	26	46	2	40	14	74
10 - 20	2.03	26	46	2	40	14	74
20 - 30	1.24	16	28	1	24	9	45
30 - 40	0.82	10	19	1	16	6	30
40 - 50	0.57	7	13	1	11	4	21
50 - 60	0.40	5	9	0	8	3	15
60 - 80	0.27	7	12	1	11	4	20
80 - 100	0.18	5	8	0	7	3	13
100 - 140	0.07	4	6	0	6	2	10
Total		**104**	**187**	**9**	**163**	**59**	**302**

Calculations for mass sand transport at all other locations are shown in Appendix 4. The calculated mass sand transport at all the sampling locations, for all the sampling periods during the research, is shown in Table 8.

Table 8. Calculated aeolian transport (kg m^{-1}), at all the sampling locations, for six sampling periods.

	2008			2009		
	A	B	C	D	E	F
Location	aeolian transport kg m^{-1}					
1	1	2	0	0	0	4
2	14	41	3	4	1	1
3	-	-	2	0	0	1
4	-	-	1	0	0	1
5	-	-	1	1	0	3
6	6	61	407	> 578*	378	> 767*
7	4	3	4	6	4	19
8	2	2	1	3	3	5
9	22	12	85	17	2	98
10	184	294	22	94	50	360
11	> 420*	> 473*	13	78	288	> 647*
12	-	-	18	141	66	549
13	104	187	9	163	59	302
14	-	-	5	81	68	156
15	-	-	-	307	144	1353
16	551	> 607*	755	98	158	1491
17	> 1276*	> 635*	1070	130	47	1788
18	8	2	0	0	1	4
19	3	2	0	1	1	4
20	2	4	0	2	1	6
21	89	39	111	4	6	27
22	-	-	-	20	102	304
23	2	0	11	0	0	36
24	0	1	0	0	0	1
25	2	1	9	0	0	7
26	130	68	429	4	22	325
27	13	13	392	2	13	158
28	26	> 416*	40	6	18	85
29	19	2	19	29	4	41
30	24	2	17	6	2	11
31	20	1	46	-	-	-
32	0	0	1	-	-	-

* minimal value as dust trap filled up during erosion event

The values in Table 8 that are marked with * show minimal values from locations with a single dust trap placed at 30 cm height, that filled up during an erosion event. The dust traps at some of these locations were raised up to 60 cm height and the coefficient for that height used to calculate the estimated aeolian transport and this applies to some of the highest values reported in the table. The spatial distribution of the average calculated aeolian transport for all the sampling periods is shown in Fig. 27.

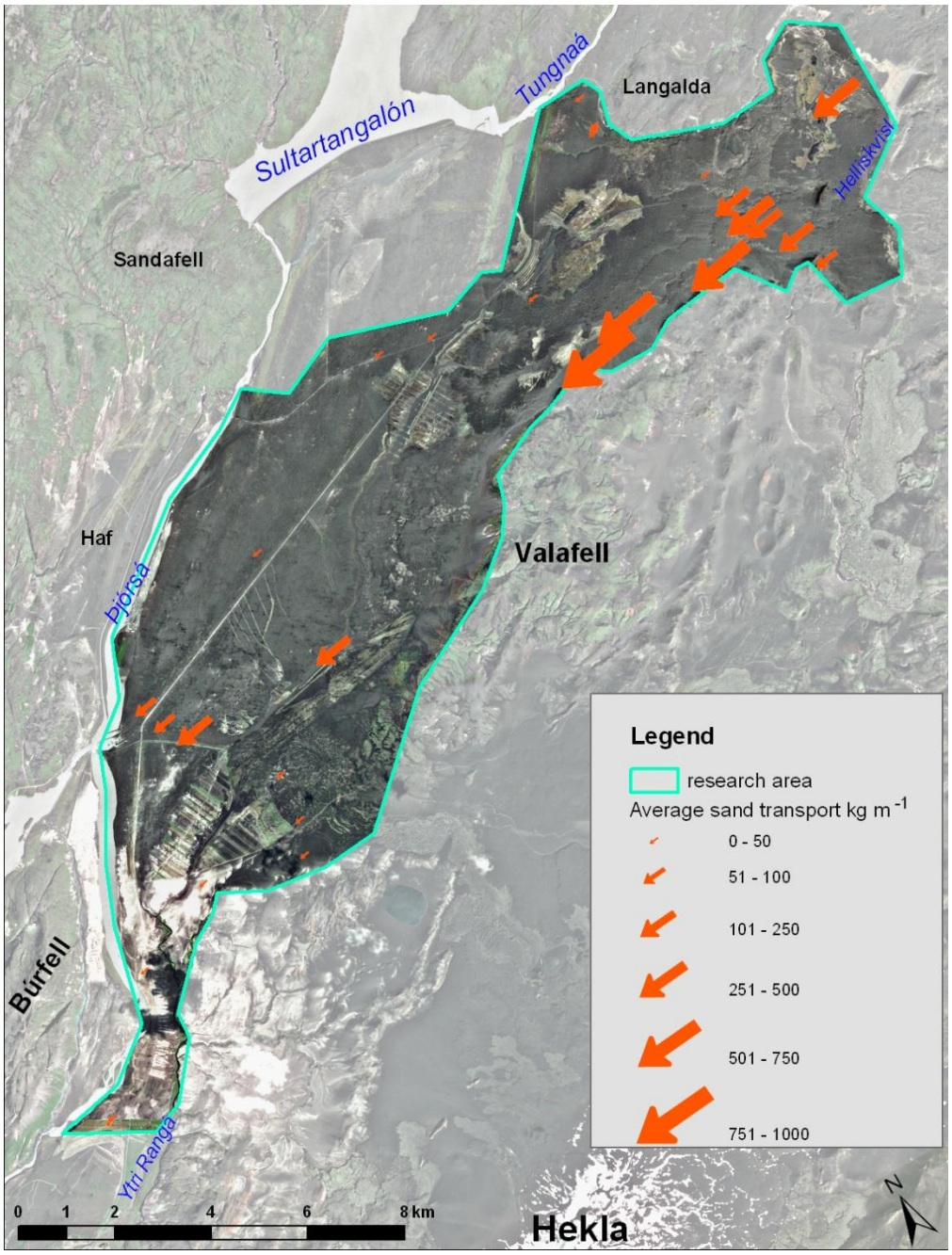

Figure 27. The average calculated aeolian transport at all locations, for all sampling periods.

The erosion events are very different in intensity both between locations and within the same location (see Appendix 5). Because of this variability the standard error of the average aeolian transport was calculated for each location, and it ranged from < 1 kg m^{-1} in locations with little erosion, up to 379 kg m^{-1} in locations with intense erosion events. To gain a clearer picture of the erosion susceptibility of each location the most intensive erosion event at each location is shown in Fig. 28.

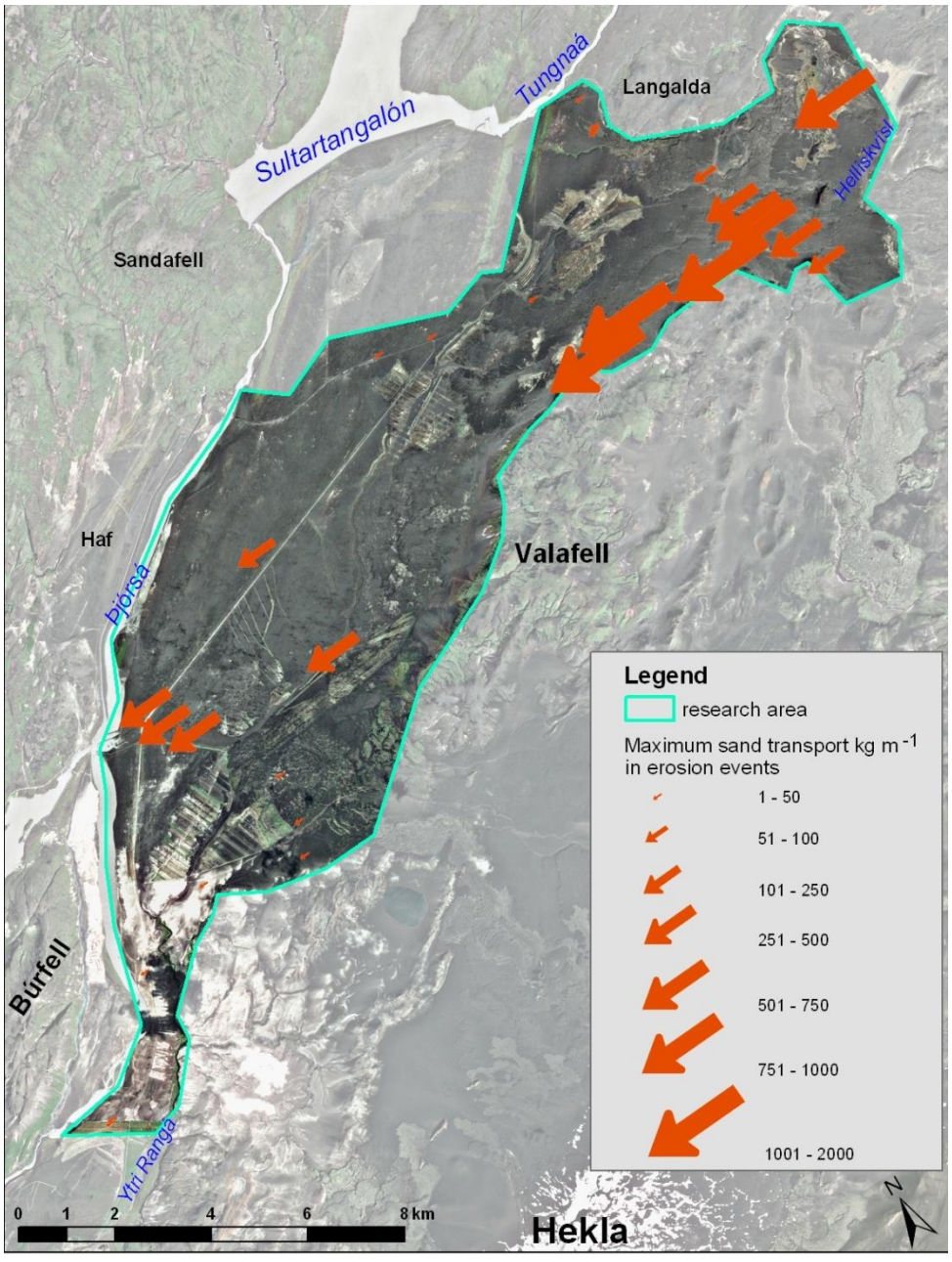

Figure 28. The maximum calculated aeolian transport in a single erosion event, at all locations, for all sampling periods.

Weather conditions

The weather conditions were recorded throughout the sampling period. Table 9 shows the weather conditions at location no 21 during the six erosion events, including some of the important weather factors that affect erosion such as wind speed, air humidity and air temperature.

Table 9. Weather conditions during the erosion events in 2008 and 2009 at location no 21.

Erosion event	Date	Length in hours and minutes	Temperature range	Air humidity range	Average of 10 min mean wind speed $	Average of 10 min maximum wind speed $	Maximum wind speed in storm event $
			°C	%	m s^{-1}	m s^{-1}	m s^{-1}
A	4th June 2008	10 hr 30 min	9.3 - 13.9	43 - 73	13.4	16.7	19.2
B	1st July 2008	14 hr 50 min	5.9 - 12.4	52 - 84	14.9	18.4	22.5
C	29th August 2008	8 hr 20 min	9.6 - 12.8	58 - 82	14.5	19.4	24.1
D	28th May 2009	1 hr 50 min	5.7 - 12.3	48 - 73	10.9	14.4	16.7
E	27th July 2009	4 hr 20 min	10.2 - 14.4	38 - 54	13.9	17.2	19.6
F	24th August 2009	6 hr 10 min	10.5 - 15.3	47 - 69	15.4	19.3	23.0

$: wind speed measured at 2.2 m height

Table 10 shows the weather conditions during the four erosion events, measured at location no 11 in 2009.

Table 10. Weather conditions during erosion events 2009 at location no 11.

Erosion event	Date	Length in hours and minutes	Temperature range	Air humidity range	Average of 10 min mean wind speed $	Average of 10 min maximum wind speed $	Maximum wind speed in storm event $
			°C	%	m s^{-1}	m s^{-1}	m s^{-1}
D	28th May 2009	4 hr 50 min	4.6 - 11.3	48 - 81	11.1	14.2	20.7
E	27th July 2009	12 hr 20 min	7.3 - 13.4	42 - 71	11.9	14.7	17.2
Fa	21st August	3 hr 10 min	5.4 - 7.4	56 - 68	11.4	14.6	16.1
F	24th August 2009	8 hr 30 min	8.3 - 14.4	52 - 80	13.7	17.3	21.5

$: wind speed measured at 2.2 m height

In two out of three erosion events (E and F) that were recorded at both locations (Table 9 and Table 10), the average of 10 min mean wind speed was higher at location no 21 than location no 11. The same applies to the maximum wind speed recorded in these erosion events. Despite higher wind speed at location no 21 in these erosion events, the amount of material collected

in dust traps at 15 cm height is considerably less, or 7 g and 31 g compared to 328 g and 738 g respectively at location no 11.

The wind direction during the erosion events ranged from northern to easterly winds. Observation data from the meteorological station at Búrfell, show that the main wind directions of driving sand movement in the research area are NE and E.

4.3 Sensit electronic sensors

The automated Sensit sensors give important information about the relation between sand transport and weather conditions. Three Sensit sensors were placed at location no 21 during the whole research period, mounted at 7.5 cm, 15 cm and 30 cm height. Data from the Sensit sensor mounted at 15 cm height, from the six erosion events that occurred at location no 21 are plotted in Fig. 29.

At location no 21, the Sensit sensor mounted at 7.5 cm height did not give reliable information in 2009 due to technical problems. Based on data from 2008 the average output from the Sensit sensor at 7.5 cm height was about 7% higher than from the Sensit sensor at 15 cm height, but it varied from 2-16%. The average output from the sensor mounted at 30 cm was about 67% of the output from the sensor at 15 cm height but the range was between 63-73%. This was compared to the amount of sediment that was collected in dust trap at this location for the same sampling periods in 2008. The average amount collected at 30 cm height is about 63% of what was collected at 15 cm height which can be considered quite similar to the results obtained by the Sensit sensor (67%) but it varied from 54-71%.

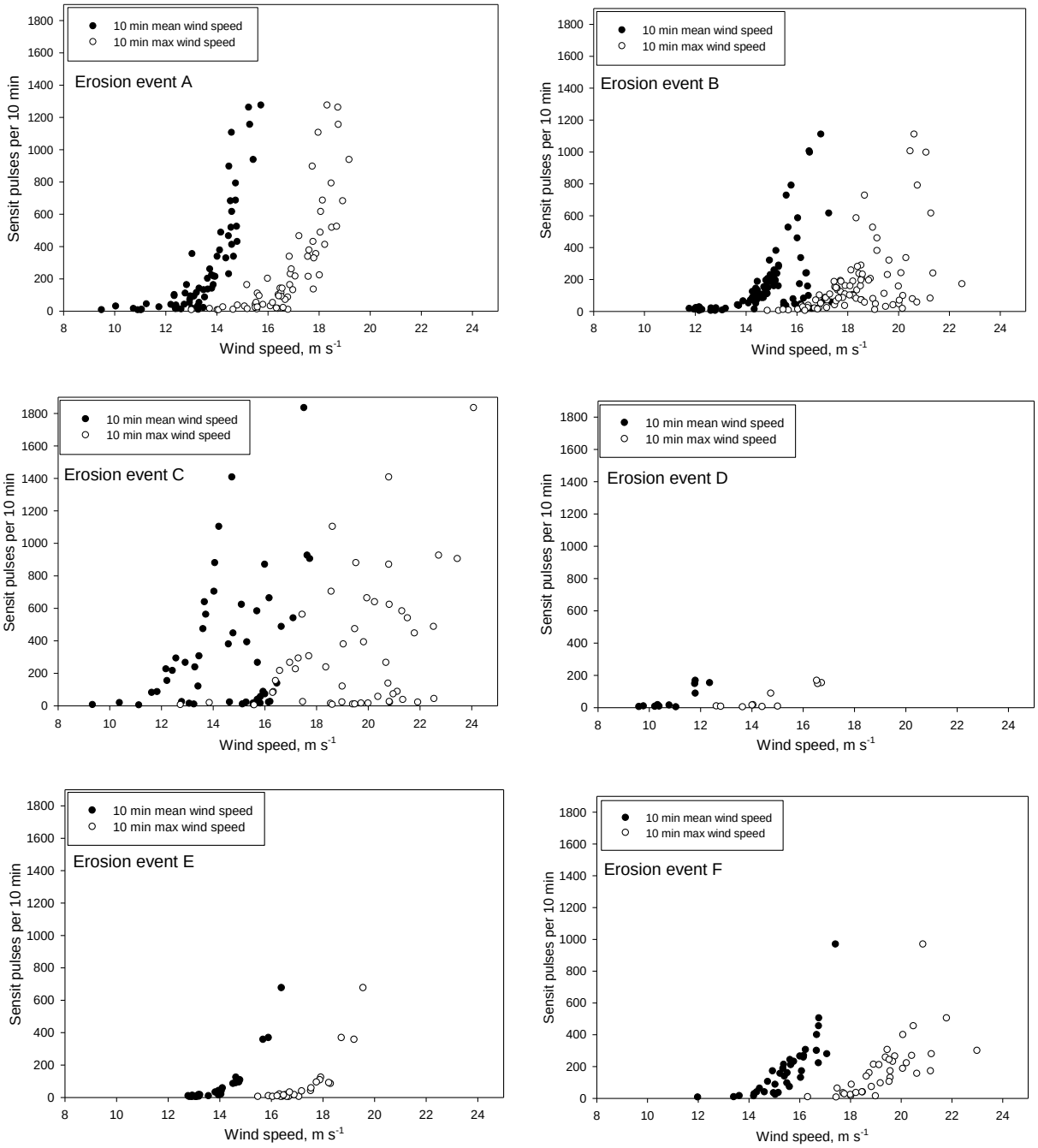

Figure 29. The relationship between 10 min mean wind speed, 10 min maximum wind speed and Sensit pulses counted for the same 10 min intervals at 15 cm height, during six erosion events at location no 21.

One Sensit sensor mounted at 15 cm height was placed at location no 11 in 2009. Three erosion events were recorded at this location on the same dates as at location no 21 but one additional erosion event was also recorded there on the 21st of August. These erosion events

are all plotted in Fig. 30 (note different scale from Fig. 29 as erosion event F resulted in very high pulse counts).

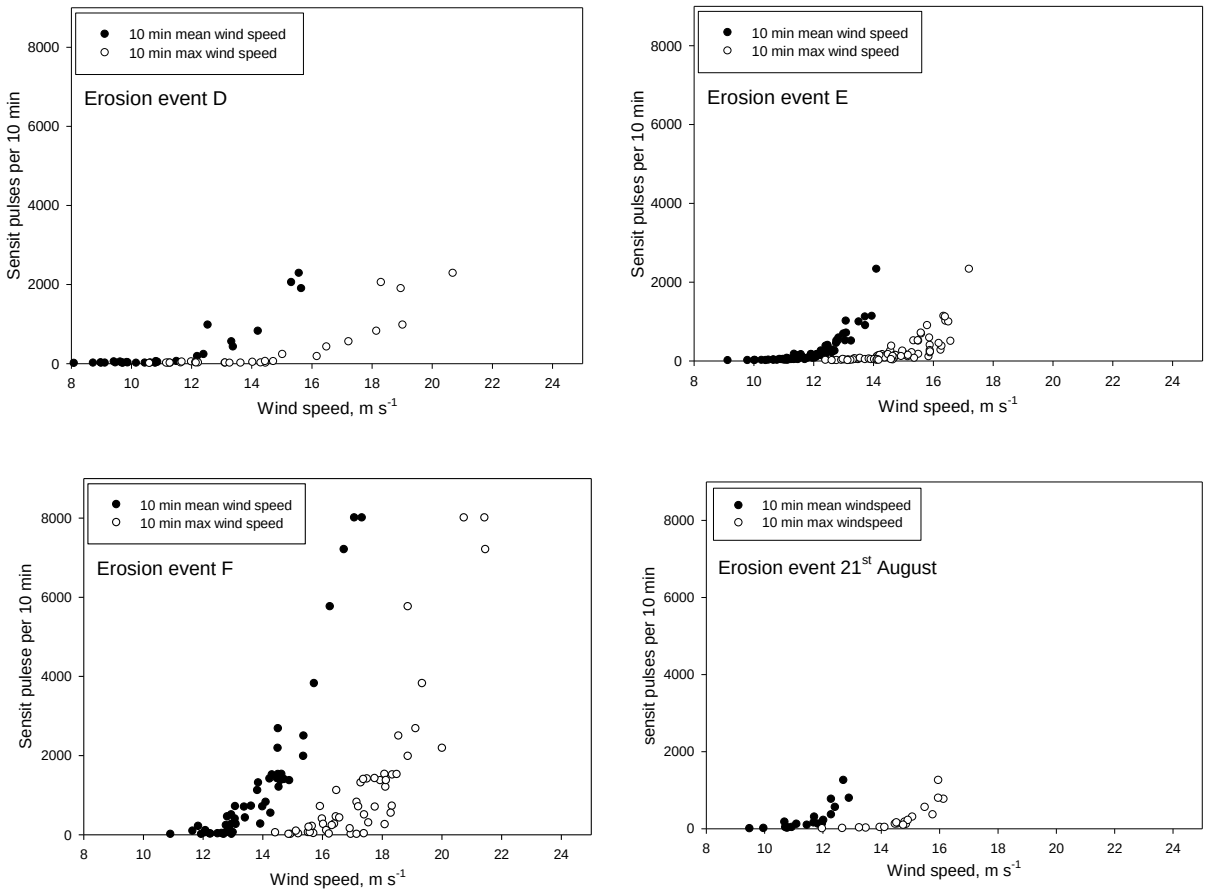

Figure 30. The relationship between 10 min mean wind speed, 10 min maximum wind speed and Sensit pulses per 10 min during four erosion events at location no 11.

During the erosion events the main distribution of Sensit pulses at location no 21 shows less than 400 per 10 minutes although they reach higher number, especially during the third erosion event when they are >1800. At location no 11 there are considerably higher number of pulses counted per 10 min interval than at location no 21. The highest count reached almost 8000 pulses per 10 min in the sixth erosion event, compared to approximately 1000 at location no 21.

Threshold value

To obtain the threshold value, the lowest wind velocity at which saltation activity is first recorded is determined. Based on 10 min mean wind speed the fluid threshold value at

location no 21 varied between erosion events from 10.1 m s^{-1} to 13.2 m s^{-1} for wind measured at 2.2 m height, with the average threshold at 11.4 m s^{-1}. At location no 11 the average fluid threshold value was 10.8 m s^{-1}, but the range was from 9.1 m s^{-1} to 13.0 m s^{-1}.

Correlation between Sensit outputs and measured movement

It is difficult to quantify the sediment movement based on Sensit data only because such calculations assume a linear relationship between Sensit particle count and sediment discharge which is not always the case (van Donk and Skidmore, 2001). The correlation between 10 min mean wind speed and Sensit particle count was calculated using a simple nonlinear regression (f=a*b^x). At location no 11 the correlation was very strong ($r > 0.90$) in all three erosion events measured there (D, E and F) with r^2 ranging from 0.89 - 0.94. At location no 21 the correlation proved to be strong or very strong ($r > 0.70$) in four erosion events (A, D, E and F) with r^2 ranging from 0.77 - 0.99 but in two erosion events (B and C) the correlation was weak ($r < 0.39$) or modest (r 0.40-0.69), with r^2 ranging from 0.16 – 0.25.

The relationship between Sensit particle count (pulses) and sediment discharge can be different from one erosion event to the next due to meteorological factors and also between areas because the mass behind each particle count is based on physical characteristics such as grain size and density. The results show that this applies to the research area based on comparison between results obtained by the sensors and the traps. At location no 21, each Sensit pulse represents 0.003 - 0.007 g in different erosion events but at location no 11 the amount ranged between 0.009 - 0.018 g in different erosion events. Care has to be taken when interpreting the Sensit counts. Over long periods with alternating aeolian activity and quieter periods, background noise can influence the results (higher counts). Rainfall can also contribute to Sensit pulses. Therefore, short intensive storms are best to establish the relationship between counts and the mass transported. For further calculations using the Sensit data, the average amount of sediment per Sensit pulse, the factor of 0.005 g for location no 11 and 0.012 g for location no 21 will be used.

Based on data from the erosion events where the r^2 was >0.5, regression equations were computed to predict mass sand flux (kg m^{-1} hr^{-1}), for erosion events where the 10 min mean wind speed reaches up to 18 m sec^{-1} (Fig 31).

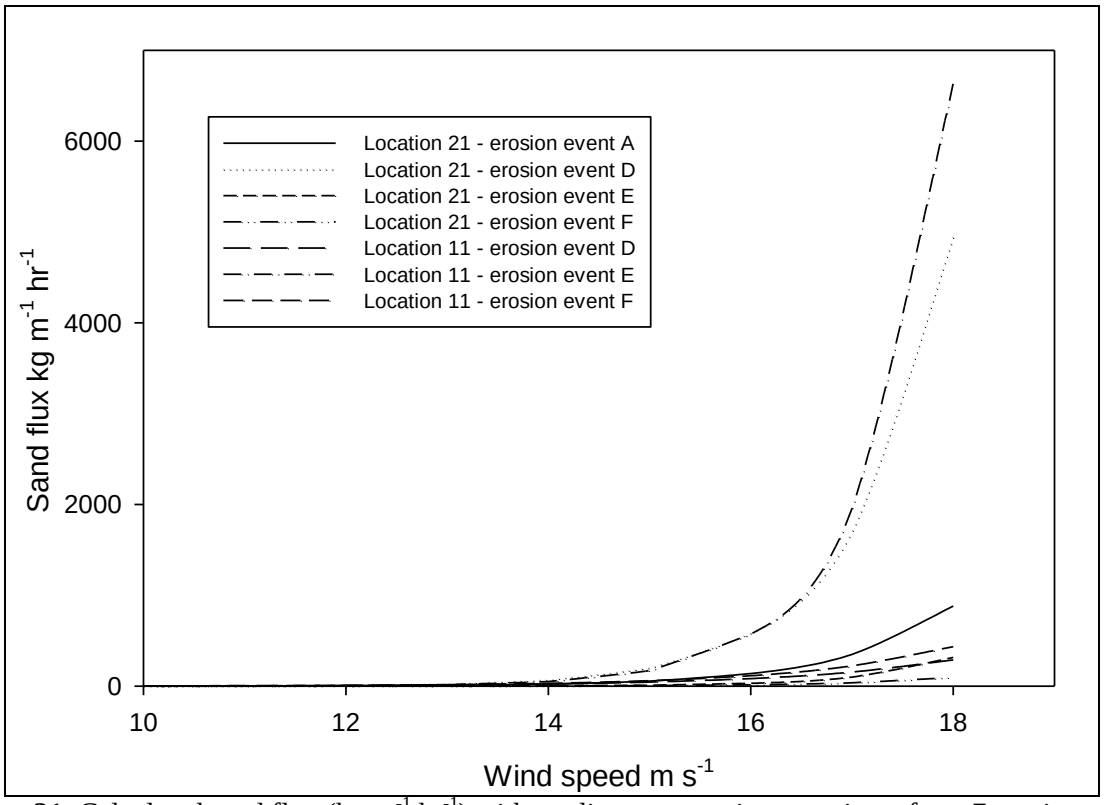

Figure 31. Calculated sand flux (kg m^{-1} hr^{-1}) with nonlinear regression equations, from 7 erosion events, bases on 10 min mean wind speed.

4.4 Effect of reclamation efforts on sand movement

The effect of reclamation efforts on sand movement was estimated in two areas, at locations no 6, 7 and 8 near Helliskvísl and at locations no 31 and 32 near Búrfell. At location no 6, near Helliskvísl, the vegetation cover was <5% outside the reclamation area and the soil erosion class was sand field with very severe erosion (5). Inside the reclamation area at locations no 7 and 8 the vegetation cover was 61-80% and the erosion class was sand field with considerable erosion (3). Near Búrfell the vegetation cover outside the reclamation area, at location no 31, was <5 % and the erosion class was sand/pumice field with very severe erosion (5). Inside the reclamation area the vegetation cover was >60% and the soil erosion classified as slight erosion (2).

Measurements were made in all five locations in 2008 but only at locations no 6, 7 and 8 in 2009. A set of four dust traps was placed at location no 6 during three sampling periods, from June to August 2008 and from May until the end of June 2009. At all other locations one dust trap mounted at 30 cm height was used.

To estimate the effect of reclamation on sand movement, the measured mass transport outside of the reclamation areas (locations no 6 and 31) was given the value of 100% and the mass transport 50 m (locations no 7 and 32) and 100 m (location no 8) inside the reclamation area was shown as ratio (%) of the erosion on the untreated areas (Fig. 32).

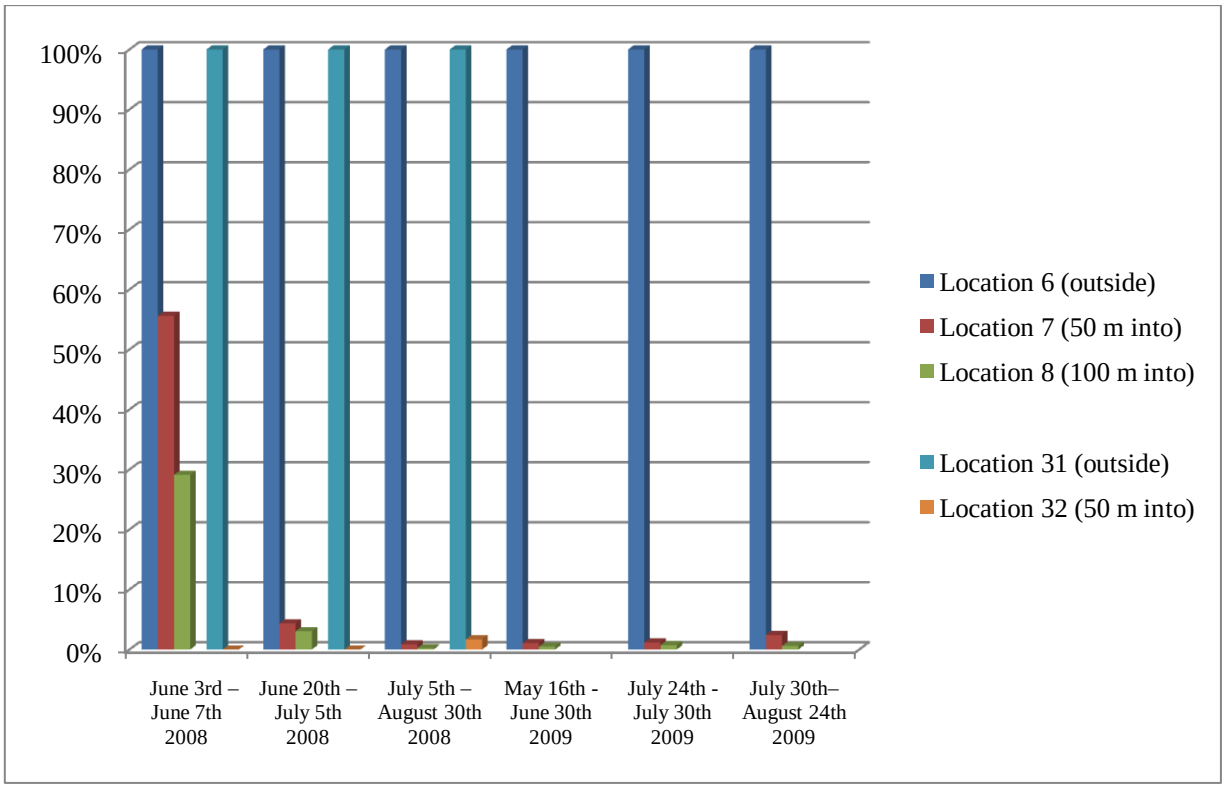

Figure 32. The ratio of calculated mass sand transport between locations outside of and inside reclamation areas.

The proportion of sand transport inside the reclamation areas is low, or <5 %, compared to the sand transport outside reclamation areas, except at locations no 7 and 8 during the first sampling period, 3rd – 7th of June 2008 (Fig. 32). However, in that erosion event, the calculated sand transport outside the reclamation area at location no 6 was low compared to all the other erosion events (Fig. 33), which indicates data noise due to low amount of material. It should, however, be noted that the height curves for the transport within the reclaimed areas may be different from those outside, so the difference outside of and inside reclamation areas shown in Fig. 32 is more an indication of the influence of reclamation efforts than a quantitative estimate.

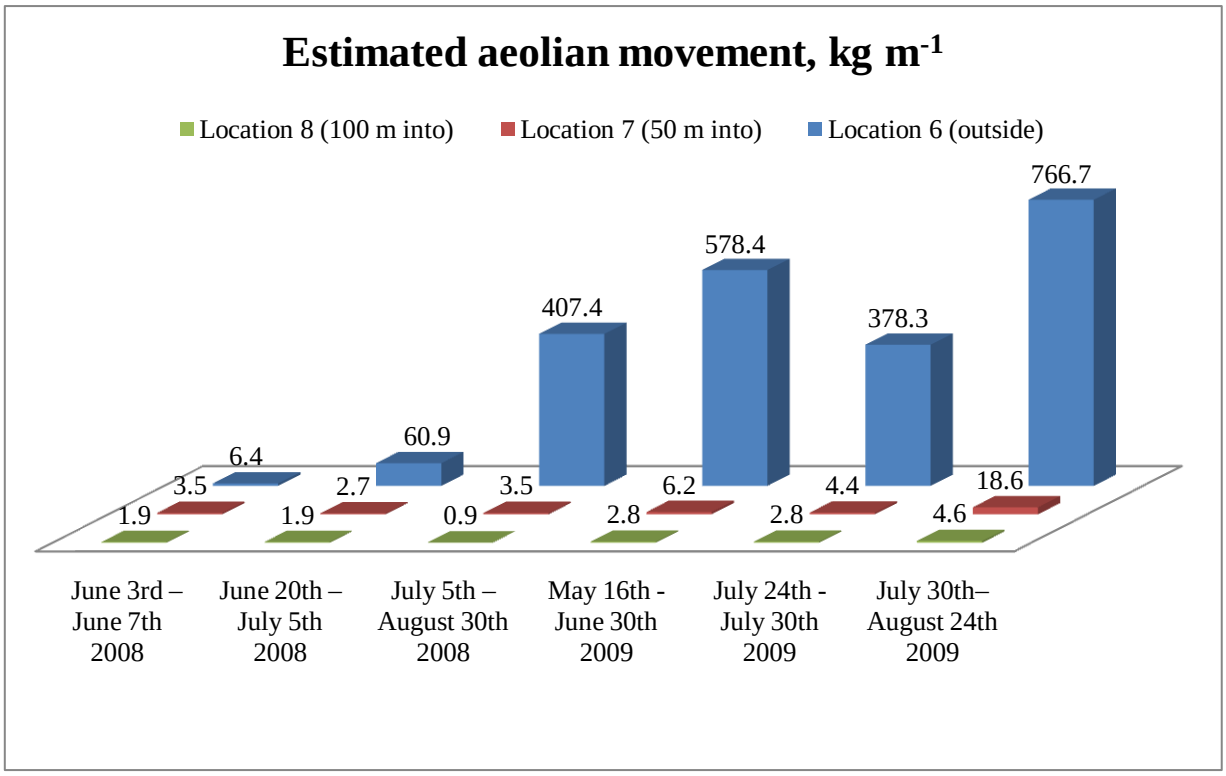

Figure 33. The differences in calculated sand transport outside (location no 6) and inside (locations no 7 and 8) the reclamation areas near Helliskvísl.

To estimate the effect of reclamation efforts on the grain size distribution of the aeolian material, samples collected in dust traps placed outside and inside the reclamation areas were sieved. The samples near Helliskvísl were collected in August 2009 but samples from locations near Búrfell were collected in August 2008. All the samples were taken from dust traps mounted at 30 cm height.

Grain size parameters show that the mean grain size at locations no 6, 7 and 8 was 917, 215 and 140µm respectively and at locations no 31 and 32 it was 3431 and 86µm respectively (Table 6). This result shows that near Búrfell (location no 32) only very fine sand and silt were transported into the reclamation area, but near Helliskvísl (locations no 7 and 8) the grain size carried into the reclamation area ranged from silt to very coarse sand (Fig. 34).

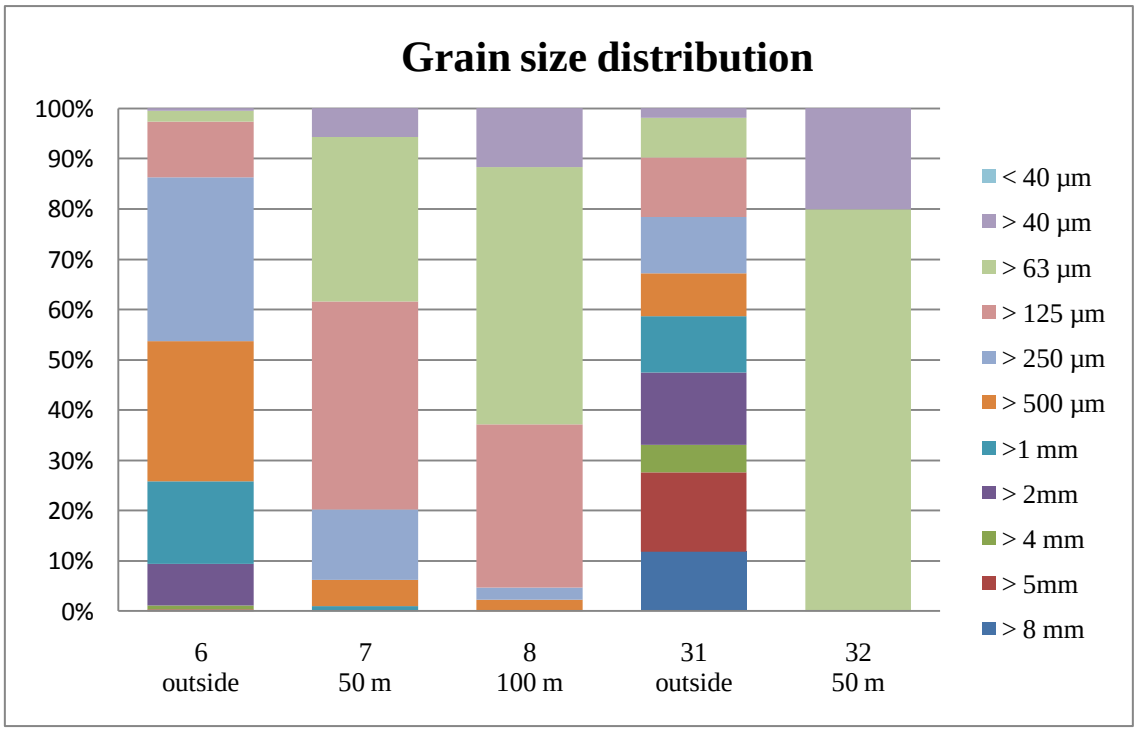

Figure 34. Grain size distribution of samples collected outside (locations no 6 and 31) and inside (locations no 7, 8 and 32) reclamation areas.

4.5 Environmental factors

The research area was mapped in the field and by using remote sensing to gather information on soil erosion, surface roughness, rock outcrop, vegetation cover, loose materials on surface and waterways.

Soil erosion

Most of the research area is classified with very severe or severe erosion, 61% and 27% respectively. Most of the remaining 12% are revegetated areas that still have considerable erosion according to the field estimate (Fig. 35).

There are three erosion forms according to the Icelandic classification scheme (Arnalds et al., 1997) that dominate in the research area: sandy lava (about 72%), sand fields (about 24%) and sandy lag gravel (about 4%).

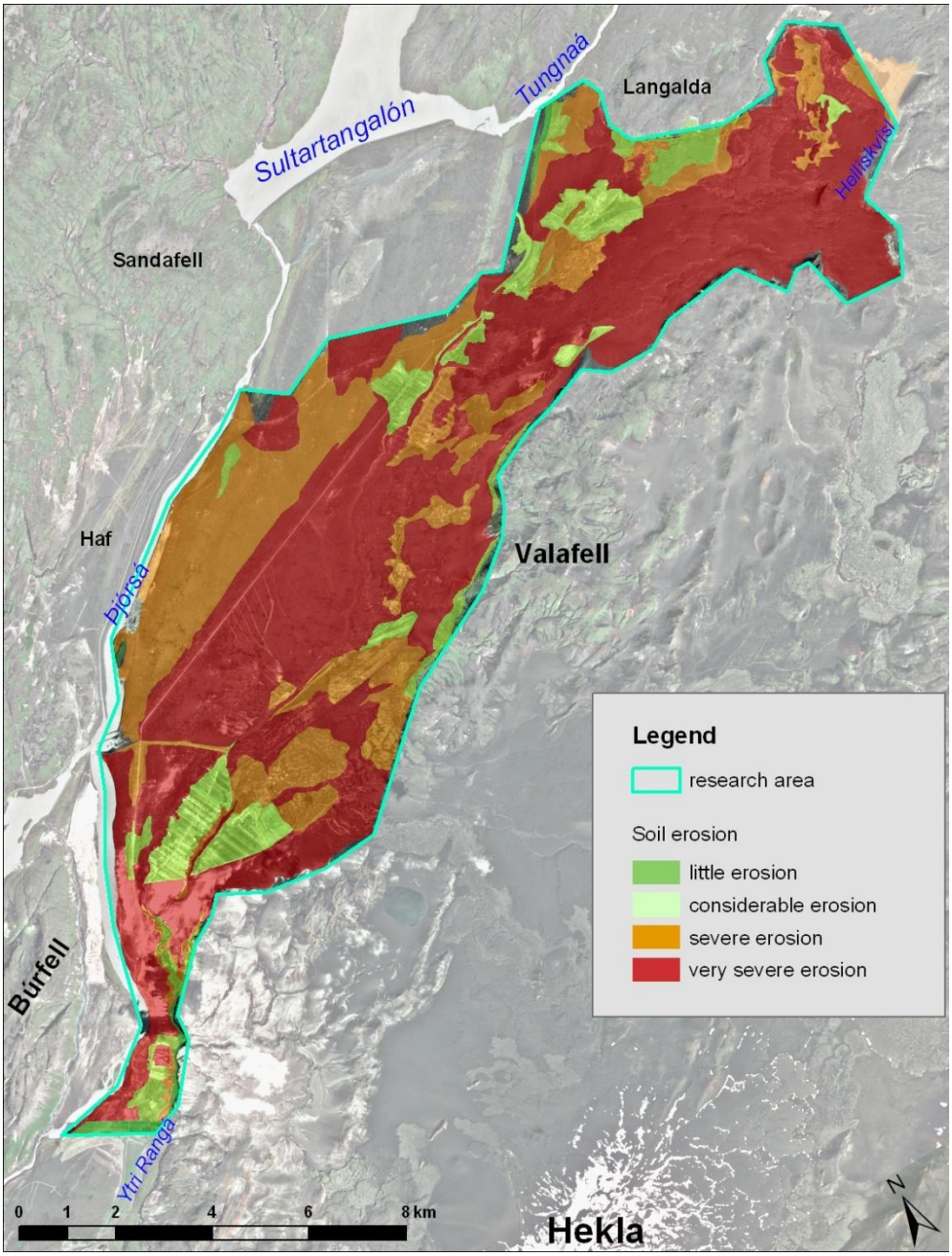

Figure 35. Soil erosion classification of the research area.

Surface roughness

The surface roughness in this research refers to meso-scale surface features such as stones, rocks and lava formations. More than half of the research area is classified as having smooth or rather smooth surface, 22% and 33% respectively. Only 11% of the area has very rough surface with surface features > 150 cm high and the remaining 34% is classified with rough surface (Fig. 36).

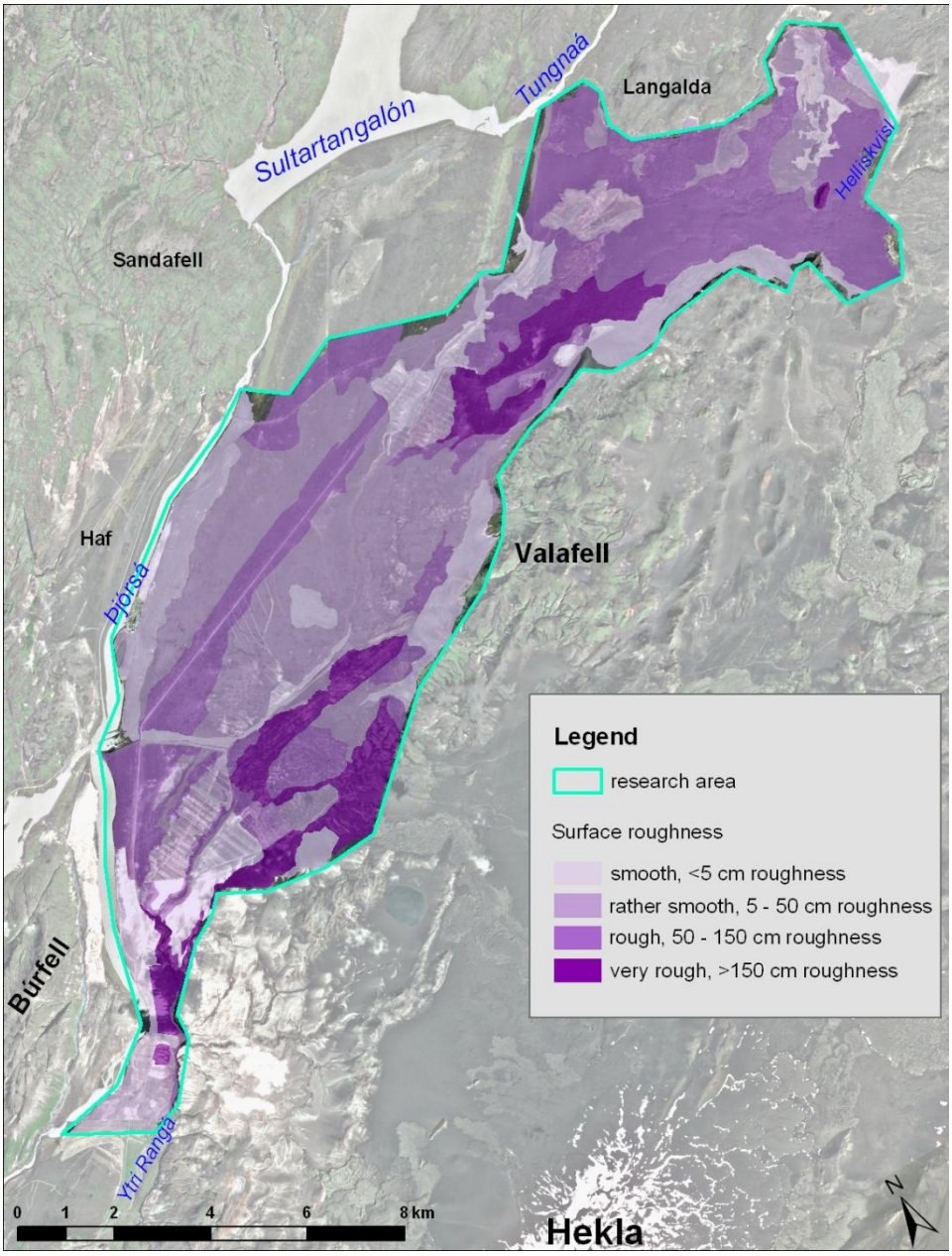

Figure 36. Surface roughness classification of the research area.

Wind profiles where the wind speed was measured at three different heights were also used to estimate the wind effect based on surface roughness. Wind profiles were taken on surfaces classified as smooth, rather smooth, rough and very rough but the result showed that there was no significant difference ($p > 0.05$) between the wind profiles on smooth and rather smooth surfaces. There was also no significant difference ($p > 0.05$) between the wind profiles on rough and very rough surfaces. Smooth and rather smooth proved to be significantly different ($p < 0.01$) from rough and very rough surfaces.

Rock outcrop

Rock outcrop in this research refers to stones >10 cm in diameter. Only 13% of the research area had no rock outcrop. Most of the research area was classified with rock outcrop 1-20% and 21-40% or 42% and 38% respectively. The remaining 7% of the research area had rock outcrop with > 40% cover (Fig. 37).

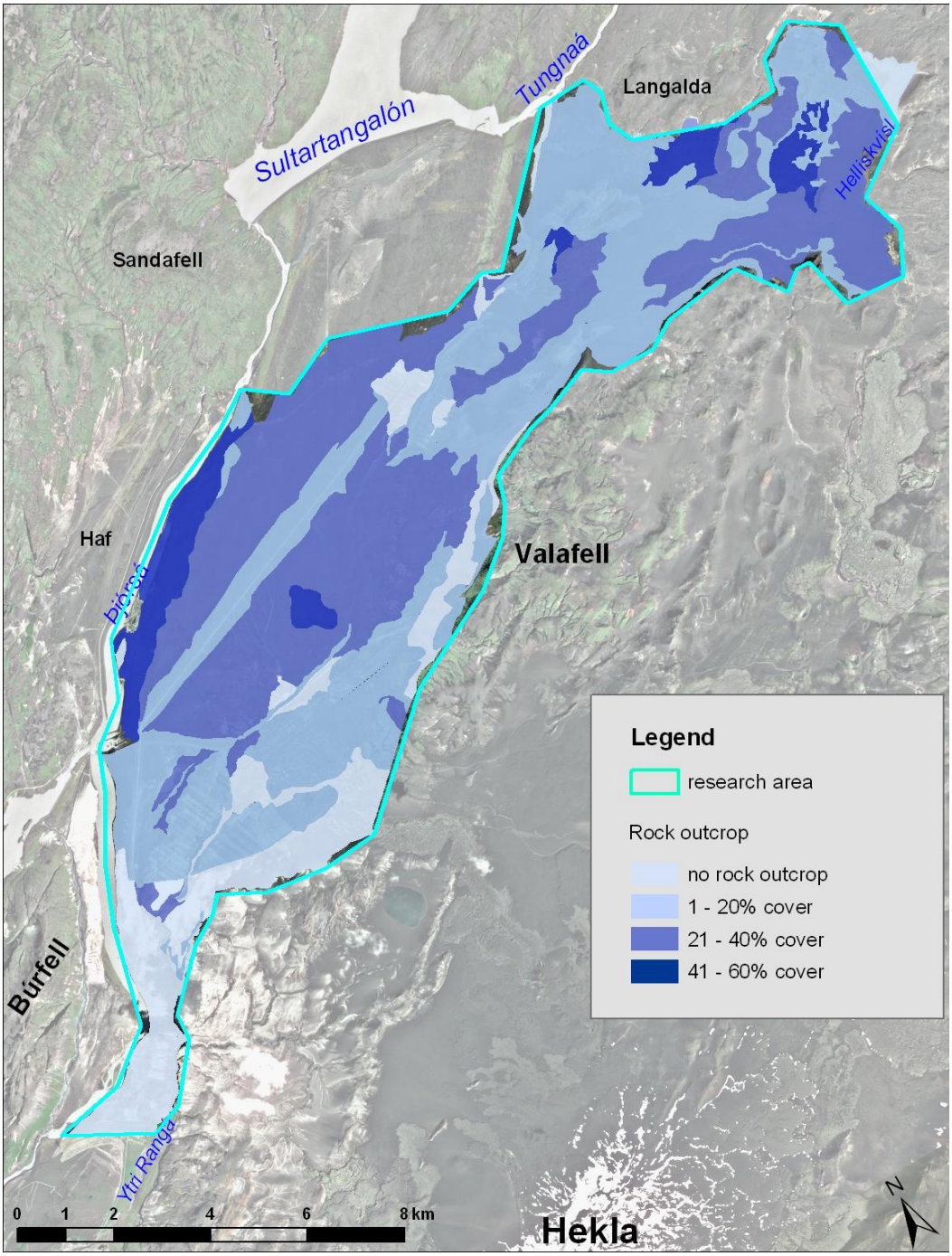

Figure 37. Rock outcrop classification of the research area.

Vegetation cover

Most of the research area is sparsely vegetated with 69% of the area with < 20% vegetation cover. The sparsely vegetated areas were divided further into classes with 0-5%, 6-10%, 11-15% and 16-20% cover and these classes covered 34%, 25%, 7% and 3%, respectively, of the research area. Approximately13% of the research area had 21- 40% vegetation cover and 9% of the whole area had 41- 60% vegetation cover. Densely vegetated areas with > 80% cover were only 9% of the research area (Fig. 38).

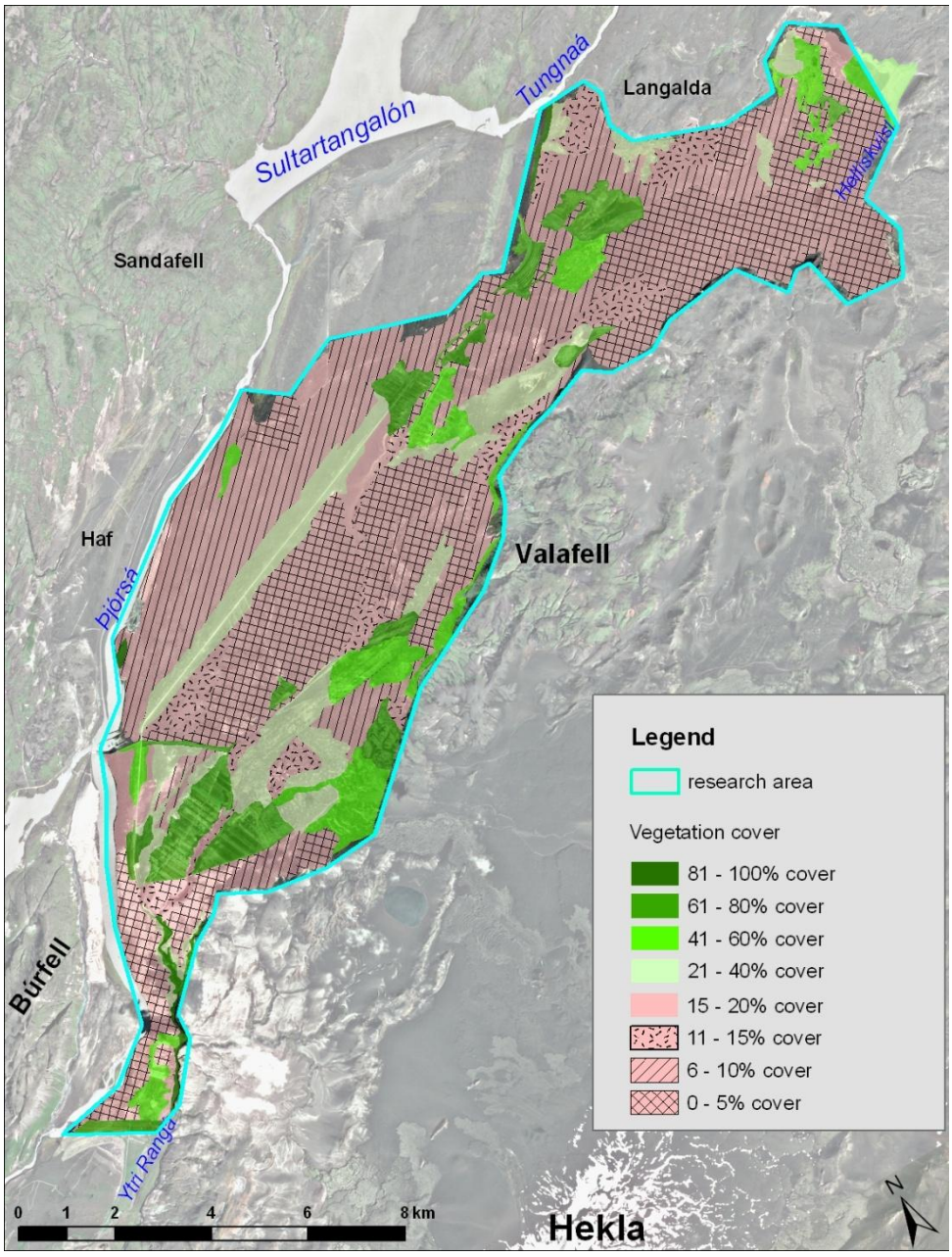

Figure 38. Vegetation cover classification of the research area.

Loose materials on the surface

Part of the field mapping was to estimate the amount of loose materials on the surface that can be transported with aeolian processes, especially sand and pumice. Most of the research area, except the reclamation areas, had > 40% of the surface covered with loose materials and 17% had > 80% cover of loose materials (Fig 39).

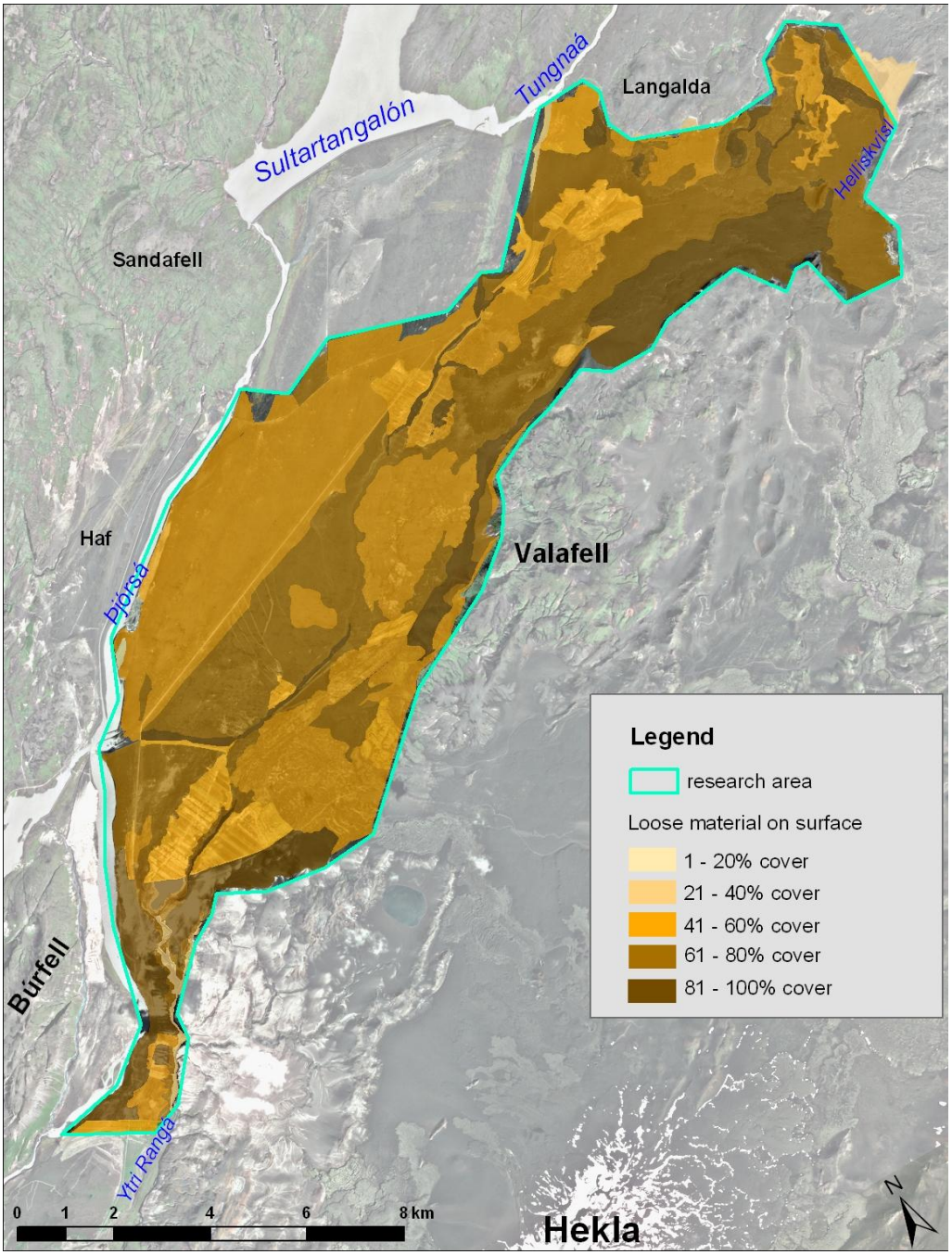

Figure 39. Loose materials on the surface (sand and pumice), that can be transported by aeolian processes.

Water erosion

All waterways within the research area are active only during short periods (winter thaw etc.) but are otherwise dry. All well defined waterways were mapped as well as two floodplains that are both at the foothills of Valafell (Fig. 40).

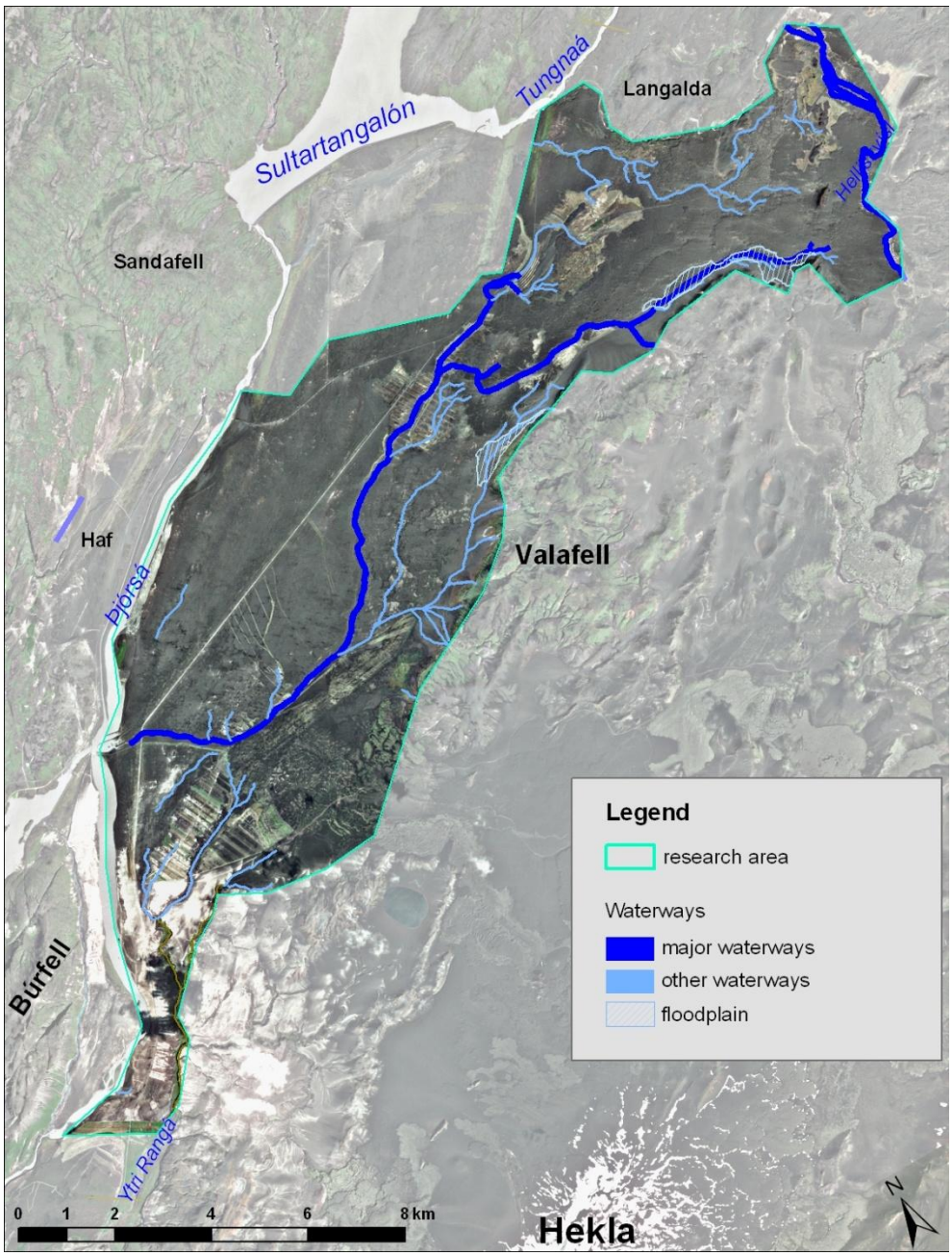

Figure 40. Rivers, floodplains and waterways in the research area.

There is one major waterway that is most prominent in the research area and it´s length is about 27 km. Part of it is well defined as hay bales have been used to steer the water flow into

confined channels. Many other waterways were mapped and most of them are formed where runoff water gathers into flow channels in the sandy lava fields on frozen ground and also at the foothills of Valafell. The total length of these other waterways is about 74 km, giving waterways a total of 101 km.

Grain size distribution and sorting of grains

Based on the grain size distribution and other grain size parameters, the research area was divided into three sections (Fig. 26). There is a considerable difference in sand transport between locations within the south-western part of the research area, depending on the amount of pumice on surface. The locations in areas closest to Hekla, within a 12 km radius from the mountain, have the highest proportion of coarse grains, with the mean grain size > 3000 µm and they are also very poorly or poorly sorted with σ >2600 (Table 6). The sorting of grains at these locations is not normalized (Fig. 41) and the uneven distribution can reduce the erodibility as a high proportion of coarse grains can form a resistant layer (Gillette and Stockton, 1989).

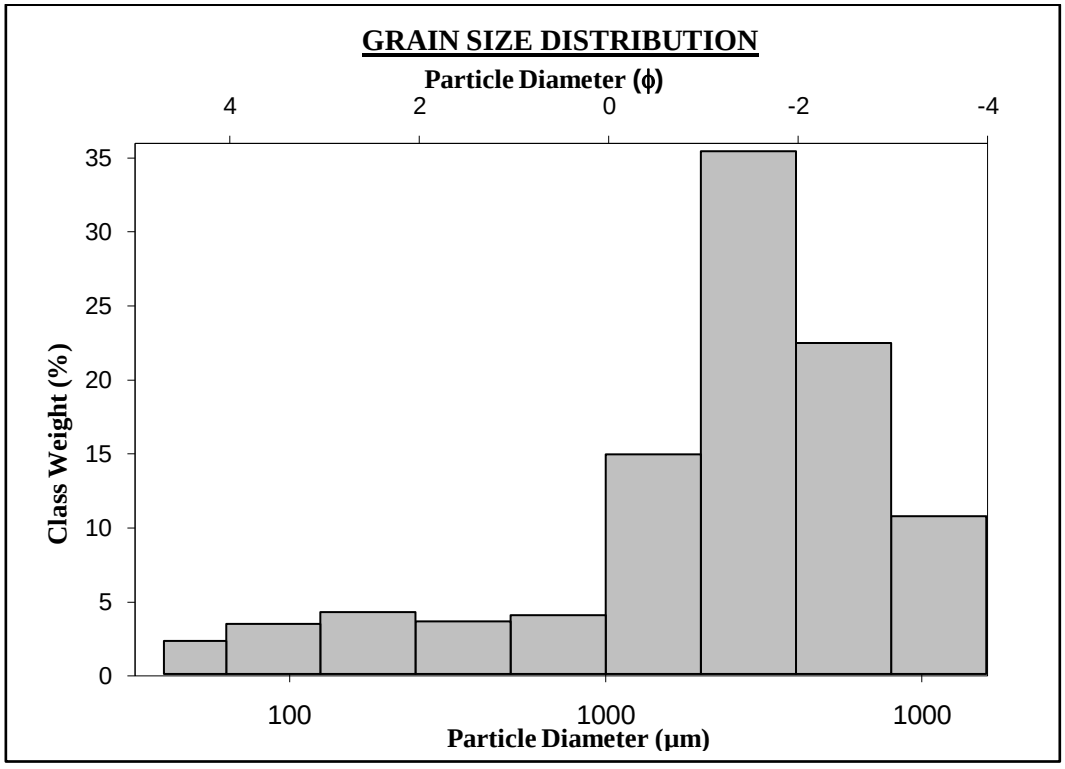

Figure 41. Frequency plot of grains size distribution from a sample collected in dust trap at location no 29 which is in the south-western section and within a 12 km radius from Hekla.

The other locations within the south-western section which are further away from Hekla have much lower proportion of coarse grains with the mean grain size ranging from 796-1593 µm. They are also poorly sorted with σ ranging from ~1250-2000 and the distribution in grain size in these locations is closer to normal distribution (Fig. 42).

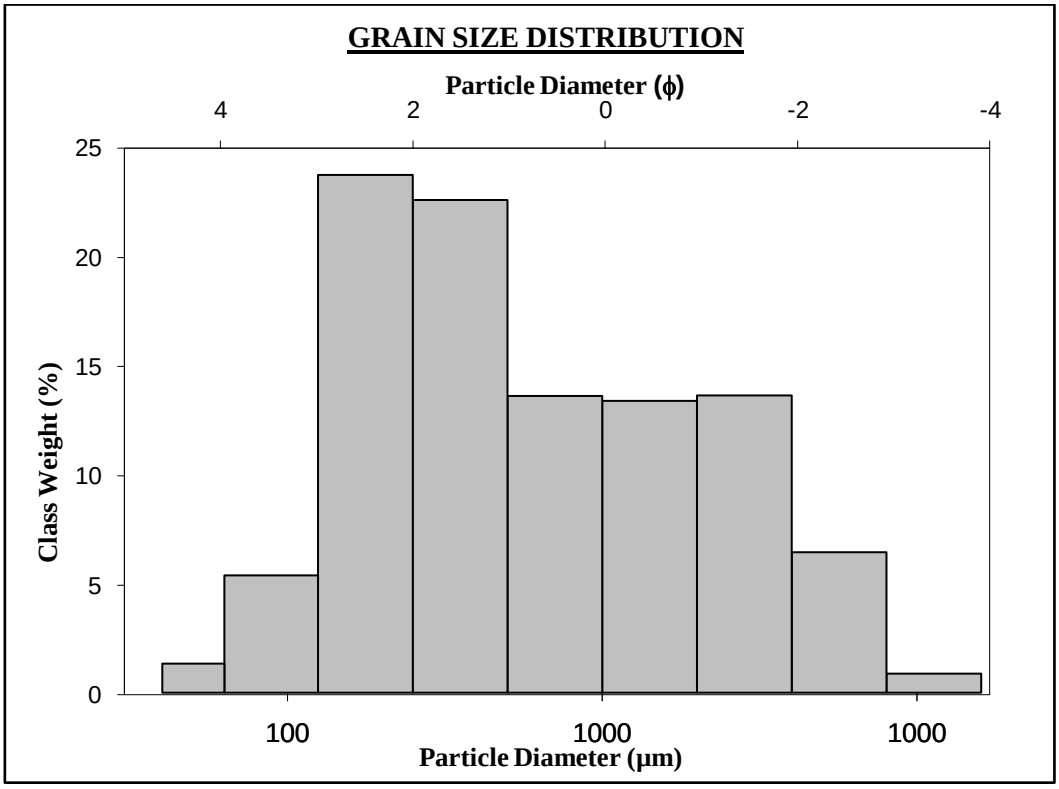

Figure 42. Frequency plot of grains size distribution from a sample collected in dust trap at location no 26 which is in the south-western section but outside the 12 km radius from Hekla.

In the sandy areas in the north-eastern part and near Helliskvísl, both the grain size and the sorting has a value of <1000. The grain size distribution of samples collected in dust traps in the north-eastern part is close to normal distribution (Fig. 43).

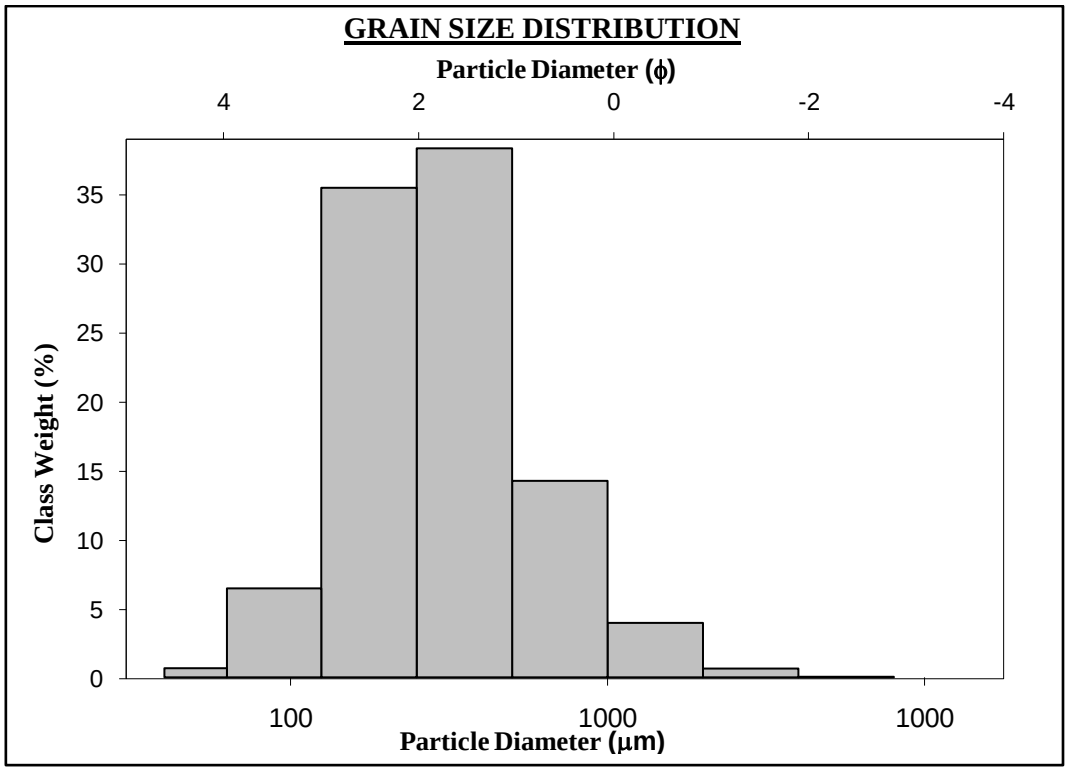

Figure 43. Frequency plot of grain size distribution from a sample collected in dust trap at location no 11 which is in the north-eastern part of the research area.

4.6 Image classification and spatial analysis

Image classification

A SPOT5 image taken in August 2009 was classified with supervised classification. Eighteen classes or areas were used as a base for the classification. Each class was chosen based on pixel values in the SPOT image which represent a certain surface type (Fig. 44).

First, the representative areas for the most distinctive features or pixel values like vegetated areas and white pumice fields were chosen. For other less distinctive classes the representative areas were also chosen based on factors known from the field mapping such as lava fields and areas sparsely vegetated with Lyme grass.

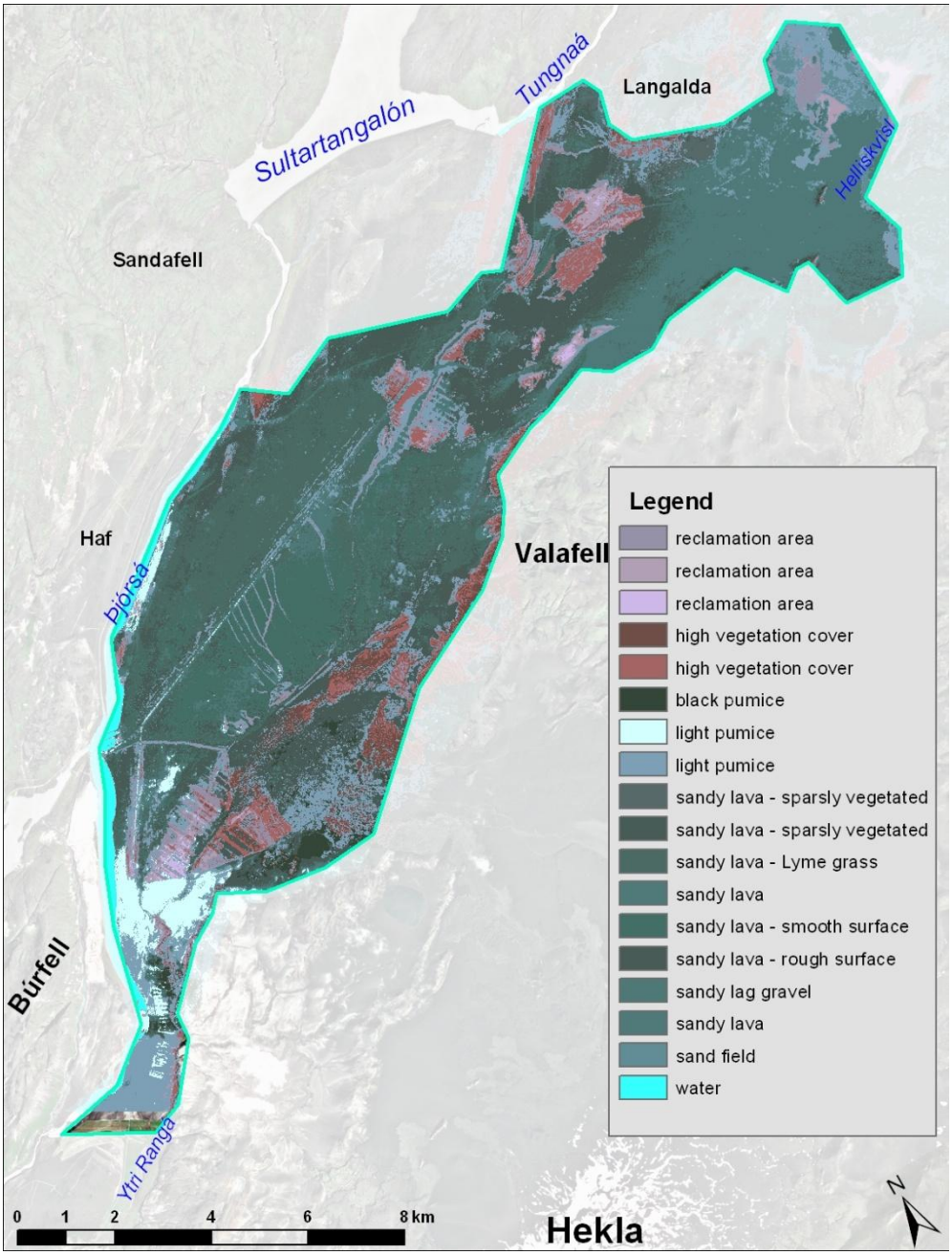

Figure 44. A supervised classification of a SPOT image from 2009.

To simplify the classified image, classes were grouped together based on their susceptibility to erosion and given value accordingly from 1-6, where 1 represents the lowest susceptibility and 6 the highest. The grouping was the following: 1) All the vegetated areas including reclamation areas. 2) Areas with black or light pumice. 3) Lava fields with very rough surface and lava fields with sparse vegetation (often 10-15% cover). 4) Lava fields sparsely vegetated with Lyme grass (often 5-10% cover). 5) Lava field with smooth surface, but a high

percentage of rock outcrop (often 20-40%). 6) Sand fields, sandy lag gravel and sandy lava, all with very sparse vegetation and a high percentage of loose material on surface. These simplified classes are shown in Fig. 45. To link the classification to aeolian transport in the research area, the calculated transport in the most intensive erosion event at each location is also shown in Fig. 45.

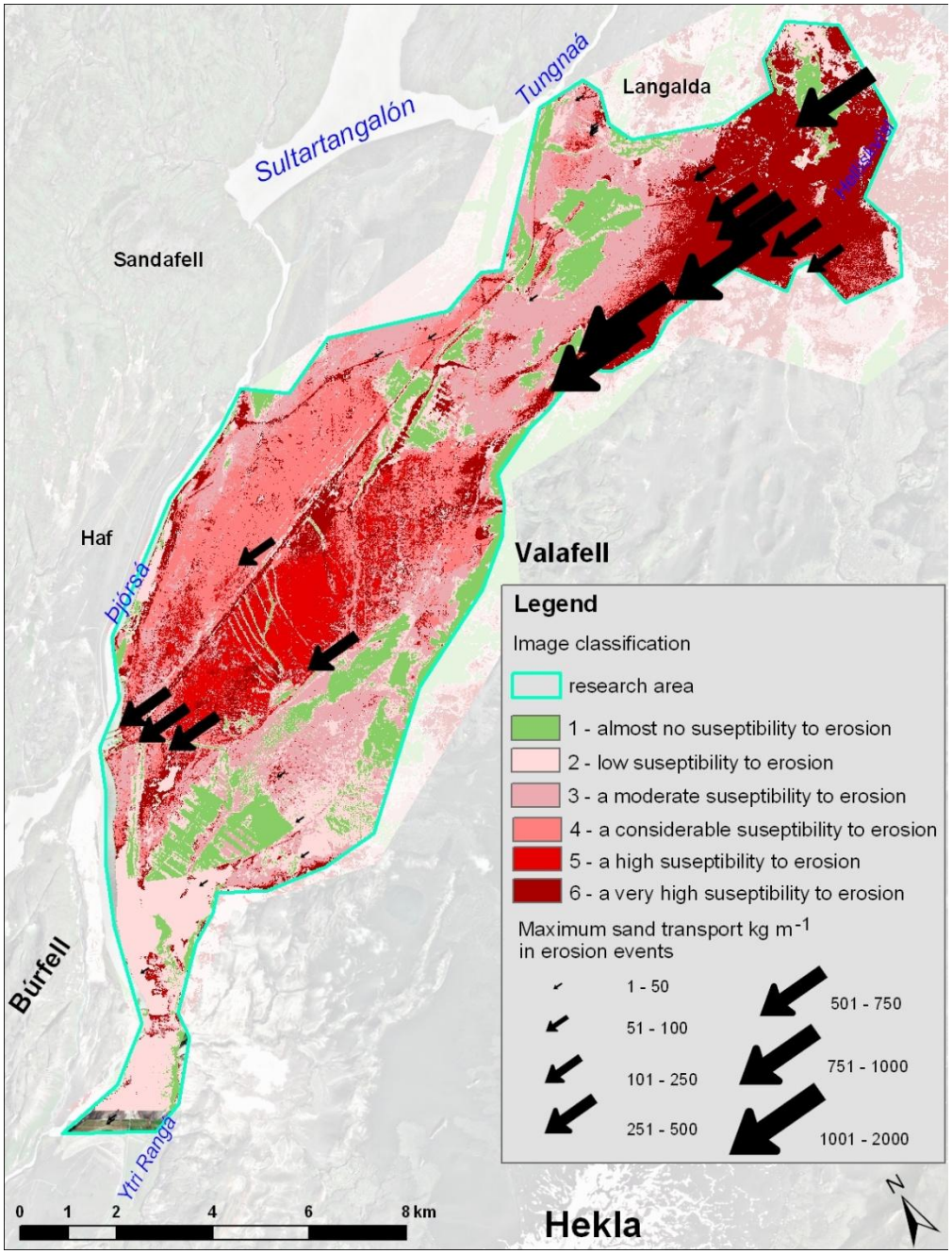

Figure 45. A supervised classification of a SPOT image of the research area, simplified based on estimated susceptibility to erosion. The calculated aeolian transport in the most intensive erosion event is shown with arrows.

Spatial analysis

Spatial analysis was used to estimate the effect of environmental factors. That was done by creating a model, based on surface characteristics, which would identify areas with high susceptibility to erosion. Each data layer (Figs. 35-40) was rasterized and reclassified based on attribute values, given in the field mapping e.g. erosion severity and vegetation cover (see Appendix 2). In the reclassification each cell was given a value from 1 to 7, reflecting susceptibility to aeolian transport. The highest values were given where there is little or no hindrance to sand movement, e.g. very severe soil erosion and high quantity of loose material on surface. The lowest values were given where there are considerable effects that decrease sand movement, e.g. high percentage of vegetation cover and rock outcrop (Table 11).

Table 11. Cell values for reclassified data layers based on attributes from field mapping

	New cell values based on layer attributes						
Raster layer	**7**	**6**	**5**	**4**	**3**	**2**	**1**
Vegetation cover (%)	0-5 %	6-10%	11-20 %	21-40 %	*	41-60 %	> 60%
Rock outcrop (%)	*	0%	*	1-20 %	21-40 %	41-60 %	> 60%
Soil erosion	very severe	*	severe	*	considerable	*	ittle or slight
Loose material (%)	81-100%	61-80%	*	41-60%	*	21-40%	<20%
Surface roughness	*	*	oth/rather smo	*	ough/very rougl	*	*
Grain size distribution	sand	*	mostly sand	*	*	*	pumice
Major dry waterways (m)	0-200	*	200-300	*	*	300-500	*
Other dry waterways (m)	*	*	0-100	100-200	*	200-300	300-500

* cell values not used

Based on the wind profiles, the surface roughness was divided into only two classes, instead of four as in the field mapping, because there was no significant difference ($p > 0.05$) between smooth and rather smooth surfaces and also there was no significant difference ($p > 0.05$) between the wind profiles on rough and very rough surfaces. Dry waterways were drawn as lines and not polygons as the other data layers. To estimate the effect of water erosion, a 500 m wide buffer zone was created around the waterways and given different values based on the distance from the waterway and its size.

All the reclassified data layers were then combined using the *Raster Calculator*, to estimate the highest probability of intense wind erosion within the research area (Fig. 46). The equation used was *probability = (vegetation cover) + (rock outcrop) + (soil erosion) + (loose materials) + (surface roughness) + (grain size) + (major waterways) + (other waterways)*.

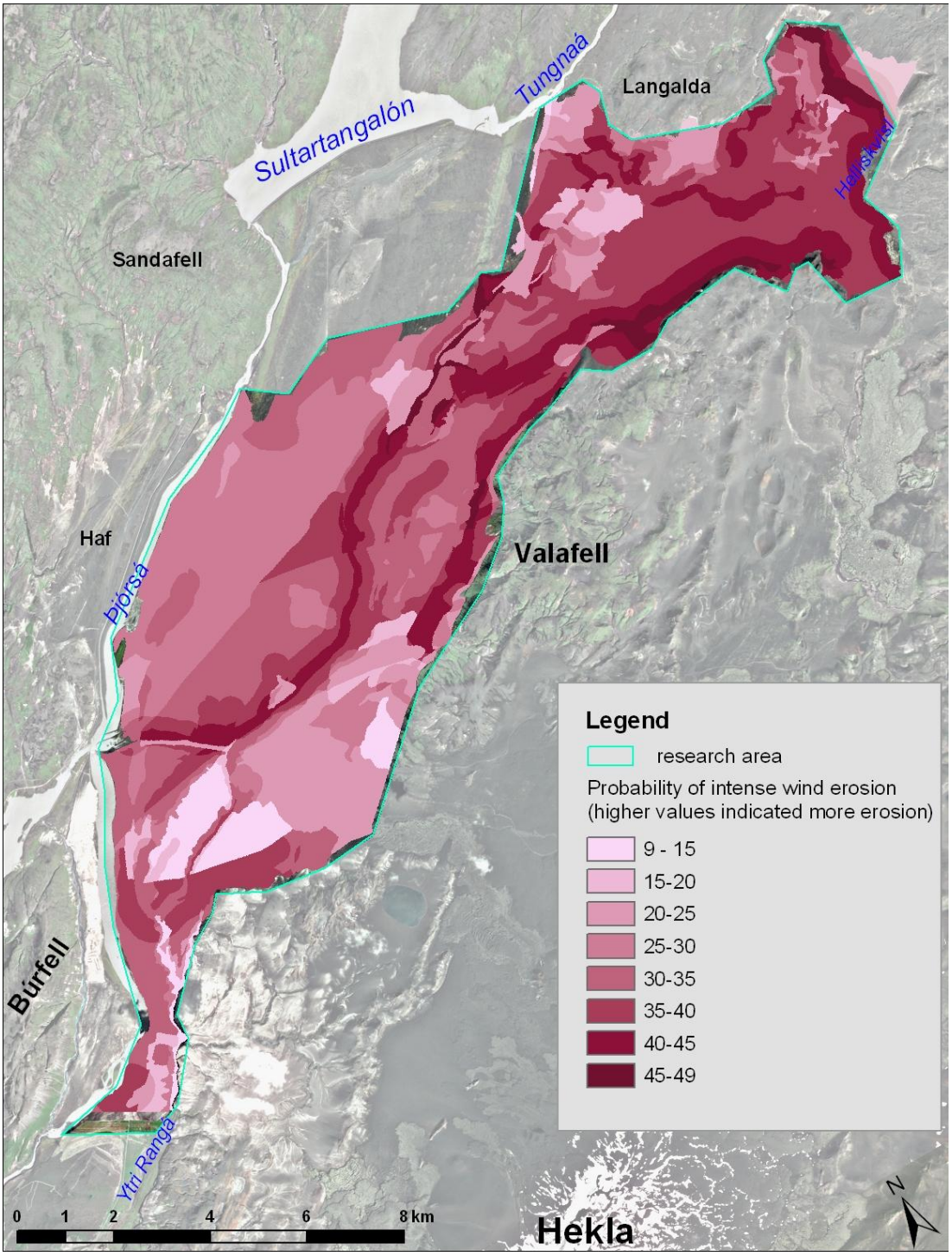

Figure 46. Probability of intense wind erosion within the research area. Calculations based on spatial analysis from the field data, where the highest values indicate the calculated highest intensity of sand transport.

The results from the spatial analysis were compared to the calculated wind erosion, based on field measurements with dust traps. The spatial distribution of probable intensity of wind

erosion and the measured sand transport in the most intensive erosion event at each location is shown in Fig. 47.

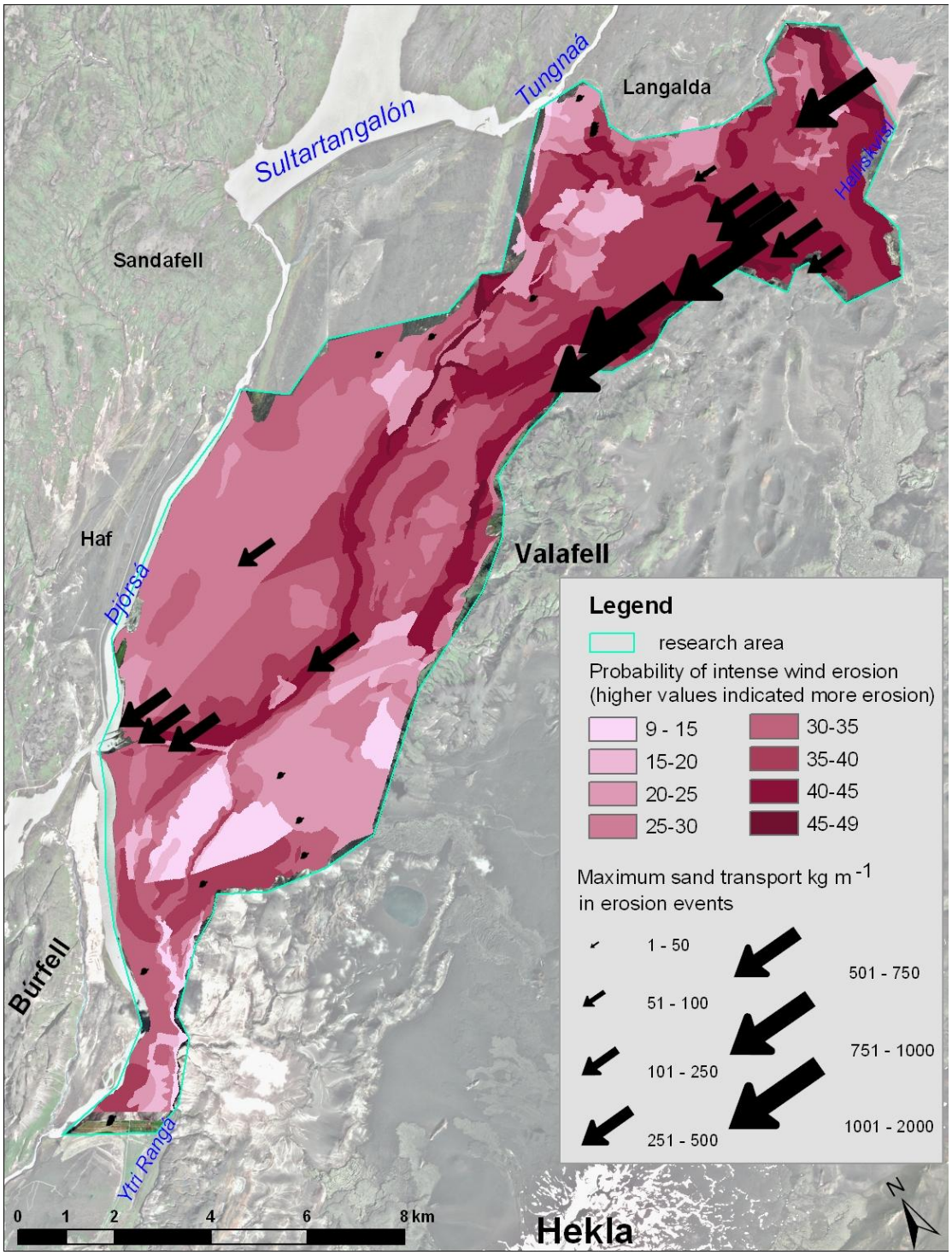

Figure 47. The probable intensity of wind erosion within the research area and the calculated maximum sand transport in the most intensive erosion event. The maximum sand transport is shown with arrows.

Principal component analysis was used to further analyse this relationship of maximum sand transport and the different surface characteristics used in the spatial analysis (Fig 48).

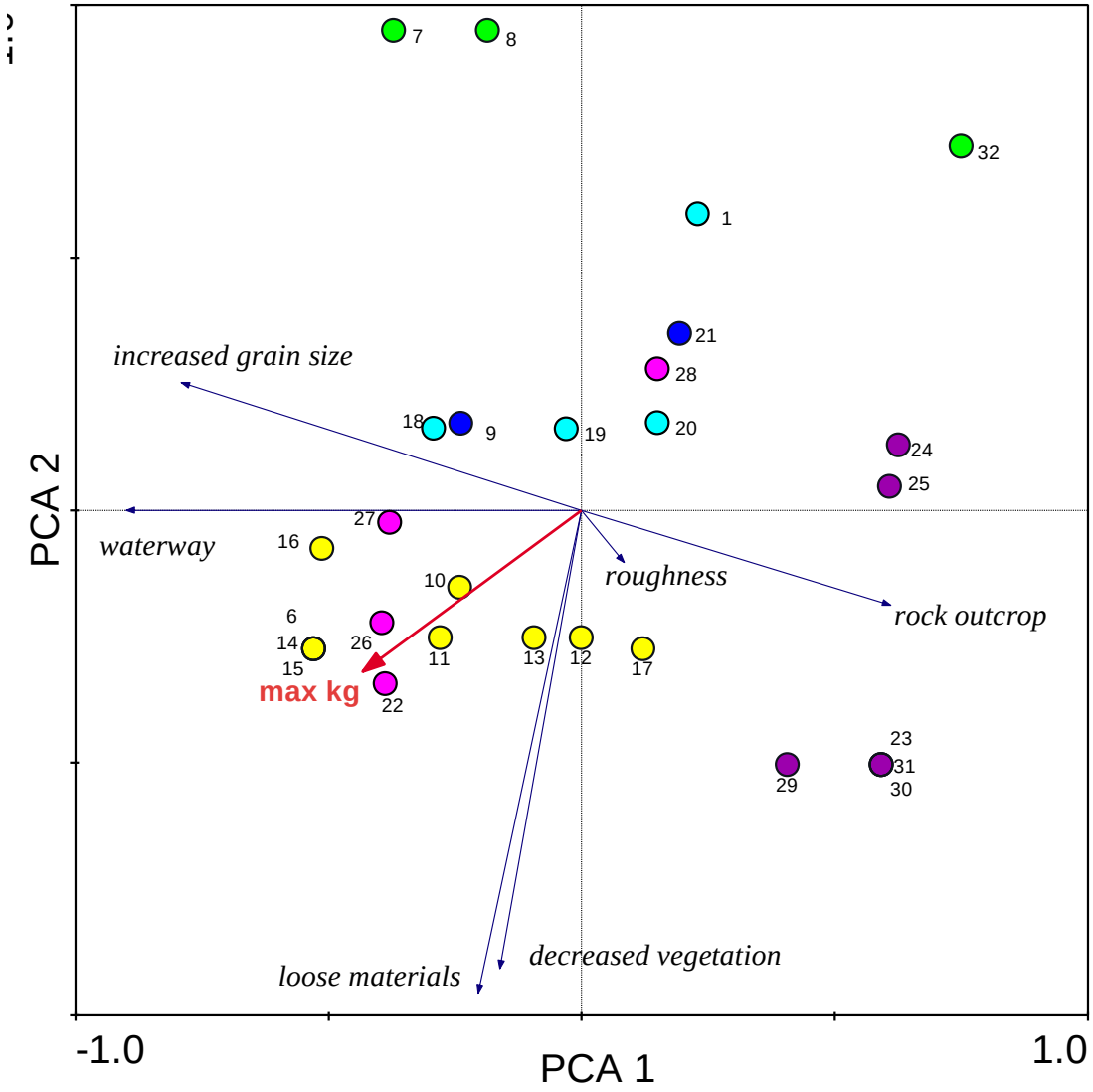

Figure 48. Principal component analysis of surface characteristics used in the spatial analysis.

The principal component analysis showed that the eigenvalues for the first and second principal components are 0.42 and 0.30 respectively and the correlation with the sand transport is 0.59 for the first principal component and 0.54 for the second principal component. The amount of loose sandy materials on surface and reduced vegetation cover appear to effect wind erosion the most, but the effect of grain size (more erosion with reduced grain size) and other surface characteristics are also important factors.

To further analyse the connection between the calculated maximum wind erosion based on dust traps measurements, the probability of wind erosion based on spatial analysis and the estimated susceptibility to erosion based on image classification the calculated values are shown in Table 12. Locations no 2, 3, 4 and 5 are excluded as reclamation work was done there after the field mapping in the area.

Table 12. Calculated maximum wind erosion based on dust trap measurements, probable intensity of wind erosion based on spatial analysis and classification value based on image classification. Locations no 2-5 are excluded.

Location	Maximum wind erosion, kg m^{-1}	Probable intensity of wind erosion	Classification value **&**
1	4	23	4
6	767	46	6
7	19	24	1
8	5	24	1
9	98	32	6
10	360	41	6
11	647	42	6
12	549	39	6
13	302	40	6
14	156	46	6
15	1353	46	6
16	1491	44	6
17	1788	39	6
18	8	37	3
19	4	31	3
20	6	31	3
21	111	30	4
22	304	44	5
23	36	35	2
24	1	22	2
25	9	23	3
26	429	41	5
27	392	39	4
28	416	33	4
29	41	37	2
30	24	35	2
31	46	35	2
32	1	11	1

Highest values in each column are highlighted

& simplified classification values based on estimated susceptibility to erosion (Fig. 45)

The logarithm (log10) of maximum wind erosion was used to calculate a linear regression between: a) maximum wind erosion and probable intensity of wind erosion and b) maximum wind erosion and classification values. It showed that there is a stronger correlation between

wind erosion and probable intensity than between maximum wind erosion and classification values, with r^2 as 0.70 and 0.65 respectively.

To see if more reliable estimates of the probability off intense wind erosion within the research area could be gained, further analysis on the field mapping attributes was done. The method used was to multiply all the reclassified data layers from the field mapping and thereby enhancing the effect of each extreme factor. This calculation method resulted in much weaker correlation between maximum wind erosion and probable intensity with r^2 as only 0.30 and will therefore not be used.

5. Discussion

Wind erosion has been investigated for decades but measurements in the field have proven to be difficult (e.g. Stout, 1998; Zobeck et al., 2003). Variations are associated with the frequency and magnitude of single storms (Morgan, 1986) and many field studies have shown that due to meteorological factors and surface conditions, both temporal and spatial variations in sand flux are often found within a field (e.g. Stout and Zobeck, 1996; Visser et al., 2004). Inadequate sampling frequency in space and time, often caused by shortage of resources, results in lack of knowledge of the spatial and temporal variation of the magnitude of material transported by aeolian activity (Chappell et al., 2003). The problem of extrapolating data from small plots to higher scales is also one of the difficulties associated with the determination of erosion (Stroosnijder, 2005). All these factors can affect the results in wind erosion studies and have to be taken into consideration when the results are interpreted.

In this research, attempts were made to overcome some of these problems. With about 20 000 km^2 of sandy surfaces in Iceland, some with intense erosion affecting river systems and other aquatic systems as well as producing dust plumes, it is important to be able to estimate erosion in large areas. In this research new methods were used for measuring erosion simultaneously on a landscape scale and to predict erodibility based on environmental factors. These results add valuable information to our knowledge and understanding on erodibility of sandy surfaces and on wind erosion in Iceland.

5.1 Aeolian sand transport

The aim of this research was to gather information on aeolian transport on a landscape scale and to acquire knowledge about the effect that environmental factors have on sand movement. The results presented here are one of the first results reported for landscape scale measurements of sand transport in Iceland. They show that there is considerable spatial variation in sand transport within the research area (Fig. 28). At some of the locations where sand movement was measured it proved to be negligible, but in other locations the aeolian transport was very active. The sand transported each year ranged from <1 kg m^{-1} to 2981 kg m^{-1} at locations within the research area. When locations within reclamation areas and other locations with < 50 kg m^{-1} in any erosion event are excluded, the measured transport ranged

from about 110 kg m^{-1} to almost 3000 kg m^{-1} per year. At some of the most active aeolian transport sites within the research area the mass sand transport was >1 t m^{-1} per summer and at location no 17 it was almost 3 t m^{-1} in the summer 2008 (Table 7).

The aeolian transport at the more active sites within the research area seem to be of the same order of magnitude as found in other research in Iceland (e.g. Sigurjónsson et al. 1999; Gísladóttir, 2000; Arnalds et al., 2001; Sigurjónsson, 2002; Arnalds and Gísladóttir, 2009; Arnalds, 2010). Erosion events differ in both, intensiveness and length, as well as in other meteorological conditions and individual storms are therefore difficult to compare. In the research area the most intensive erosion was about 150 kg m^{-1} hr^{-1} compared to about 200 kg m^{-1} hr^{-1} in Hólsfjöll (Arnalds and Gísladóttir, 2009).

Regression equations can be used to calculate possible sand transport with variable climatic variables. The weather stations and Sensit sensors were placed at locations no 11 and 21 and are therefore used for regression calculations. Figure 31 shows the calculated mass sand flux based on erosion events where r^2 between sand transport and 10 min average wind speed was > 0.5. The relationship was calculated for wind speed up to 18 m s^{-1}. Two of the curves showed very high sand flux values or 5000-6000 kg m^{-1} hr^{-1}. These curves indicate more intensive wind erosion than other research in Iceland has shown, for example Kjaran et al. (2006) calculated 10-42 years recurrence of saltation in the magnitude 5000-6000 kg m^{-1} day^{-1} for much higher wind speed than 18 m s^{-1}. No actual measurements have been done in Iceland at similar weather conditions (average 10 min wind speed at 18 m s^{-1}) but the fact that they are so much higher than the other sand flux values indicates that these curves might not give realistic values. The others curves showed from 100 to 900 kg m^{-1} h^{-1} (Fig. 49).

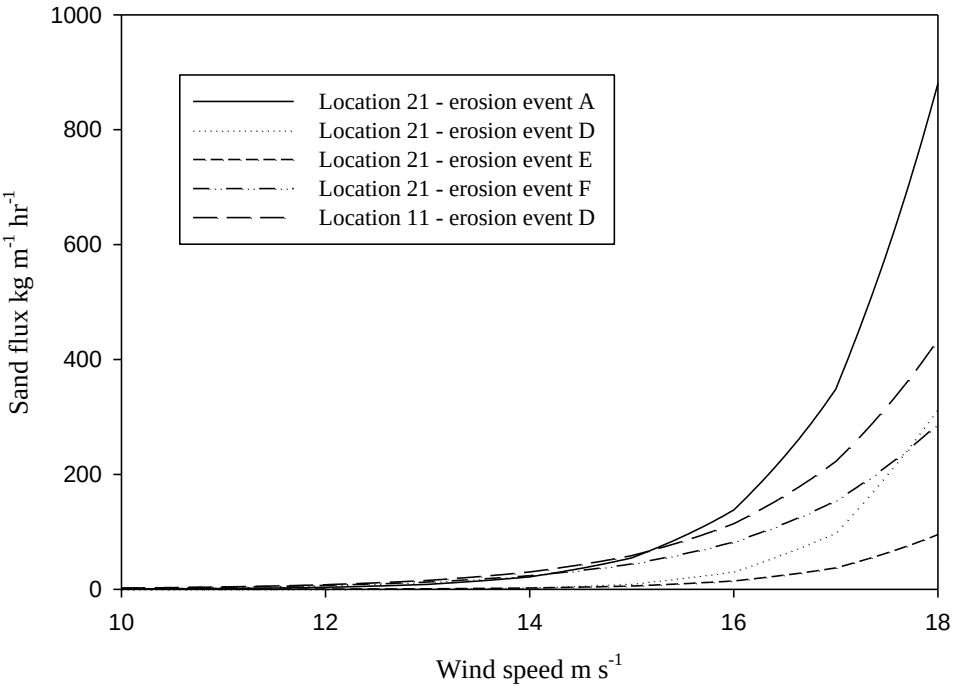

Figure 49. Calculated sand flux (kg m^{-1} h^{-1}) with nonlinear regression equations, based on data from 5 locations, using 10 min mean wind speed, up to 18 m s^{-1}.

By assuming that the average storm length is 5-10 hours these curves, excluding the curve for storm event A, show similar values to other areas in Iceland were aeolian transport has been measured (Arnalds, 2010).

However, locations no 11 and 21 which were used for the regression calculations in Fig. 49 do not have the most intensive erosion events within the research area. Therefore it can be assumed that at the locations with the most intense wind erosion, the aeolian transport can be considerably more than the calculated sand flux shown in Figure 49.

Interaction between aeolian and fluvial processes

The interactions between aeolian and fluvial processes appear to be quite effective in the research area but no measurements were made on the water erosion except the mapping of dry waterways and floodplains. Visser and Sterk (2001) argued that wind and water erosion should be studied simultaneously in semi-arid zones, where the two processes contribute about equally to soil degradation. The results from this research support this theory because when the distribution of dry waterways is compared to the measured sand transport, it appears to be obvious that sediment from the fluvial processes act as an active source for aeolian processes

and vice versa. There were seven dust trap locations in close vicinity, or less than 250 m, of the major waterways (locations no 6, 13, 15, 16, 22, 26 and 27). Some of these locations have the most intense erosion events and all these locations had calculated wind erosion >300 kg m^{-1} during the most intensive erosion event. There were six locations, no 9, 10, 11, 14, 18 and 29, within 250 m from the other waterways. Location no 18 is placed on top of a thick lava field, above the waterway and is therefore not affected by sediment from the waterway. Location no 29 is in a pumice field where large grain size reduces the erosion intensity. The other locations have the maximum wind erosion ranging from 98 to 647 kg m^{-1}. Only four locations (12, 17, 21 and 29) with intense erosion events (> 50 kg m^{-1}) are not located in the vicinity of a waterway. These results indicate that the waterways are an active source of material. When the total length of waterways within the research area, about 100 km, is taken into consideration it can be assumed that they transport considerable quantities of material both into the research area and between areas from the north-eastern part to the south-western part, and into the Þjórsá river.

Active sediment sources maintain the sand movement but if no new material is added to the area, the surface generally tends to become more stable as erodible components are preferentially removed and the availability of erodible source material becomes limiting (Rose, 1998; Shao et al., 1993). This is in accordance with little wind erosion in locations no 1, 18, 19 and 20 in the north-western part which is always < 10 kg m^{-1}. There are no obvious active sources near those locations but factors like soil erosion and vegetation cover indicate some erodibility. The most intensive mass sand transport in the research area appears to be where there are active sources that transport new material into the area. The Helliskvísl river transports for example new material into the north-eastern part but these active sources are not only fluvial because new material is also transported into the research area by aeolian processes. This conclusion is based on data from the national soil erosion survey of Iceland (Arnalds et al., 1997) which shows severe erosion in adjacent areas northeast of the research area. Eroding material from these areas is likely carried by prevailing wind into the research area. This and the Helliskvísl river can partly explain why the most intensive wind erosion is in the north-eastern part of the research area. However the intensity of aeolian transport decreases considerably from the north-eastern part to the south-western part (Fig 28). Therefore my conclusion is that the aeolian sediment fed by the active sediment sources in the

north-eastern part is partly transported by fluvial processes further into the research area and into the river Þjórsá.

Aeolian sediment transport is commonly influenced by factors such as topography which can cause an increase or decrease in transport potential, and these variations in the intensity of processes result in aeolian and fluvial events having different magnitude-frequency characteristics (Bullard and Livingstone, 2002). Analysis based on topography was not part of this research mostly because only 20 m contour lines were available for the area which is not detailed enough where abrupt vertical differences occur in otherwise a fairly flat area as the research area is.

Effect of environmental factors

Spatial variations can be caused by many factors. The spatial difference in sand transport can in large part be explained by the surface characteristics such as grains size distribution, soil erosion, fluvial processes, surface roughness, vegetation cover and rock outcrop (Fig. 47).

To interpret the results and for establishing a relationship between mass transport and environmental factors, the dust traps locations were grouped by the most dominant spatial and/or environmental factors.

a) Land reclamation greatly reduces aeolian sediment transport. Locations no 3, 4, 5, 7, 8 and 32 are all within reclamation areas. The vegetation has the most affect on the wind erosion, resulting in mass sand transport in any erosion event <20 kg m^{-1}. At location no 2 Lyme grass was seeded around the dust traps in June 2008 so except for the first two storm events, location no 2 can be grouped with other locations affected by reclamation work.
b) The coarse pumice close to Hekla is less susceptible to aeolian transport than the finer volcanic materials. Locations no 23, 24, 25, 29, 30 and 31 are closest to Hekla, all being within 12 km radius from the volcano. Pumice is dominant on the surface at these locations and the mean grain size is > 3000µm. There are several factors that indicate high erodibility such as no rock outcrop, smooth surface, severe erosion and no vegetation cover. However, the mass sand transport at these locations is always <50 kg m^{-1}. Therefore the high proportion of coarse grains in the grain size distribution is

likely to be a dominant factor that affects the sand transport rather than other environmental factors. The mass sand transport might possibly be underestimated because of the large diameter of the pumice. Because of the grain size distribution theses locations also probably have a higher proportion of surface creep, which is not measured.

c) Locations no 22, 26, 27 and 28 are a little further away from Hekla, but still within a 15 km radius from the mountain. There is also some pumice on surface but the mean grain size is finer than at the locations in group b, ranging from about 800-1600µm. The sand transport reaches up to 430 kg m^{-1} during erosion events at these locations which confirms that the grain size distribution is a dominant factor explaining the sand movement in the area, as could be expected. Most of these locations are also close to a major waterway which acts as an active sediment source for aeolian activity.

d) Availability of erodible source material increases the erosion susceptibility. Location no 6 near Helliskvísl and locations no 10, 11 12, 13, 14, 15, 16 and 17, all in the north-eastern part, proved to have the highest transport rates within the research area. Based on the surface classification they have the highest proportion of loose material on surface, as well as severe erosion and very little vegetation cover. Locations no 6, 13, 15 and 16 are close to a major waterway but the other locations are not fed directly by sediment sources but as mentioned earlier there is an active aeolian sediment source adjacent to the north-eastern part of the research area.

e) Locations no 9 and 21 are also in sandy areas but the sand transport is considerably less than at locations in group d, or always <120 kg m^{-1} in any erosion event. These locations are classified with severe erosion (surface classification) but the amount of loose material on surface is 40-60% which can explain the difference from locations in group d where the amount is > 80%. These locations are also further away from active sediment sources than group d.

f) Locations no 1, 18, 19 and 20 are all in sandy areas but there is not a very high percentage of loose material on surface and there are no active sources that feed the sand transport in these areas, resulting in very little sand transport or < 10 kg m^{-1}.

This grouping of locations is compared to the maximum intensity of sand transport within the research area in Fig. 50. It shows that the calculated maximum sand transport is well explained by the surface characteristics and environmental factors.

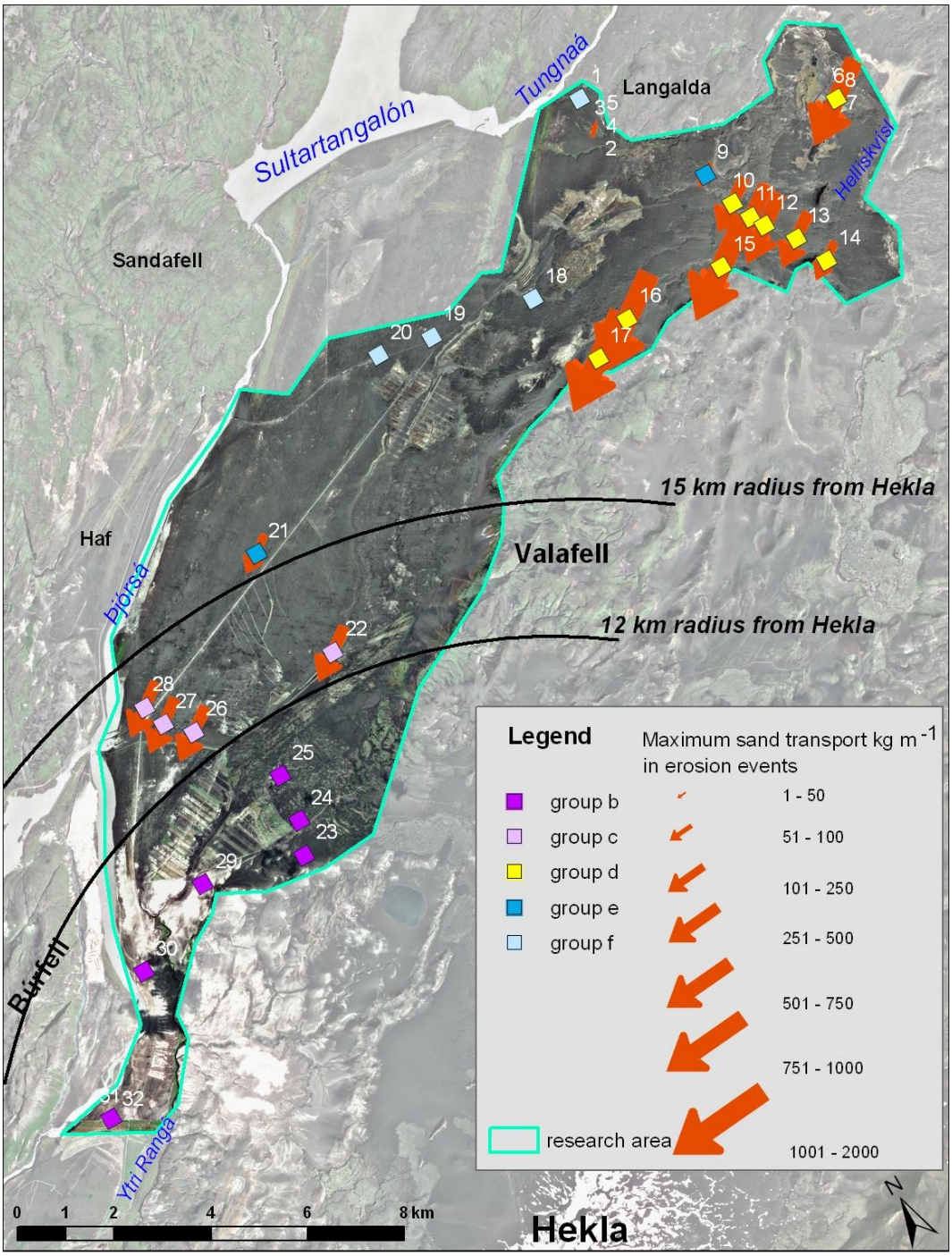

Figure 50. The grouping of locations (boxes), based on surface characteristics and environmental factors, compared to the maximum mass sand transport (arrows). Group a, reclamation areas are excluded.

These results also show an active pathway for sand transport, from the north-eastern part, along the hillsides of Valafell and through the research area into Þjórsá river, which greatly influences the erosion processes in the research area. This result is in accordance with Arnalds theory of pathways for aeolian sand-drift which he described for Northeast Iceland (Arnalds 1992).

The principal component analysis (Fig 48) is in good agreement with the grouping of locations based on field characteristics (Fig 50) and supports this method of combining field work with GIS analysis techniques.

It is important to keep in mind that the research was done at a landscape scale and the weather conditions, especially wind speed, but also air humidity, can vary within the area. Precipitation in the north-eastern part of the research area could for example explain why an erosion event in August 2008 proved to be the least intensive at some of the locations there, when the same erosion event proved to be the most intensive at some of the location in the south-western part (Table 7). Another factor that might affect the spatial difference in aeolian sediment transport in the research area is the fetch effect. The total flux increases with the fetch length (Zobeck et al., 2003) and the increase becomes more significant as the wind velocity increases (Dong et al., 2004). No measurement where made on the actual fetch length but factors like surface roughness, reclamation work and closeness to active sediment sources affect the fetch length within the area.

By looking at the whole research area and the difference on mass sand transport within the area, it indicates that the fundamental differences in the erodibility of the surface causes this difference in mass sand transport, rather than meteorological factors. This conclusion is in accordance with results from Stout (2007) when he measured wind erosion in two areas with similar weather conditions but different surface type.

Spatial analysis and image classification

Dust trap measurements give point data but by using data, based on field mapping, for environmental factors that control the wind erosion rates such as vegetation cover, soil erosion and amount of loose materials on the surface, it is possible to expand the dust trap data to a

landscape scale. Both spatial analysis based on field mapping and image classification is useful to assess spatial variability of the various environmental data.

The prediction of probable intensity of wind erosion based on spatial analysis from the field mapping is not fully in accordance with the measurement from the dust traps (Table 12), but with r^2 of 0.70 there seems to be a strong relationship between the probable intensity of wind erosion and the most active sand transport areas (Fig. 47). It is, however, important to keep in mind that the values given in each category in the spatial analysis (Table 11) are proxies of how they affect and contribute to the aeolian processes.

Based on the image classification the results show that there is a good agreement between measured erosion values and estimates of erosion susceptibility based on surface characteristics, with r^2 of 0.65. As shown in Figure 45, conditions conductive to high erosion rates are in the north-eastern area and along the slopes of Valafell which is in good agreement with the measured sand transport. By applying the knowledge gained from field mapping to the image interpretation used in supervised image classification and comparing that to dust trap measurements the erosion susceptibility can by predicted on a landscape scale. These results are in accordance with Walsh et al. (1998) which concluded that fieldwork will always be an integral part of geomorphologically based research but field techniques should be amalgamated with the techniques of remote sensing and GIS to allow for spatial relationships at various scales.

Grain size

Research in Iceland has shown that Icelandic conditions in relation to wind erosion are in many ways unique (Arnalds et al., 2001). An example of that is that the definition of the nonerodible soil fraction >0.84 mm, as is used in wind erosion models (Zoback et al., 2003) does not apply to Icelandic conditions. Arnalds (1990) showed that up to 2 mm coarse grains can be transported by wind in Iceland. The results from this research show that soil grains (pumice) >8 mm can be transported by saltation (Fig. 25). Furthermore, the proportion of large grains such as >2 mm and especially >8 mm must be underrated because of the small openings of the dust traps (~2 x 5 cm), thus increasing the probability of colliding with the sides of the openings. Despite this fact, grains >2 mm were >10% in eight of the twenty samples shown in

Fig. 24. It is also worth noting that 40% and 42% of the grains collected in the 100 cm trap (Fig. 22) were >1 mm, demonstrating how meaningless the 0.84 mm limit can be in Iceland.

There appears to be a connection between the amount of aeolian transport and grain size parameters such as the mean grain size and the sorting of the material collected in dust traps. Locations with poorly sorted samples have less sand transport than locations where the material is better sorted. This is in accordance with what has been stated before that aeolian entrainment and transport are most effective where sediment has been pre-sorted, by wind and/or water (Pye and Zoar, 1990; Bullard and Livingstone, 2002).

The amount of sand collected in dust traps at 60 cm and 100 cm height (Appendix 3) indicate that the saltation layer is high or well above 1 m. Yet the movement at 100 cm height is only 3-13% of what it is 0-10 cm above the surface, with one exception where it is 21%. The grain size distribution of samples collected at 60 and 100 cm height show a high proportion of coarse grains (Fig. 22 and 23) and this is in accordance with results from Dong et al. (2002) on the variation of sand flux with height, which showed that the average saltation height increases with both wind speed and sand size.

Another example of the uniqueness of wind erosion in Iceland is that the curves showing the height distribution of sand transport (Fig. 26) are not as steep as similar curves based on research in other countries (e.g. Zobeck et al., 2003; van Donk and Skidmore, 2001; Han et al., 2004), which often have little sand transport above 20 cm height. Research at Hólsfjöll, in North Iceland (Arnalds and Gísladóttir, 2009) showed similar curves as were obtained in the sandy areas in the north-eastern part of the research area (Fig 25). The curve from the south-western area, characterized by pumice on the surface, is a little less steep compared to the curves from the other surface types (Fig. 25).

The difference in steepness of the height distribution curves can be at least partly explained by the density. Quartz grains which have the specific density of 2.65 cm^{-3} is the most common aeolian sediment in most countries. In Iceland, due to the volcanic origin, glass and pumice are an extensive part of sediment with density of 1.5-2.9 cm^{-3} and 0.5-1.0 cm^{-3} respectively (Arnalds 1990).

Threshold value

The average threshold values were 10.8 m s^{-1} at location no 11 and 11.4 m s^{-1} at location no 21. In this research data from 10 min average wind speed was used to find the threshold values but threshold values are more accurate if the wind speed is measured using shorter time intervals, seconds rather than minutes and it decreases with shorter time intervals (Stout, 1998). The data loggers were programmed to gather data every 1 minute in erosion events but the 1 minute data proved to be inaccurate due to too high noise restrictions in the programming of the data loggers. Therefore the one minute data was excluded in the results. Longer time spans (10 min average versus 1 min average) might explain slightly higher threshold values at this research site than at Hólsfjöll (Arnalds and Gísladóttir, 2009) and south of the Langjökull Glacier (Gísladóttir, 2000).

The difference of 0.6 m s^{-1} in the average threshold values between locations no 11 and 21 is in accordance with the results from the spatial analysis of the environmental factors. The threshold value is lower at location no 11, with finer surface materials and the estimated potential for wind erosion higher than at location no 21 (Fig. 46). This result supports Stout´s conclusion that it is the erodibility of an area that determines the threshold values rather than differences in climatic conditions (Stout, 2007).

Methods and equipment

The single dust trap method used in this research appears to be a successful method to measure wind erosion on a landscape scale. The fact that the distribution of sediments by height is very similar between sampling periods at locations where more than one set of samples were obtained from a set of four dust traps, supports the credibility of this method.

My results showed that data for wind erosion acquired by dust traps were not completely comparable with data from Sensit sensors. Based on measurement from location no 21 in 2008, the ratio of output from the Sensit sensors at 15 and 30 cm height is similar to the ratio between material collected in dust traps in 15 and 30 cm height or 67% and 63% respectively. When all the data from the Sensit sensors is compared to the amount of material collected in dust traps there is a considerable difference, both between sites and between erosion events. Each Sensit output represents 0.003 g to 0.018 g per Sensit pulse. The average amount of

Sensit pulses representing 1g is 0.005 in location no 11 but up to 0.012 in location no 21. This difference can´t be explained by the mean grain size as it is similar at both locations, or ~400µm, but the grain size sorting might partly explain this as it is poorer in location no 21 or about 600 compared to 380 in location no 11, indicating a higher proportion of coarse grains in location no 21 which will affect the outcome. However, the fact that the data loggers were programmed to reduce noise, for example from rain drop or flies, might also reduce the amount of Sensit counts during erosion events, especially when the wind speed is close to the threshold value. Van Donk and Skimore (2001) also questioned the applicability of Sensit sensors for quantification of sediment flux.

The dust trap measurements proved to be quite reliable in spite of adverse weather conditions. The exception from that were at locations no 2, 3, 4 and 5. The dust trap at location no 2, was placed in early spring 2008. The first erosion event gave reliable information but then Lyme grass was seeded around the dust trap in June 2008. The growth of the Lyme grass affected the wind erosion and resulted in less material collected at that location throughout the research period. Dust traps at locations no 3, 4 and 5 were also placed within the reclamation area after the seeding to see the possible effect. The samples that were collected from these dust traps inside the reclamation area after the seeding were too small to give reliable information about any trends after reclamation started but the small amount collected indicates that the reclamation successfully decreased wind erosion in the area.

Erosion models

In this research I choose to use field measurements and compare them with environmental factors estimated by field mapping, remote sensing and image interpretation. Numerous wind erosion modelling systems have been developed to quantify soil loss and dust emissions at the field, regional and global scales, but few have been applied specifically to assess spatio-temporal patterns in land erodibility (Webb and McGowan, 2009). Namikas and Sherman (1998) found that none of the available models at that time proved to be broadly applicable in the sense that they could provide acceptable accuracy at a wide range of sites.

This research was conducted in a large heterogeneous area, which make model validations difficult, as the field should be homogeneous for model validations (Zobeck et al., 2003). Most

modelling on aeolian transport is based on wind tunnel and field measurement where the mean grain size is silt and fine sand (e.g. Namikas and Sherman, 1998; Namikas, 2003). Icelandic soils and environmental conditions, as mentioned earlier, are in many ways unique in a global perspective and because of that most erosion models would need to be adjusted to Icelandic conditions. Because of the heterogeneity of the research area and its uniqueness, regarding the amount of pumice on surface, models that have been adjusted to Icelandic conditions (Sigurjónsson, 2002; Kjaran et al., 2006) were not used in this research.

Factors that may affect the results

Several factors must be taken into consideration when the wind erosion results are interpreted. The sand movement was only measured during late spring and summer which results in uncertainties because of temporal variation on wind erosion within the year. Wind erosion can also take place during the winter and erosion events at low temperatures can be even more intense based on the effect of low temperature on the amount of water vapour in the air and its impact on particle cohesion (McKenna Neuman, 2003). Particle entrainment is easier at lower temperatures than higher and for a given wind speed a particle 40-50% larger in diameter can be entrained in very cold air when compared with very warm air (McKenna Neuman, 2003). Arnalds and Gísladóttir (2009) found a considerable decrease in the threshold value in a storm event after the surface had frozen, compared to other measurements at higher temperatures. In this research the temperature was well above cero during all the erosion events (Tables 9 and 10) and therefore the effect of very low temperatures on the threshold value can´t be estimated.

Another factor that affects the results is that the research lasted only for two years which is a short time for field measurements where weather conditions can vary considerably between years. The inter-annual variability of parameters such as wind velocity and rainfall can only be ascertained from long term data obtained using standard methods (Lal, 1994). During the two summers that the research was conducted, the weather was mostly calm with few erosion events, but the average figures of wind speed, precipitation, air humidity and temperature are similar to the years before (Table 1). However, the average wind speed during the summermonths is considerably lower than the yearly average of 7.1 m s^{-1}. The results of the mass sand transport might therefore have some uncertainty both regarding inter-annual

variation and also regarding long time temporal variation, especially because since 1995 there have been, on average, fewer and less intensive storms than the decades before that (http://www.vedur.is/vedur/frodleikur/greinar/nr/1801).

The fact that no measurements were made of surface creep may also affect the accuracy of the results for total sand movement. Sampling at several heights, including the surface creep, up to a height of 1 m will generally ensure capture of over 99% of the creep/saltation sediment (Stout and Zobeck, 1996). Estimates of mass transport may be biased when creep is not measured since 7-25% of soil movement can by moved by creep (Chepil, 1945) or even up to 40% of the transported mass (Zobeck et al., 2003).

At several locations the dust traps filled up repeatedly (see Appendix 3). This may reduce the amount of calculated wind erosion, especially at locations where only one dust trap was located. An additional factor that may have reduced the amount of calculated wind erosion in areas with a large proportion of pumice on the surface is that the dust traps opening slots are so small (20 x 45 mm in diameter) that the biggest grains can hardly fit into the slot and are therefore more likely to bounce of the dust trap than to enter it. Given the high proportion of grains > 4mm (Fig. 24) this might show considerably less wind erosion in the south-western part than is in reality. Surface measurements might therefore be more useful than BSNE dust traps to measure the sand movement more accurately at the locations in the south-western part of the research area.

The fact that it was not possible to obtain measurements with a set of four dust traps in all the locations within the research area because of the scarcity of storms might have reduced the accuracy of the height distribution curves used for calculation at each site. However, when all the factors that may have affected the calculated wind erosion are taken into account it is clear that most of the effects decrease the estimated wind erosion rather than increase it. Therefore it is safe to assume the overall mass sand transport in the research area is not overestimated.

5.2 Effect of reclamation on wind erosion

The results from measuring sand transport with dust traps outside the reclamation areas and inside them at 50 m intervals show clearly that the vegetation cover in the reclamation areas

have detrimental effect on the sand transport (Fig. 32 and 33). The grain size parameters (Table 6) show that the mean grain size decreases considerably at locations inside the reclamation areas as only the finest grains are transported into the reclamation areas (Fig. 34). However the calculation of mass sand transport at the sites inside the reclamation areas might be affected by the fact that a set of four dust traps was not located inside the reclamation areas to calculate the height distribution of eroding material. Because of the difference in grain size parameters, the coefficients used for the calculation of wind erosion inside the reclamation areas might not give accurate values. It can be stated, however, that the wind erosion is greater by an order of magnitude outside reclamation areas compared to erosion within them.

Even though the calculation of wind erosion within the reclamation areas might be biased, the amount of material collected in dust traps outside and inside of reclamation areas shows relative quantities of aeolian material transported into the reclamation areas. This shows that often large quantities of material are deposited at the first 50 m and it indicates that the stress in that area is considerable. It would therefore be valuable to obtain better estimates of transport over the first 10 m of vegetation next to an unstable wind erosion area. This result also emphasises the importance of creating continuous reclamation areas to avoid sediment entrainment between them.

This is the first time that the effect of reclamation work on wind erosion is measured in Iceland. The vegetative characteristics were not taken into account but plant flexibility is one of the characteristics that are important in estimating the affect on wind erosion (Cooke et al., 1993). Increasing rigidity increases the roughness height z_0 and thereby affects the wind speed near the surface. Further investigation of various plant characteristics in relation to wind erosion would further our understanding on the effect of vegetation on sand movement.

6. Conclusions

It has been stated that erosion is the biggest environmental problem in Iceland and the national soil erosion survey (Arnalds et al., 1997) has successfully shown the distribution and extent of the soil erosion. This research shows that a better understanding of the nature and magnitude of wind erosion is still needed, for example to be able to identify aeolian transport pathways. Here, new methods to estimate erosion susceptibility on a landscape scale are suggested as a step into that direction. My conclusion is that, both, spatial analysis based on field mapping of environmental factors and supervised image classification based on knowledge of field characteristic is a useful way of estimating soil erodibility on a landscape scale. By comparing the estimated soil erodibility with dust traps measurements the aeolian transport on a landscape scale can by quantified.

The field mapping of soil erosion based on the Icelandic classification scheme (Arnalds et al., 1997) classified > 60% of the research area with severe erosion (5). However, my results show that there is a considerable variability on wind erosion susceptibility within these areas which indicates that this classification scheme does not describe the landscape dynamics in sandy areas sufficiently. My conclusion is that a new scale, with 3-5 additional classes for areas previously classified as severe erosion, is needed. By adding classes to the current scale, areas similar to locations in group d (Fig. 50) could be identified as areas that are likely candidates for aeolian transport pathways, especially if relief characteristics also enhance wind speeds (along hillsides etc.). By adding classes to the current erosion scale it would also make it possible to observe wind erosion processes on a landscape scale, which is needed, considering the 20 000 km^2 of sandy areas in Iceland.

The new *single dust trap method* proved, in this research, to be a successful method to measure wind erosion on a landscape scale. There is considerable wind erosion within the research area where the sand transport is of the same order of magnitude as has been measured in other wind erosion researches in Iceland.

Both aeolian and fluvial processes are active in the research area. The sediment transport is mostly from northeast to southwest, both because of the prevailing north-easterly winds and also because most of the waterways run into the river Þjórsá. This indicates considerable

sediment transport into the river Þjórsá, by both these erosion processes. These results have practical value as the sediment transport can possibly affect the production of electricity further down the river at Búrfell Power Station.

Reclamation efforts have detrimental effect on wind erosion but research on the transport over the first 10 m of vegetation next to unstable wind erosion areas and of various plant characteristics in relation to wind erosion is necessary to further our understanding on the effect of vegetation on sand movement.

7. References

Aradóttir, Á.L., 2005. Restoration of birch and willow woodland on eroded areas. In: G. Halldórsson, E.S. Oddsdóttir and Ó. Eggertsson (Editors), Effects of afforestation on ecosystems, landscape and rural development. TemaNord, Reykholt, Iceland, pp. 343.

Arnalds, A., 1987. Ecosystem disturbance in Iceland. Arctic and Alpine Research, 19(4): 508-513.

Arnalds, A., 1988. Landgæði á Íslandi fyrr og nú (Past and present condition of lands in Iceland). In: A. Arnalds (Editor), Græðum Ísland, Landgræðslan 80 ára. Landgræðsla ríkisins, pp. 13-30. [In Icelandic].

Arnalds, Ó., 1990. Characterization and erosion of Andisols in Iceland. Texas A&M University, College Station, Texas.

Arnalds, Ó., 1992. Sandleiðir á Norðausturlandi (Pathways of aeolian sand-drift in Norteast Iceland). In: A. Arnalds (Editor), Græðum Ísland, Landgræðslan 1991-1992. Landgræðsla ríkisins, pp. 145-149. [In Icelandic].

Arnalds, Ó., 2004. Volcanic soils of Iceland. Catena, 56(1-3): 3-20.

Arnalds, Ó., 2008. Soils of Iceland. Jokull, 58: 409-421.

Arnalds, Ó., 2010. Dust sources and deposition of aeolian materials in Iceland. Icelandic Agricultural Sciences, 23: 3-21.

Arnalds, Ó., Gísladóttir, F.Ó. and Sigurjónsson, H., 2001. Sandy deserts of Iceland: an overview. Journal of Arid Environments, 47(3): 359-371.

Arnalds, Ó. and Kimble, J., 2001. Andisols of deserts in Iceland. Soil Science Society of America Journal, 65(6): 1778-1786.

Arnalds, Ó. and Gísladóttir, F.Ó., 2009. Mælingar á vindrofi á Hólsfjöllum (Erosion measurements at Hólsfjöll, NE Iceland), Rit LbHÍ nr 25, 43pp. [In Icelandic].

Arnalds, Ó. and Metúsalemsson, S., 2004. Sandfok af Suðurlandi 5. október 2004 (Dust emissions from South Iceland Oktober 5th 2004). Náttúrufræðingurinn, 72: 90-92. [In Icelandic]

Arnalds, Ó. and Óskarsson, H., 2009. Íslenskt jarðvegskort (A soil map of Iceland). Náttúrufræðingurinn, 78(3-4): 107-121. [In Icelandic, English summary].

Arnalds, Ó., Thórarinsdóttir, E.F., Metúsalemsson, S., Jónsson, Á., Grétarsson, E. and Árnason, A., 1997. Jarðvegsrof á Íslandi (Soil erosion in Iceland). Landgræðsla ríkisins og Rannsóknastofnun Landbúnaðarins. [In Icelandic].

Ágústdóttir, A.M. and Thórarinsdóttir, E.F., 2000. Árskógar. Report, Landgræðsla ríkisins. [In Icelandic].

Árnason, G., 1958. Uppblástur og eyðing býla í Landsveit (Desertification of farms in Landsveit farming district) In: A. Sigurjónsson (Editor), Sandgræðslan. Búnaðarfélag Íslands og Sandgræðsla ríkisins, Reykjavík, pp. 50-87. [In Icelandic].

Bagnold, R.A., 1937. The Transport of Sand by Wing. The Geographical Journal, 89(5): 409-438.

Bagnold, R.A., 1941. The Physics of Blown Sand and Desert Dunes. Willian Morrow & Company, New York.

Böhner, J., Schafer, W., Conrad, O., Gross, J. and Ringeler, A., 2003. The WEELS model: methods, results and limitations. Catena, 52: 289-308.

Blott, S.J. and Pye, K., 2001. GRADISTAT: A grain size distribution and statistics package for the analysis of unconsolidated sediments. Earth Surface Processes and Landforms, 26(11): 1237-1248.

Bullard, J.E. and Livingstone, I., 2002. Interactions between aeolian and fluvial systems in dryland environments. Area, 34(1): 8-16.

Chappell, A., McTainsh, G., Leys, J. and Strong, C., 2003. Simulations to optimize sampling of aeolian sediment transport in space and time for mapping. Earth Surface Processes and Landforms, 28(11): 1223-1241.

Chepil, W.S., 1945. Dynamics of wind erosion: III. The transport capacity of the wind. Soil Science, 60: 475-480.

Chepil, W.S., 1950. Properties of soil which influence wind erosion: II. Dry aggregate structure as an indes of erodibility. Soil Science 39: 403-414.

Conacher, A., 2009. Land degradation: A global perspective. New Zealand Geographer, 65(2): 91-94.

Cooke, R., Warren, A. and Goudie, A., 1993. Desert Geomorphology. UCL Press, London.

Dong, Z., Liu, X., Wang, H., Zhao, A. and Wang, X., 2002. The flux profile of a blowing sand cloud: a wind tunnel investigation. Geomorphology, 49: 219-230.

Dong, Z.B., Wang, H.T., Liu, X.P. and Wang, X.M., 2004. The blown sand flux over a sandy surface: a wind tunnel investigation on the fetch effect. Geomorphology, 57(1-2): 117-127.

Einarsson, M.Á., 1976. Veðurfar á Íslandi (The Climate of Iceland). Iðunn, Reykjavík. [In Icelandic].

Einarsson, M.Á., 1984. Climate of Iceland. In: H. van Loon (Editor), World Survey of Climatology: 15: Climates of the Oceans. Elsevier, Amsterdam, pp. 673-697.

Field, J.P., Breshears, D.D. and Whicker, J.J., 2009. Toward a more holistic perspective of soil erosion: Why aeolian research needs to explicitly consider fluvial processes and interactions. Aeolian Research, 1(1-2): 9-17.

Fryrear, D.W., 1986. A field dust sampler. Journal of Soil and Water Conservation, 41(2): 117-120.

Gillette, D.A. and Stockton, P.H., 1989. The effect of nonerodible particles on wind erosion of erodible surfaces. Journal of Geophysical Research, 94(10): 12885-12893.

Gísladóttir, F.Ó., Arnalds, Ó. and Gísladóttir, G., 2005. The effect of landscape and retreating glaciers on wind erosion in south Iceland. Land Degradation and Development, 16(2): 177-187.

Gísladóttir, F.Ó., 2000. Umhverfisbreytingar og vindrof sunnan Langjökuls (Environmental changes and wind erosion south of Langjökull), Háskóli Íslands, Reykjavík. [In Icelandic, English summary].

Goossens, D. and Offer, Z.Y., 2000. Wind tunnel and field calibration of six aeolian dust samplers. Atmospheric Environment, 34(7): 1043-1057.

Gregory, J.M., Wilson, G.R., Singh, U.B. and Darwish, M.M., 2004. TEAM: integrated, process-based wind-erosion model. Environmental Modelling & Software, 19(2): 205-215.

Greipsson, S. and Davy, A.J., 1997. Responses of *Leymus arenarius* to nutrients: improvement of seed production and seedling establishment for land reclamation. Journal of Applied Ecology, 34(5): 1165-1176.

Guðjónsson, G. and Gíslason, E., 1998. Vegetation map of Iceland. The Icelandic Institute of Natural History.

Gudmundsson, A., Óskarsson, N., Gronvold, K., Saemundsson, K., Sigurdsson, O., Stefánsson, R., Gíslason, S. R., Einarsson, P., Brandsdóttir, B., Larsen, G., Jóhannesson, H. and Thórdarson, T., 1992. The 1991 eruption of Hekla, Iceland. Bulletin of Volcanology, 54(3): 238-246.

Han, Z.W. et al., 2004. Observations of several characteristics of aeolian sand movement in the Taklimakan Desert. Science in China Series D-Earth Sciences, 47(1): 86-96.

Hjartarson, Á., 1995. Á Hekluslóðum (Hekla and surroundings). Árbók Ferðafélags Íslands Ferðafélag Íslands, Reykjavík, 257 pp. [In Icelandic].

Höskuldsson, Á., Óskarsson, N., Pedersen, R., Gronvold, K., Vogfjord, K. and Ólafsdóttir, R., 2007. The millennium eruption of Hekla in February 2000. Bulletin of Volcanology, 70(2): 169-182.

Hudson, N., 1981. Soil conservation. Batsford Academic and Educational, London.

Icelandic Meteorological Office, 2009. Weather observations from Búrfell station.

Kjaran, S.P., Sigurjónsson, H. and Björnsson, B.J., 2006. Calculation of wind erosion on the banks of the Hálslón., Landsvirkjun LV-2006/088.

Kjartanson, G., 1945. Hekla. Árbók ferðafélags Íslands. [In Icelandic].

Lal, R., 1994. Soil erosion by wind and water: Problems and prospects. In: R. Lal (Editor), Soil Erosion Research Methods. Soil and Water Conservation Society, pp. 1-9.

Lal, R. and Elliot, W., 1994. Erodibility and erosivity. In: R. Lal (Editor), Soil Erosion Research Methods. Soil and Water Conservation Society.

Landnámabók (The book of settlement), 1968 (reprint). Islensk fornrit 1.2. Hid islenska Fornritafelag, Reykjavík. [In Icelandic].

Lillesand, T.M. and Kiefer, R.W., 2004. Remote sensing and image interpretation. 5th ed. John Wiley & Sons, Inc.

McKenna Neuman, C., 2003. Effects of Temperature and Humidity upon the Entrainment of Sedimentary Particles by Wind. Boundary Layer Meteorology, 108: 61-89.

Morgan, R.P.C., 1986. Soil erosion and conservation. Longman Group UK Limited, Essex.

Namikas, S., 2003. Field measurement and numerical modelling of aeolian mass flux distributions on a sandy beach. Sedimentology, 50(2): 303-326.

Namikas, S.L. and Sherman, D.J., 1998. AEOLUS II: An interactive program for the simulation of aeolian sedimentation. Geomorphology, 22(2): 135-149.

Orradóttir, B., Archer, S.R., Arnalds, Ó., Wilding, L.P. and Thurow, T.L., 2008. Infiltration in Icelandic Andisols: The role of vegetation and soil frost. Arctic Antarctic and Alpine Research, 40(2): 412-421.

Ovadnevaite, J., Ceburnis, D., Plauskaite-Sukiene, K., Modini, R., Dupuy, R., Rimselyte, I., Ramonet, M., Kvietkus, K., Ristovski, Z., Berresheim, H. and O'Dowd, C. D., 2009.

Volcanic sulphate and arctic dust plumes over the North Atlantic Ocean. Atmospheric Environment, 43(32): 4968-4974.

Pye, K. and Tsoar, H., 1990. Aeolian sand and sand dunes. Unwin Hyman Ltd, London.

Rose, C.W., 1998. Modeling Erosion by Wind and Water. In: R. Lal, W.H. Blum, C. Valentine and B.A. Stewart (Editors), Methods for Assessment of Soil Degradation. CRC Press.

Runólfsson, S., 1986. Soil Conservation in Iceland. In: R.P.C. Morgan (Editor), Soil erosion and its control. Van Nostrand Reinhold Company, New York.

Shao, Y., 2000. Physics and Modelling of Wind Erosion. Kluwer Academic Publishers, Dordrecht.

Shao, Y., McTainsh, G.H., Leys, J.F. and Raupach, M.R., 1993. Efficiencies of sediment samplers for wind erosion measurement. Australian Journal of Soil Research, 31(4): 519-532.

Shao, Y.P., Raupach, M.R. and Leys, J.F., 1996. A model for predicting aeolian sand drift and dust entrainment on scales from paddock to region. Australian Journal of Soil Research, 34(3): 309-342.

Sigurbjarnarson, G., 1969. Áfok og uppblástur. Þættir úr sögu Haukadalsheiðar (Soil erosion on Haukadalsheiði). Náttúrufræðingurinn, 39: 68-118. [In Icelandic].

Sigurjónsson, A. (Editor), 1958. Sandgræðslan (Sand reclamation service). Búnaðarfélag Íslands og Sandgræðsla ríkisins, Reykjavík. [In Icelandic].

Sigurjónsson, H., 2002. Development of an erosion modeling system and its employment on Icelandic soils, Háskóli Íslands, Reykjavík.

Sigurjónsson, H., Gísladóttir, F.Ó. and Arnalds, Ó., 1999. Measurements of eolian processes on sandy surfaces in Iceland. Rit RALA no. 21.

Singh, U.B., Gregory, J. and Wilson, G., 1997. Texas erosion analysis model: Theory and validation, Proceedings of Wind Erosion: An International Symposium/Workshop, Manhattan, K.S.

Skidmore, E.L., 1994. Wind erosion. In: R. Lal (Editor), Soil erosion research methods. Ohio State University, pp. 265-293.

Skidmore, E.L., Hagen, L.J., Armbrust, D.V., Durar, A.A., Fryrear, D.W., Potter, K.N., Wagner, L.E. and Zobeck, T.M., 1994. Methods for investigating basic processes and conditions affecting wind erosion. In: R. Lal (Editor), Soil erosion research methods. Ohio State University, pp. 295-330.

Stallings, J.H., 1957. Soil conservation. Prentice-Hall, Inc.

Sterk, G., 1997. Wind erosion in the Sahelian zone of Niger. Wageningen University, the Netherlands.

Stout, J.E., 1998. Effect of averaging time on the apparent threshold for aeolian transport. Academic Press Ltd, pp. 395-401.

Stout, J.E., 2004. A method for establishing the critical threshold for aeolian transport in the field. Earth Surface Processes and Landforms, 29(10): 1195-1207.

Stout, J.E., 2007. Simultaneous observations of the critical aeolian threshold of two surfaces. Geomorphology, 85(1-2): 3-16.

Stout, J.E. and Fryrear, D.W., 1989. Performance of a windblown-particle sampler Transactions of the Asae, 32(6): 2041-2045.

Stout, J.E. and Zobeck, T.M., 1996. The Wolfforth field experiment: A wind erosion study. Soil Science, 161(9): 616-632.

Stroosnijder, L., 2005. Measurement of erosion: Is it possible? Catena, 64: 162-173.

ter Braak, C.J.F. and Smilauer, P., 2002. CANOCO Reference Manual and CanoDraw for WIndows User's Guide: Software for Canonical Community Ordination (version 4.5). Microcomputer Power, Ithaca, NY.

Thórarinsdóttir, E.F., 2009. Land assessment prior to reclamation work, Mapping and monitoring of nordic vegetation and landscapes. Nordic association of agricultural scientists, Hveragerði, Iceland.

Thórarinsson, S., 1961. Uppblástur á Íslandi í ljósi öskulagarannsókna (Wind erosion in Iceland based on tephrocronology). Ársrit Skógræktarfélags Íslands: 17-54. [In Icelandic].

Thórarinsson, S. and Sigvaldason, G., 1972. The Hekla Eruption of 1970. Bulletin of Volcanology, 36(2): 269-288.

Thorsteinsson. I, Ólafsson, G. and Vandyne, G.M., 1971. Range resources of Iceland. Journal of Range Management, 24(2): 86-93.

van Donk, S.J. and Skidmore, E.L., 2001. Field experiments for evaluating wind erosion models. Annals of Arid Zone, 40(3): 281-302.

Vilmundardottir, O.K., Magnússon, B., Gísladóttir, G. and Thorsteinsson, T., 2010. Shoreline erosion and aeolian deposition along a recently formed hydro-electric reservoir, Blondulon, Iceland. Geomorphology, 114(4): 542-555.

Visser, S.M. and Sterk, G., 2001. Techniques for simultaneous quantification of water and wind erosion in semi-arid zones, The International Symposion: Soil research for the 21st century, Hawaii.

Visser, S.M., Sterk, G. and Snepvangers, J.J.J.C., 2004. Spatial variation in wind-blown sediment transport in geomorphic units in northern Burkina Faso using geostatistical mapping. Geoderma, 120(1-2): 95-107.

Walsh, S.J., Butler, D.R. and Malanson, G.P., 1998. An overview of scale, pattern, process relationships in geomorphology: a remote sensing and GIS perspective. Geomorphology, 21(3-4): 183-205.

Webb, N.P. and McGowan, H.A., 2009. Approaches to modelling land erodibility by wind. Progress in Physical Geography, 33(5): 587-613.

Wentworth, C.K., 1922. A scale of grade and class terms for clastic sediments. Geology, 30: 377-392.

Whisenant, S.G., 1999. Repairing Damaged Wildlands. University Press, Cambridge.

Worboys, M. and Duckham, M., 2004. GIS: A computing perspective. 2nd ed. CRC Press.

Zhang, W., Kang, J.H. and Lee, S.J., 2007. Visualization of saltating sand particle movement near a flat ground surface. Journal of Visualization, 10(1): 39-46.

Zobeck, T.M., Sterk, G., Funk, R., Rajot, J.L., Stout, J.E. and Van Pelt, R.S., 2003. Measurement and data analysis methods for field-scale wind erosion studies and model validation. Earth surface processes and landforms, 28(11): 1163-1188.

Appendix 1 Pictures of dust trap locations

Field mapping data of surface characteristics from the surrounding area is shown in text boxes.

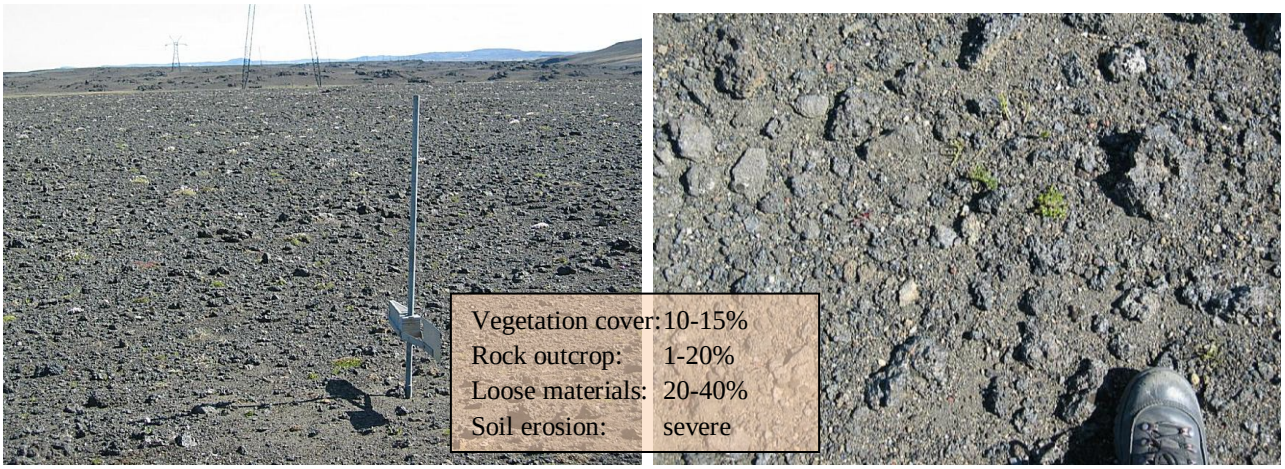

Figure A-1. Dust trap location no 1, an overview and the surface.

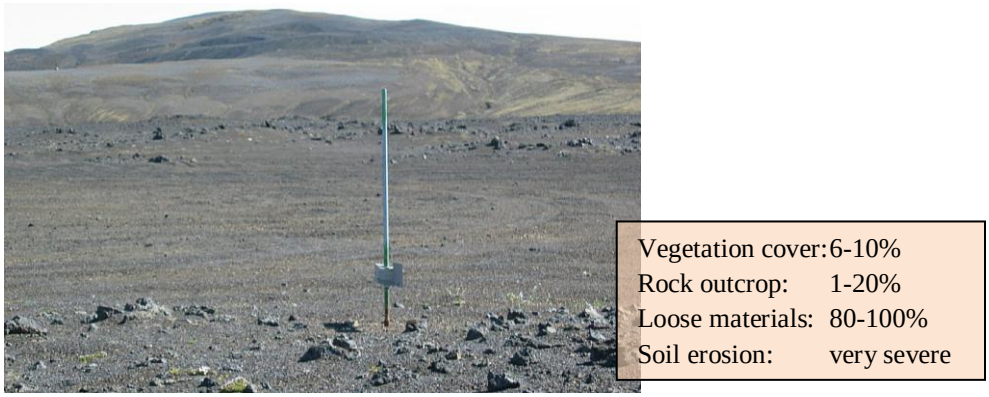

Figure A-2. Dust trap location no 2, an overview.

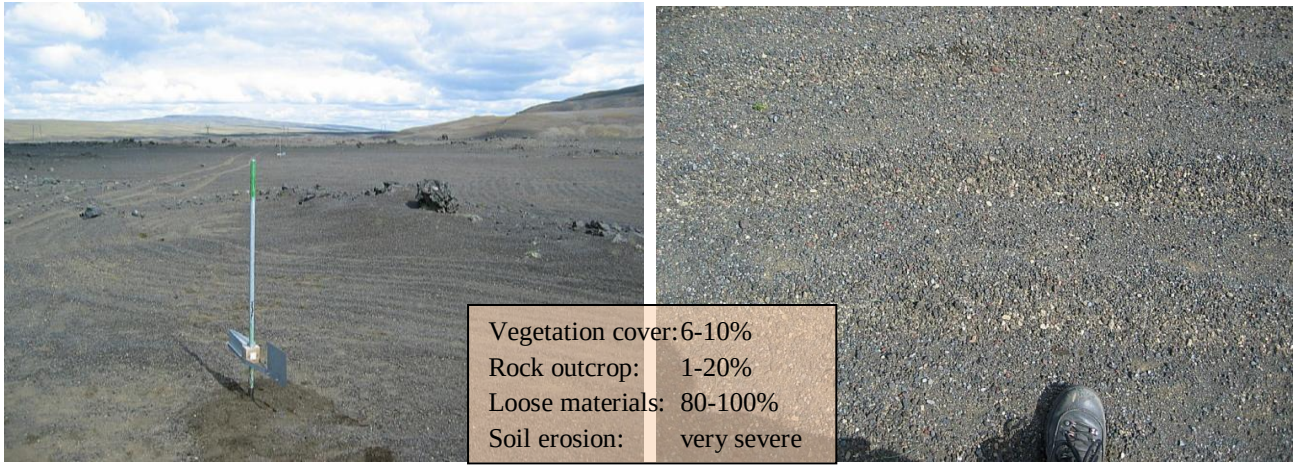

Figure A-3. Dust trap location no 3, an overview and the surface.

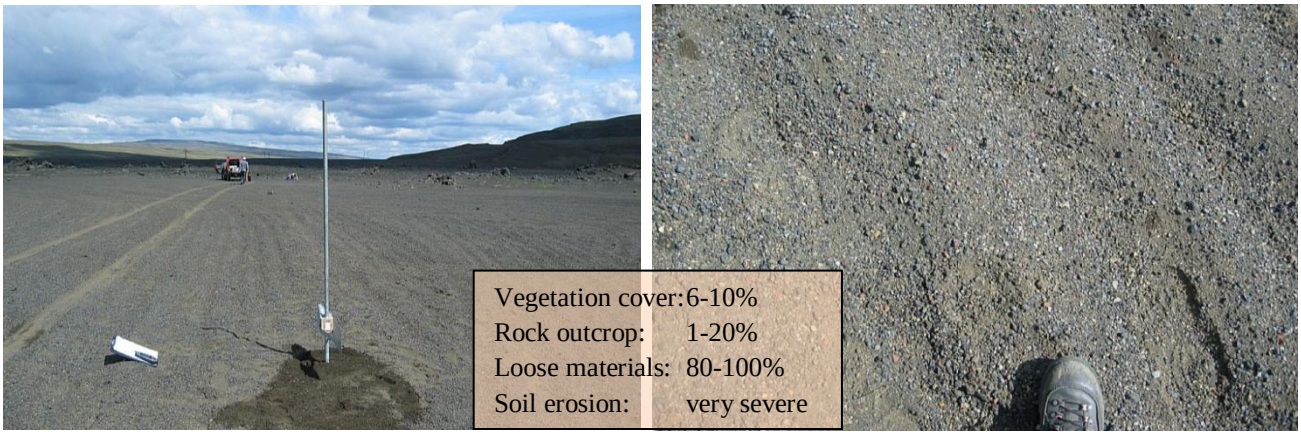

Figure A-4. Dust trap location no 4, an overview and the surface.

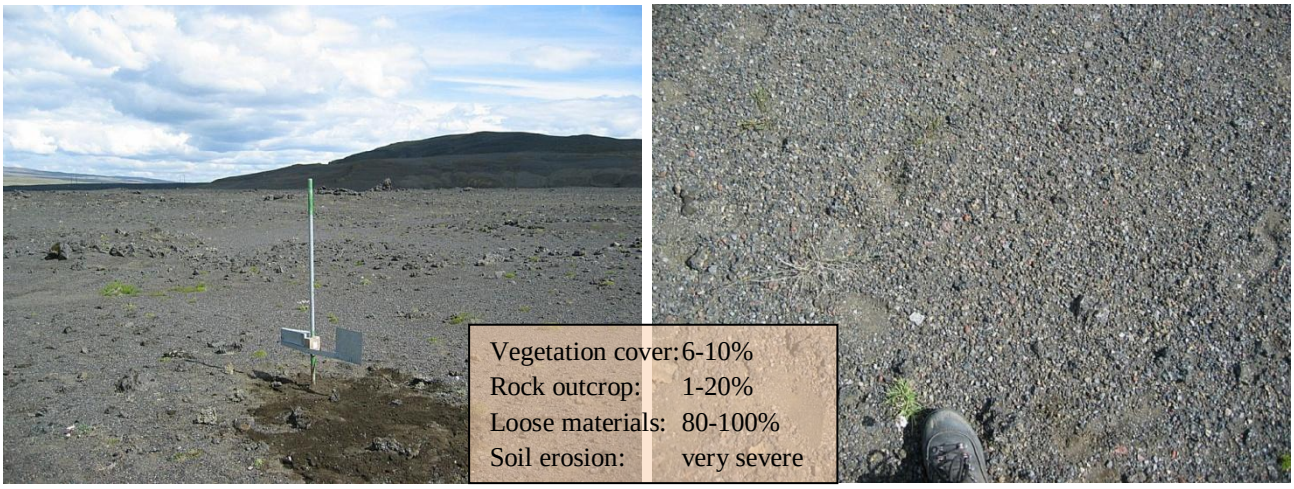

Figure A-5. Dust trap location no 5, an overview and the surface.

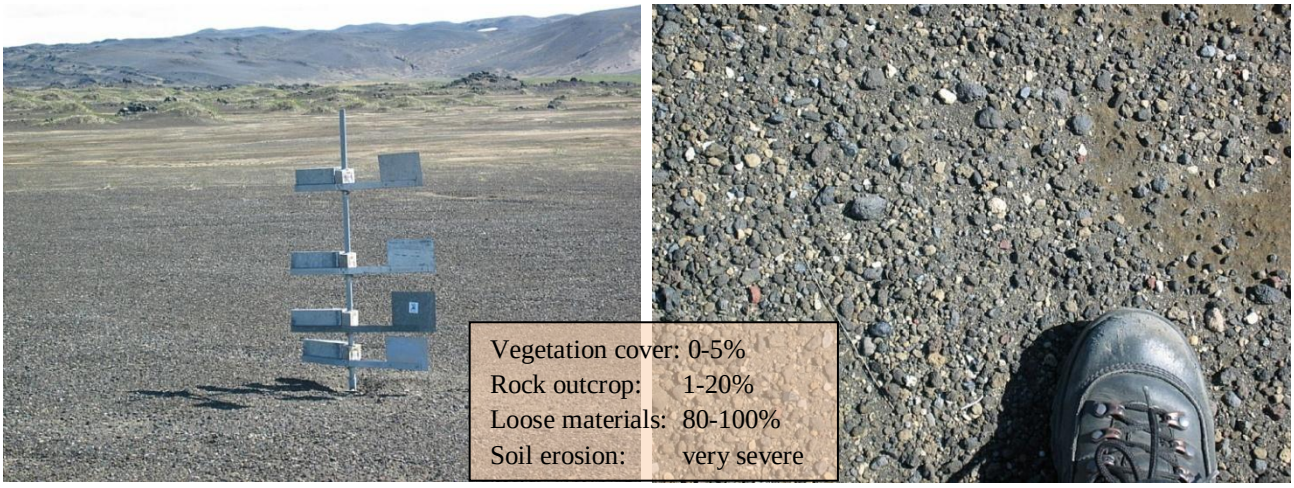

Figure A-6. Dust trap location no 6, an overview and the surface.

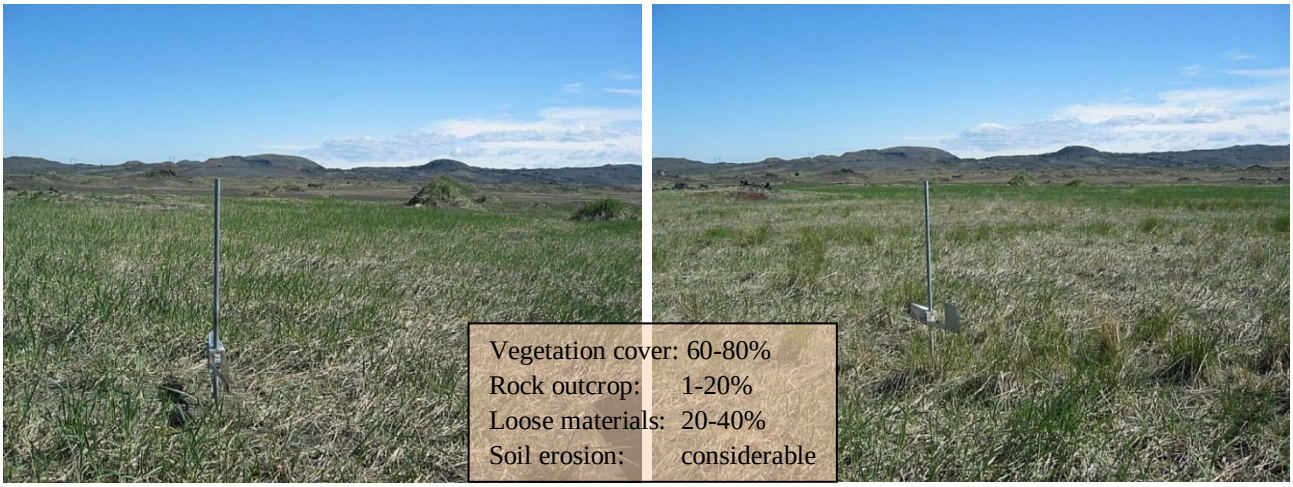

Figure A-7. Dust trap location no 7 (left) and 8 (right), an overview.

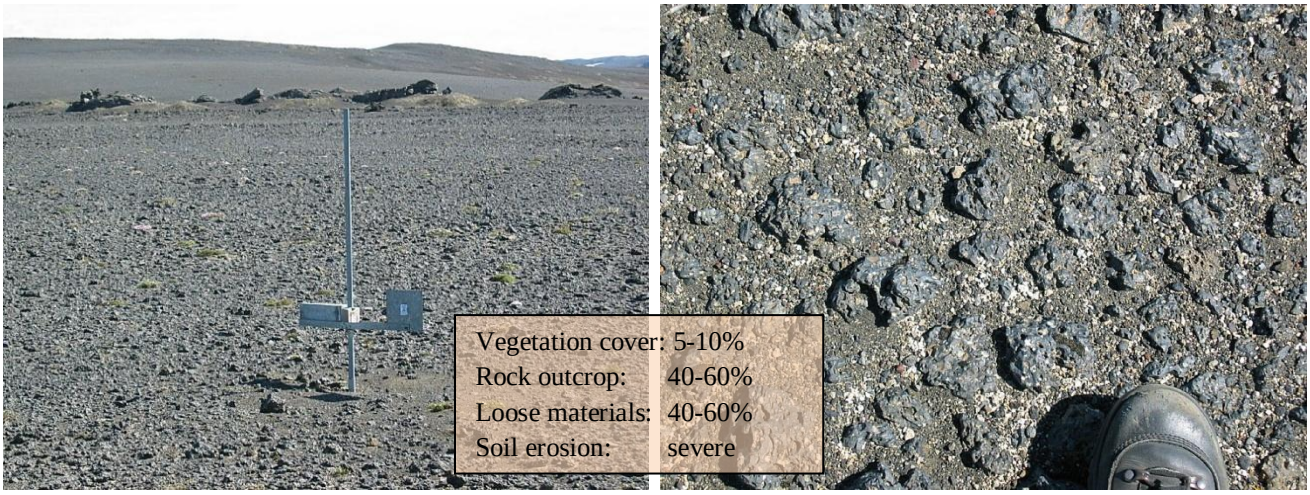

Figure A-8. Dust trap location no 9, an overview and the surface.

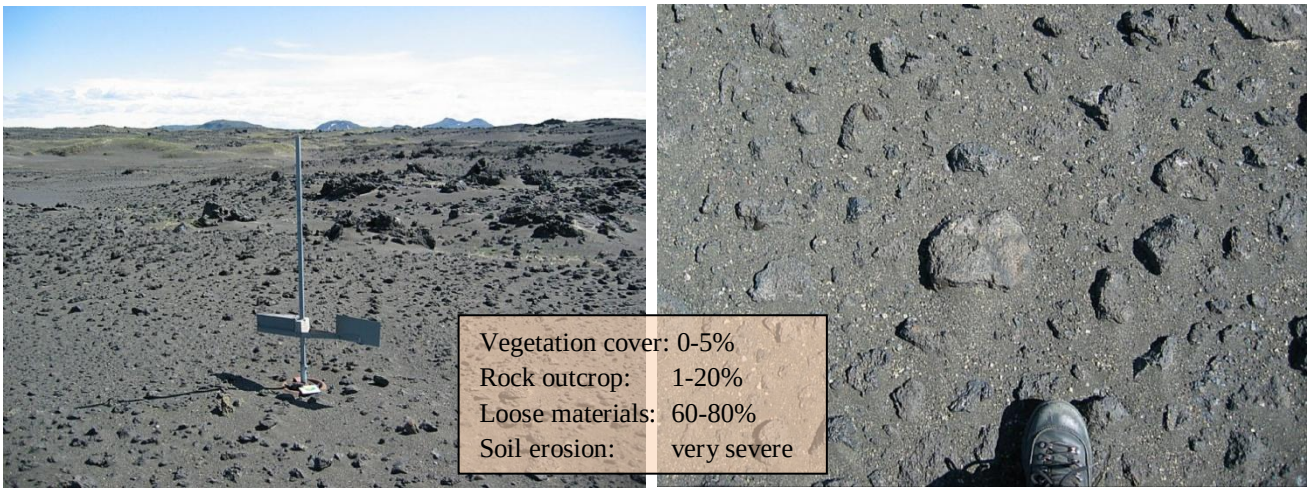

Figure A-9. Dust trap location no 10, an overview and the surface.

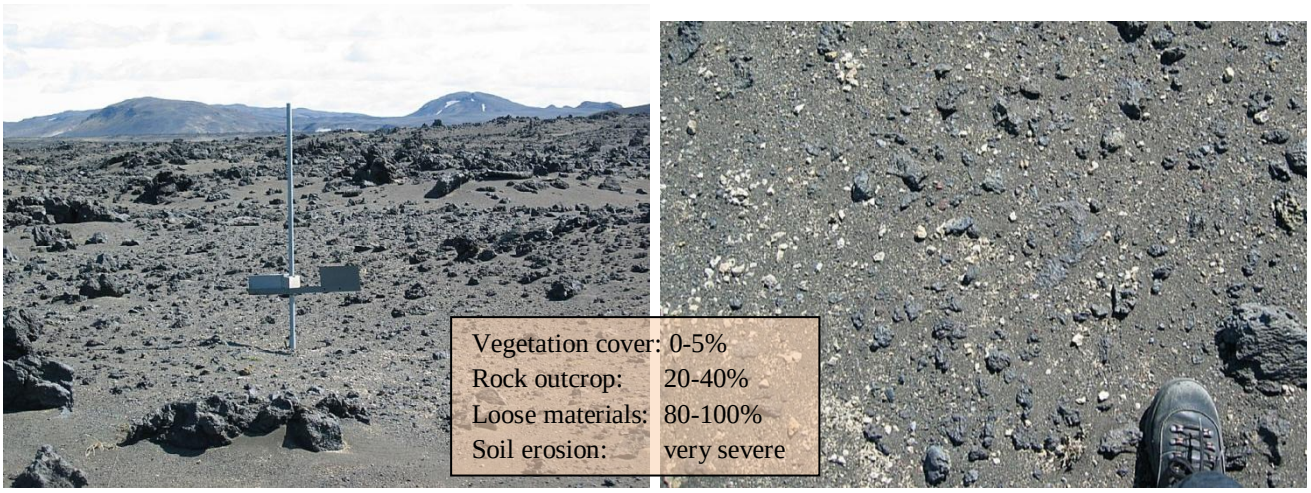

Figure A-10. Dust trap location no 11, an overview and the surface.

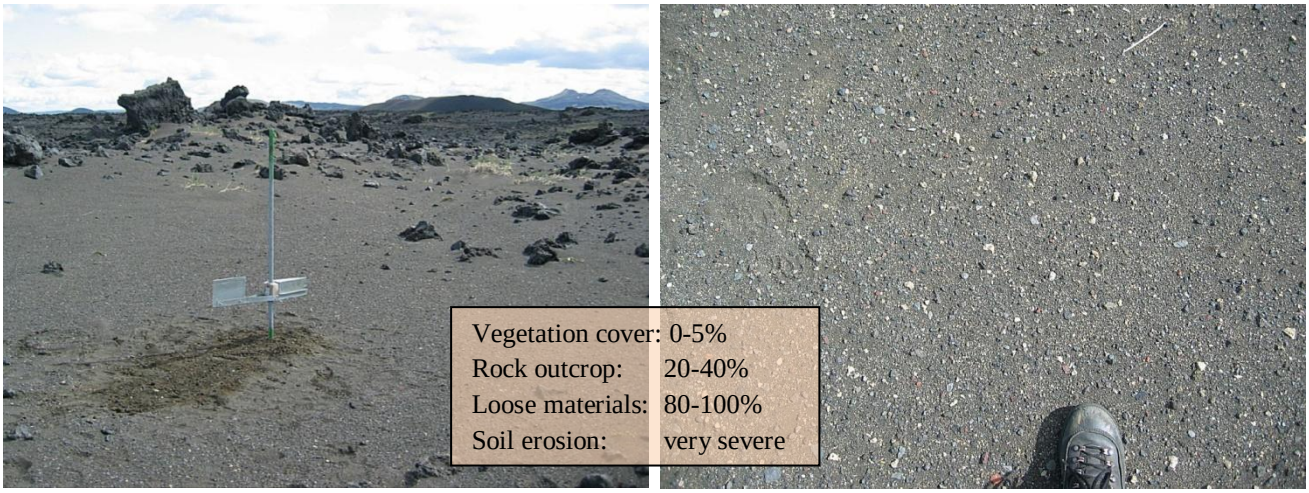

Figure A-11. Dust trap location no 12, an overview and the surface.

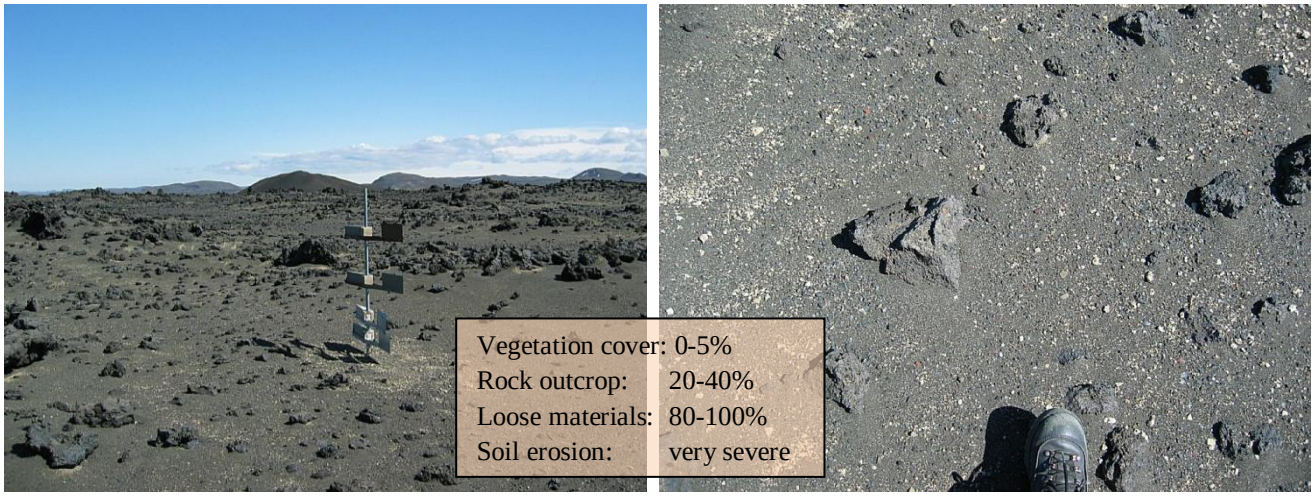

Figure A-12. Dust trap location no 13, an overview and the surface.

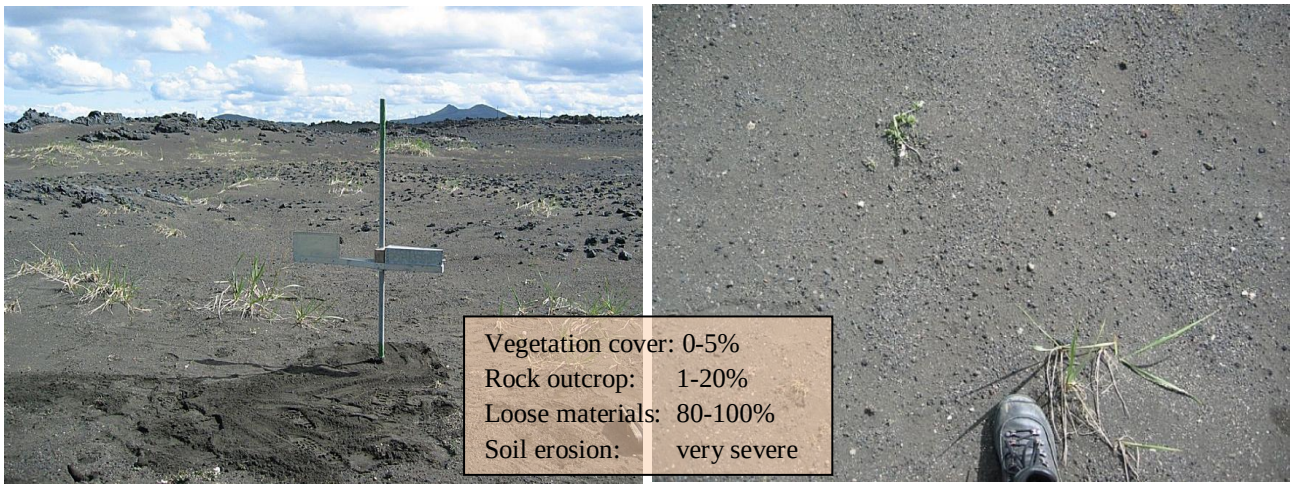

Figure A-13. Dust trap location no 14, an overview and the surface.

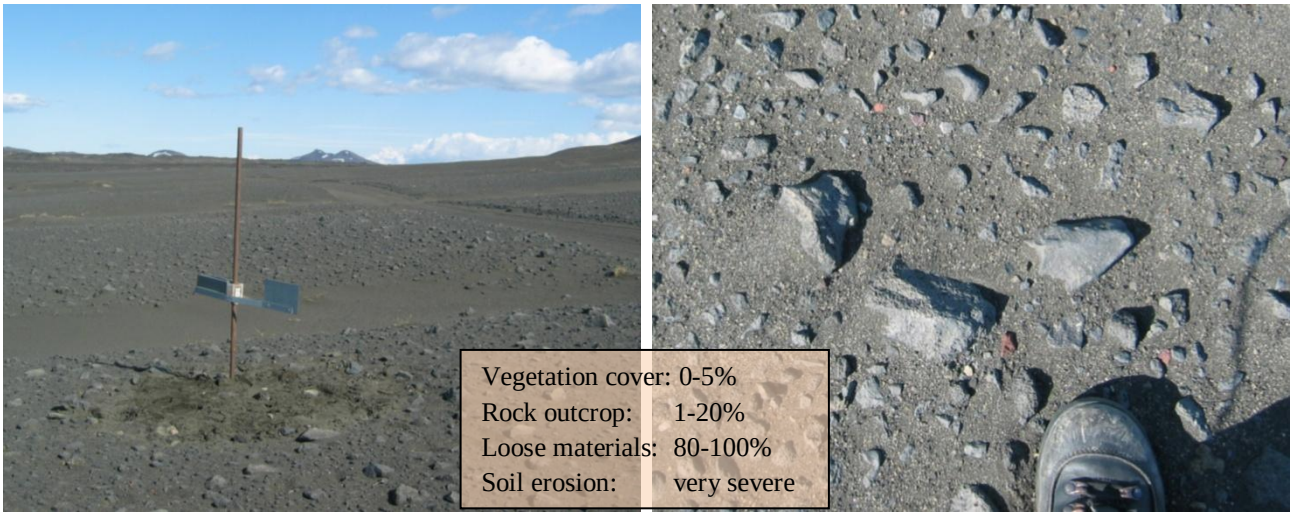

Figure A-14. Dust trap location no 15, an overview and the surface.

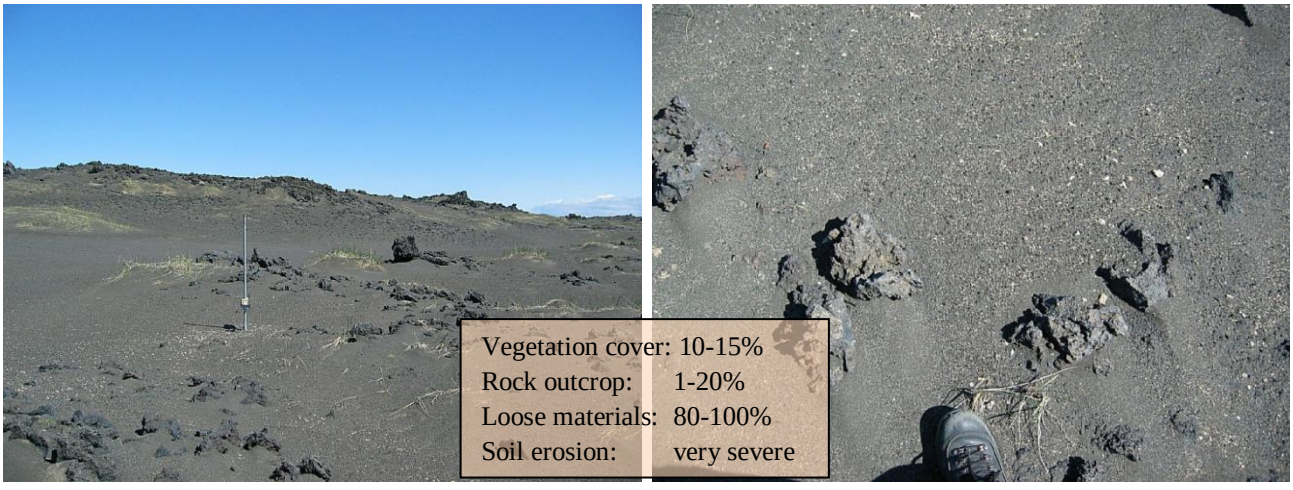

Figure A-15. Dust trap location no 16, an overview and the surface.

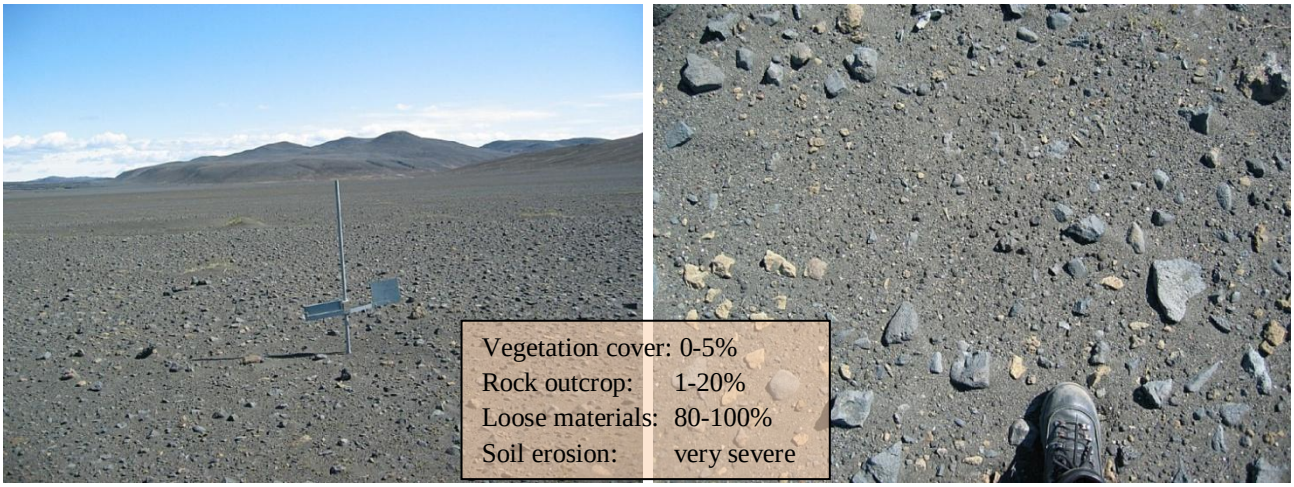

Figure A-16. Dust trap location no 17, an overview and the surface.

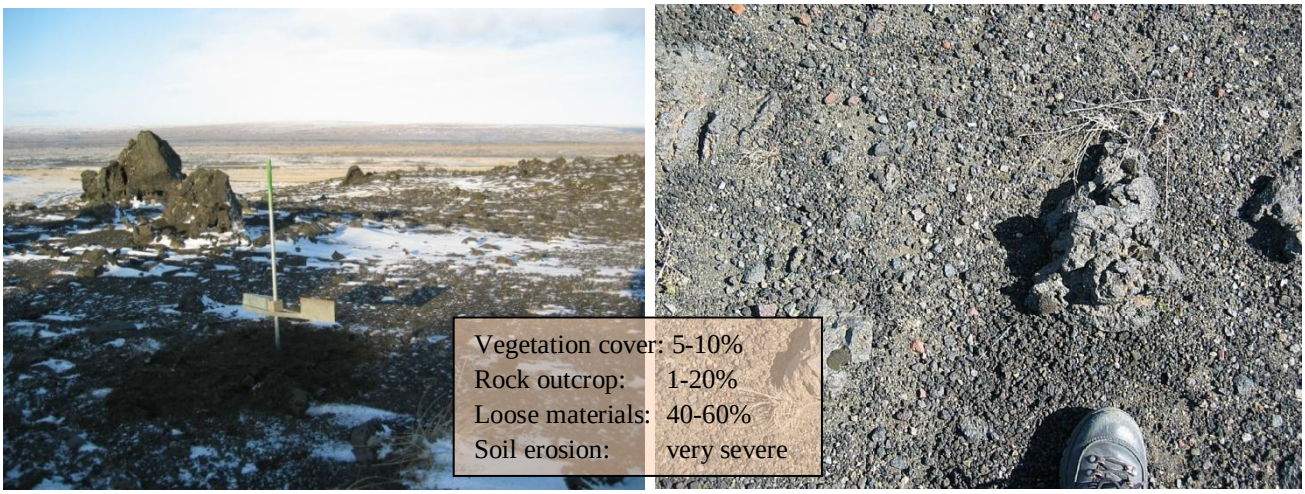

Figure A-17. Dust trap location no 18, an overview and the surface.

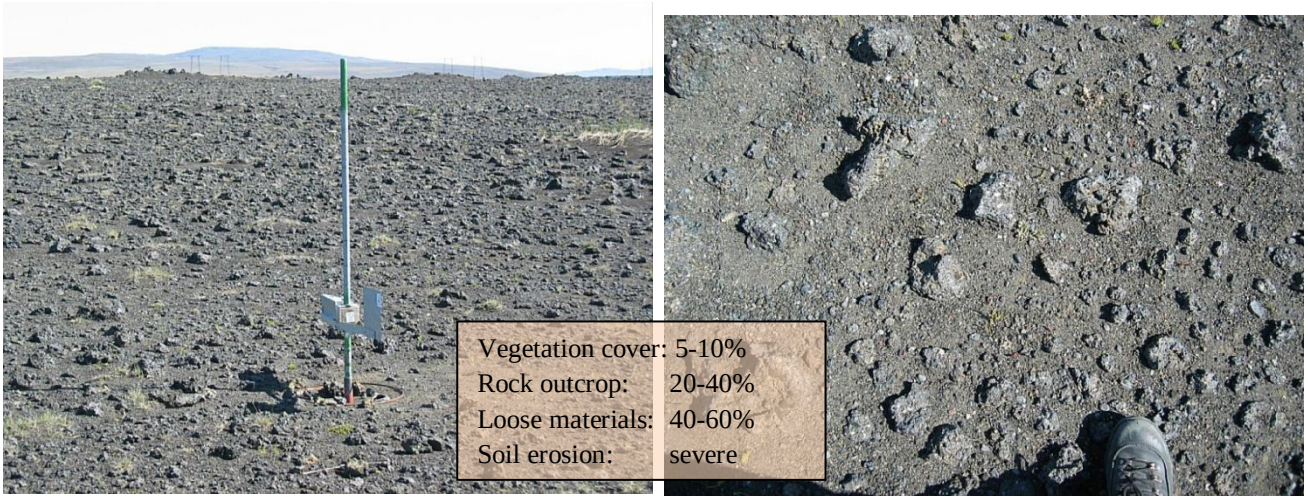

Figure A-18. Dust trap location no 19, an overview and the surface.

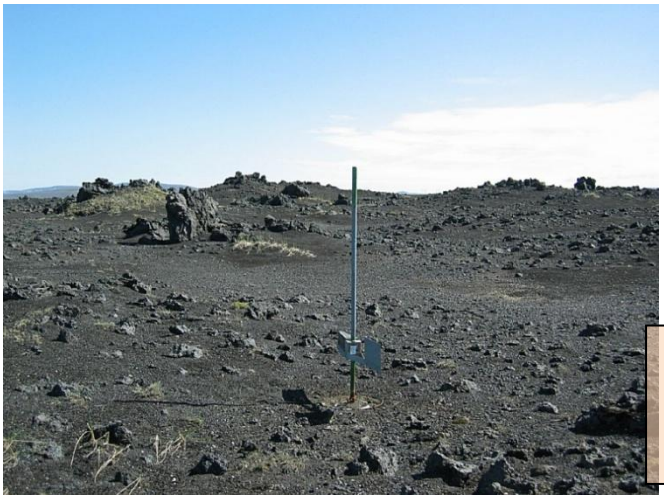

Figure A-19. Dust trap location no 20, an overview.

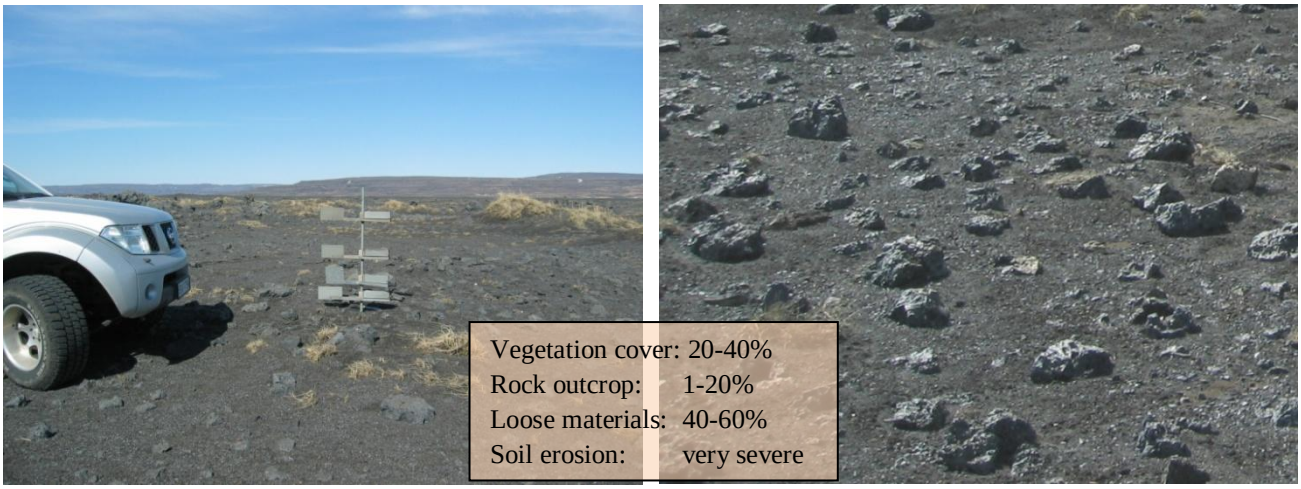

Figure A-20. Dust trap location no 21, an overview and the surface.

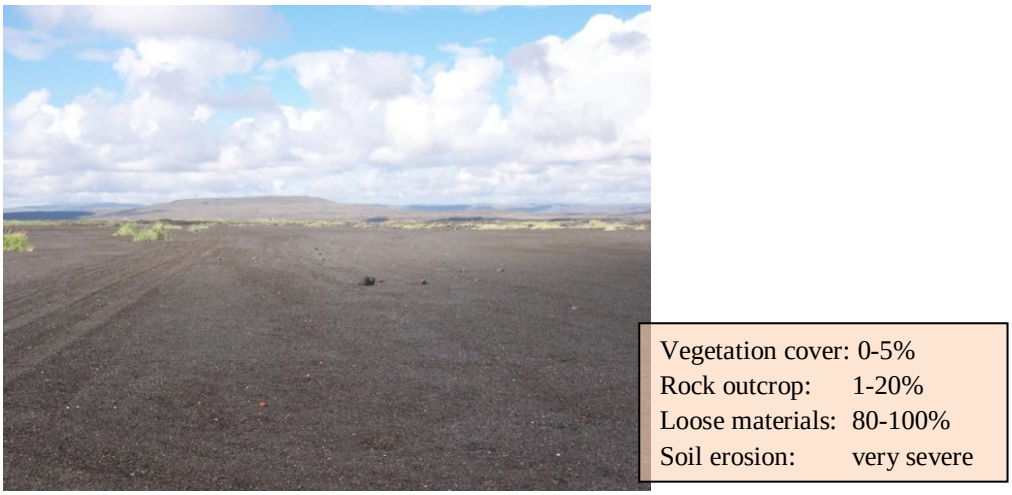

Figure A-21. Dust trap location no 22, an overview.

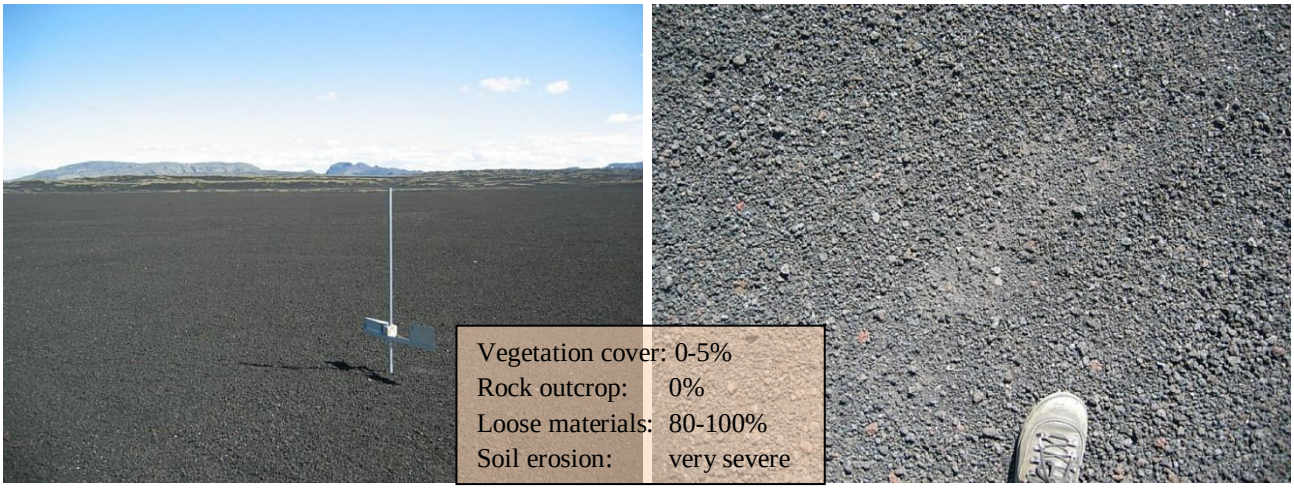

Figure A-22. Dust trap location no 23, an overview and the surface.

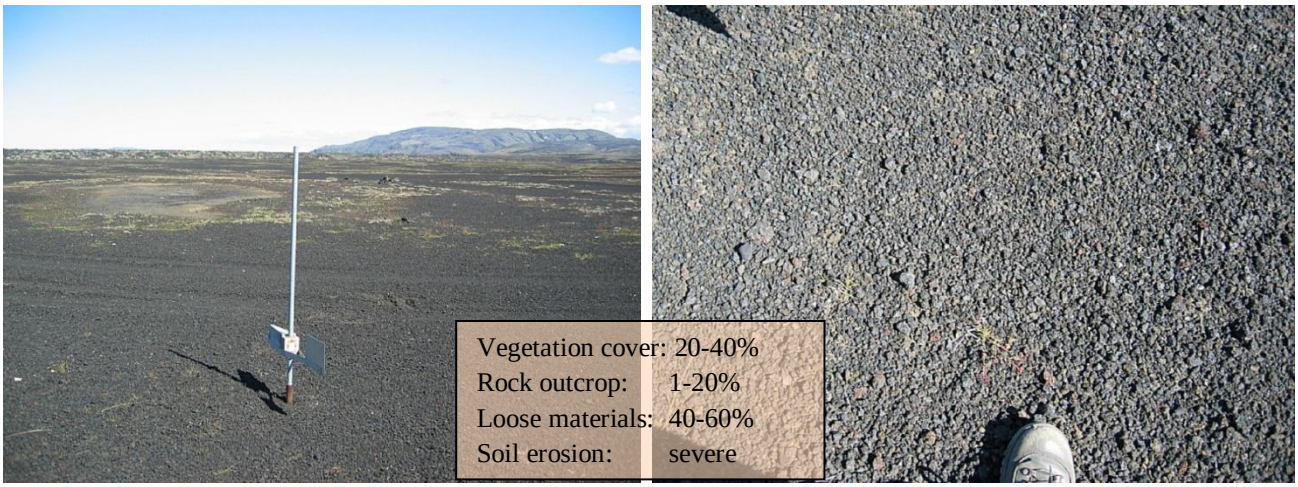

Figure A-23. Dust trap location no 24, an overview and the surface.

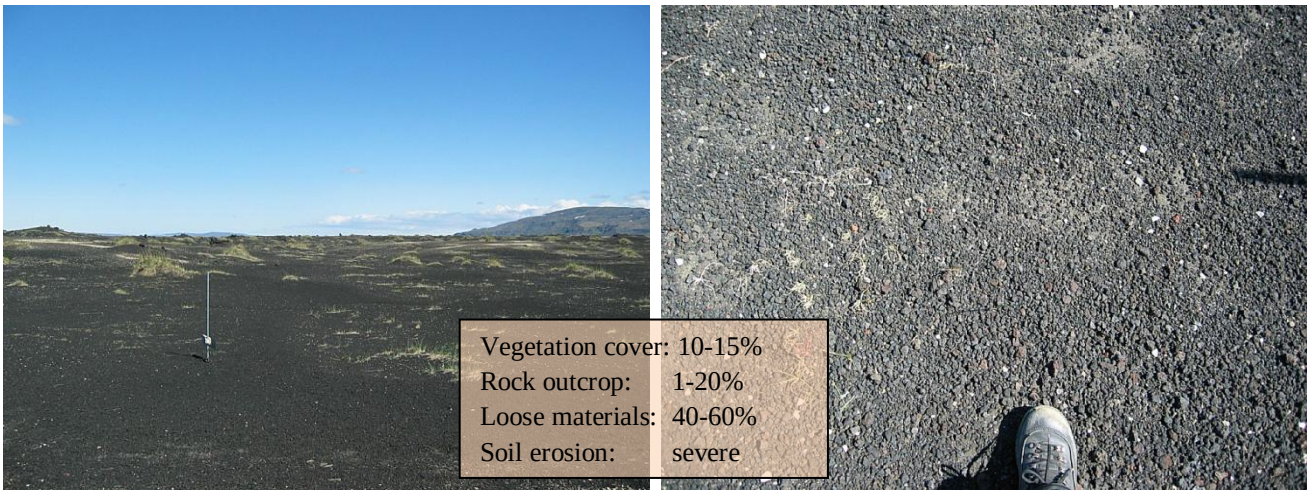

Figure A-24. Dust trap location no 25, an overview and the surface.

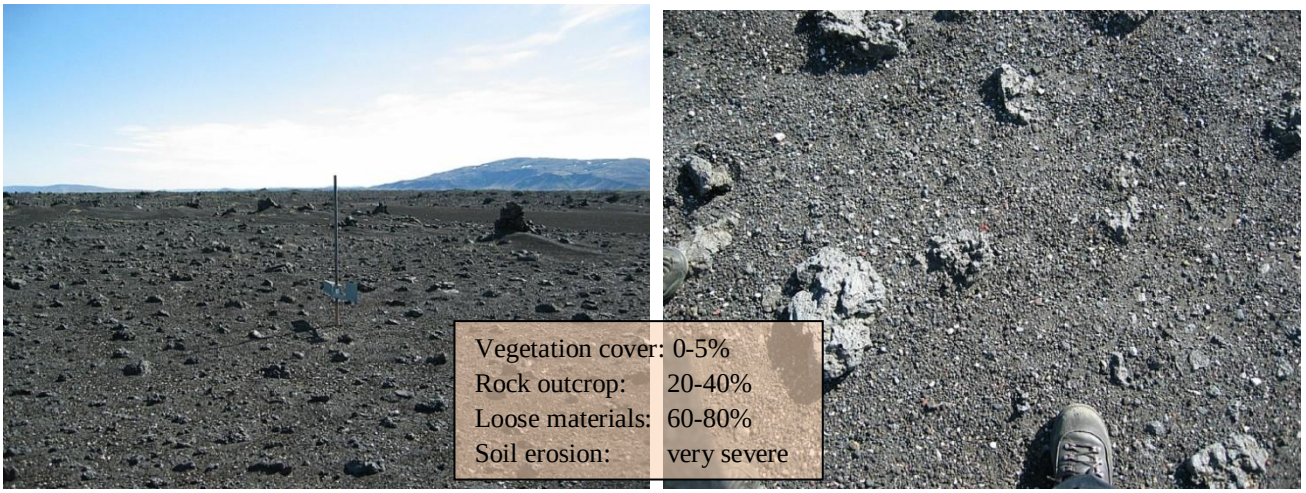

Figure A-25. Dust trap location no 26, an overview and the surface.

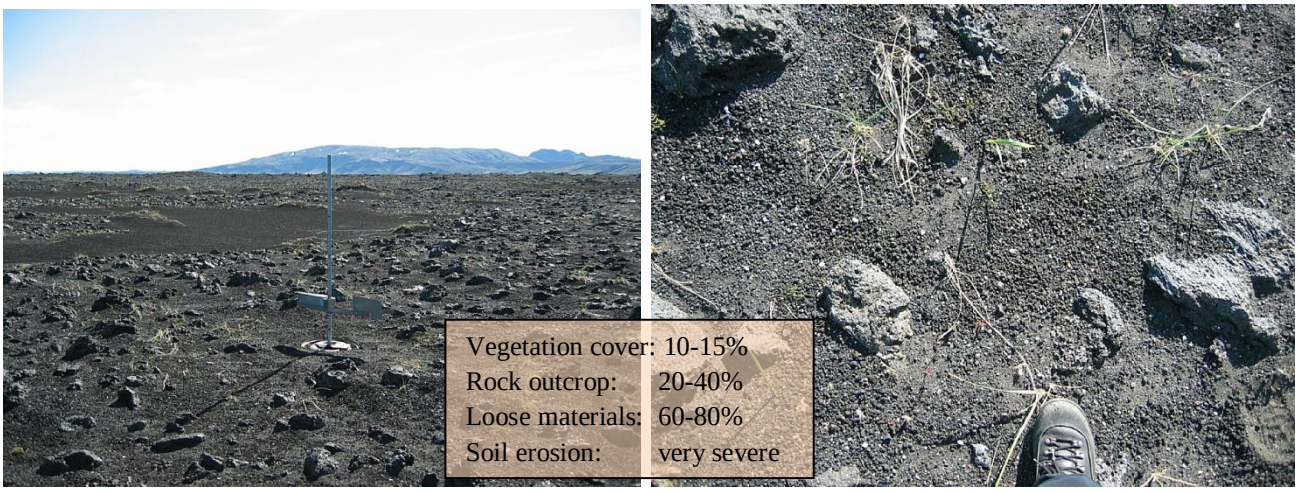

Figure A-26. Dust trap location no 27, an overview and the surface.

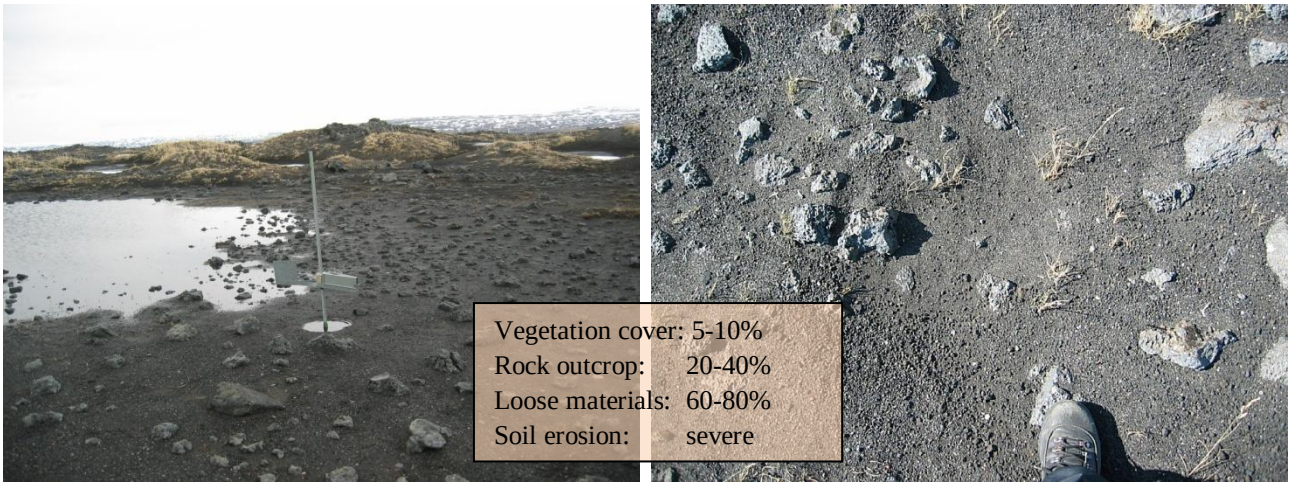

Figure A-27. Dust trap location no 28, an overview (in spring thaw 2008) and the surface.

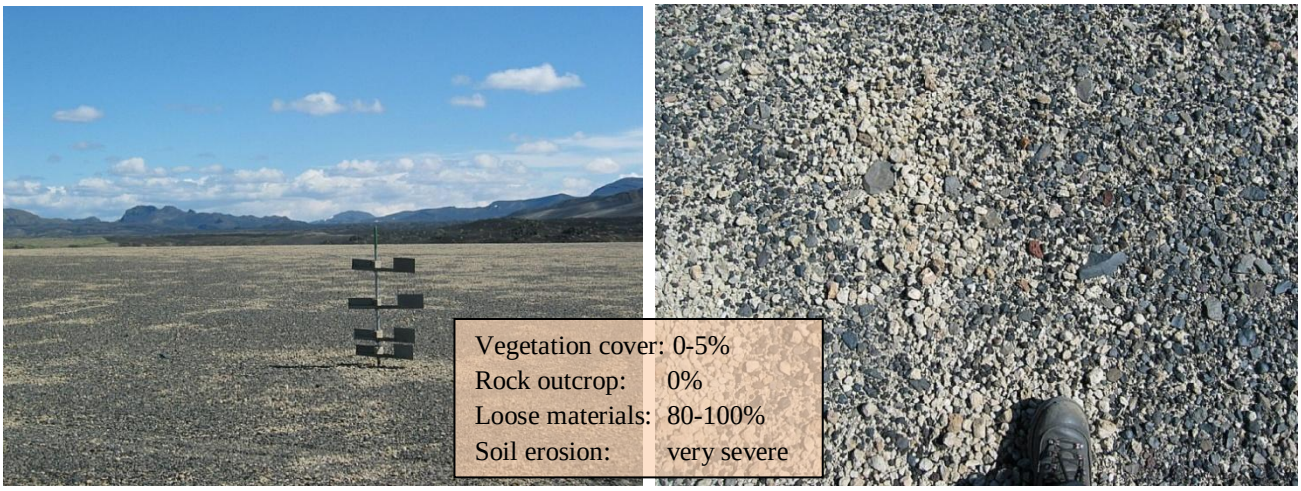

Figure A-28. Dust trap location no 29, an overview and the surface.

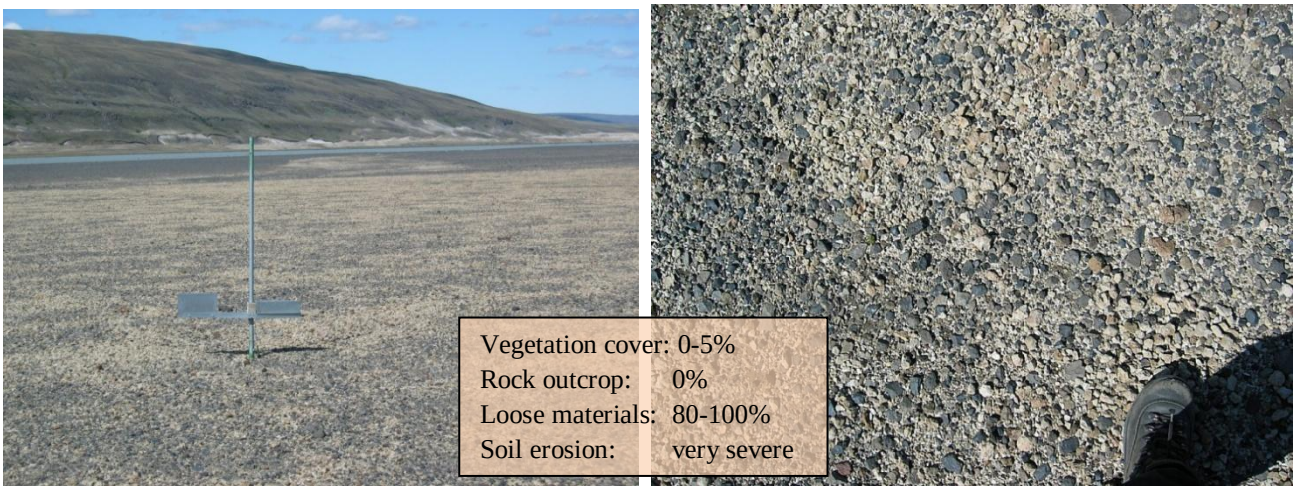

Figure A-29. Dust trap location no 30, an overview and the surface.

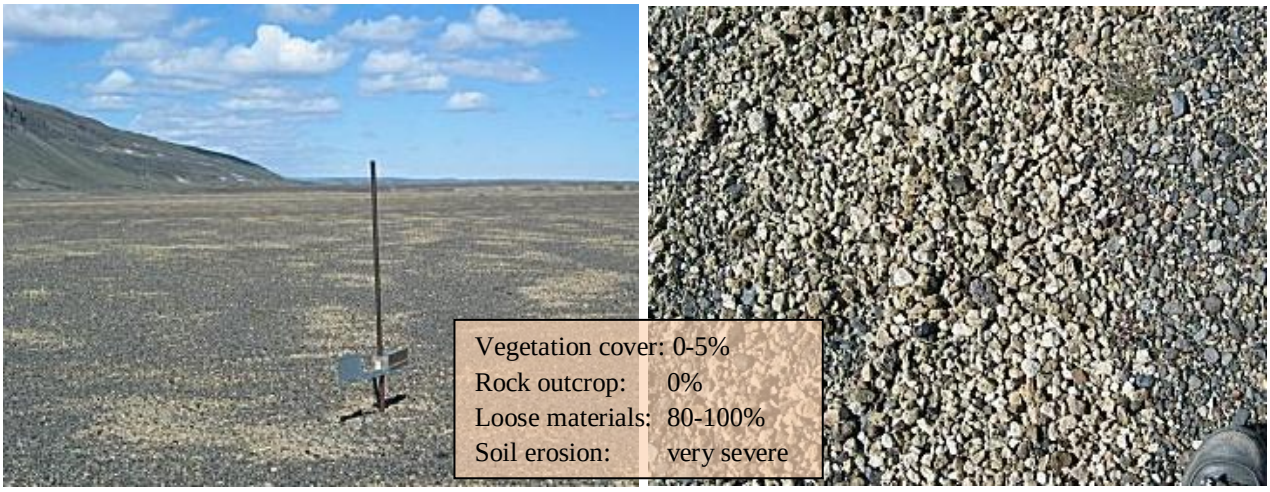

Figure A-30. Dust trap location no 31, an overview and the surface.

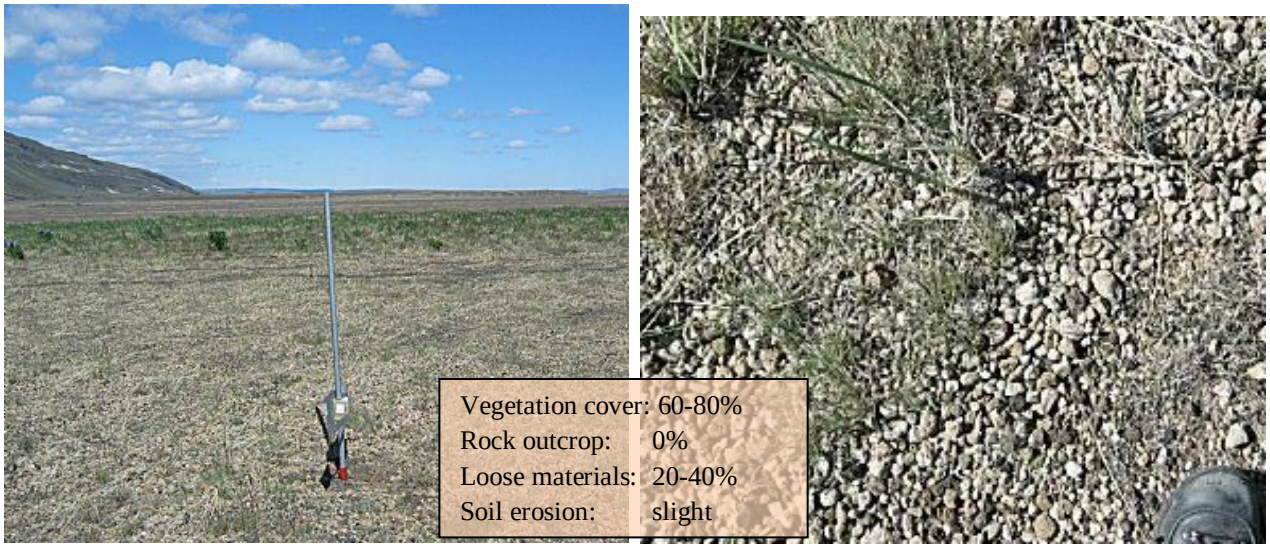

Figure A-31. Dust trap location no 32, an overview and the surface.

Appendix 2 **Field mapping system**

Mapping system used in a scale 1:15 000

Vegetation cover

1	Sparsely vegetated	0-20% cover	
		a=0-5%; b=6-10%; c=10-15%; d=15-20%	
2	Considerable	21-40% cover	
3	Half vegetated	41-60% cover	*- vegetation cover is estimated*
4	Mostly vegetated	61-80% cover	*by % cover at the soil surface*
5	Fully vegetated	81-100% cover	

Rock outcrop

0	No rock outcrop	0 %	
1	Little	1 - 20 %	*- rock outcrop*
2	Considerable	21 - 40 %	*is defined as*
3	High proportion	41 - 60 %	*rock > 10 cm*
4	Very high proportion	61 - 80 %	*in diameter*
5	Mostly covered	81 - 100 %	

Loose material (sand or pumice) on surface

0	No loose material	0 %
1	Little	1 - 20 %
2	Considerable	21 - 40 %
3	High proportion	41 - 60 %
4	Very high percentage	61 - 80 %
5	Mostly covered	81 - 100 %

Surface roughness

1	Smooth surface	< 5 cm roughness	*- surface roughness*
2	Rather smooth surface	5 - 50 cm roughness	*estimated based on*
3	Rather rough surface	51 - 150 cm roughness	*roughness within*
4	Very rough surface	>150 cm roughness	*15 m radius*

Erosion grade

0	No erosion
1	Little erosion
2	Slight erosion
3	Considerable erosion
4	Severe erosion
5	Extremely severe erosion

Soil erosion classes

A	Encroaching sand
B	Rofabards / erosion escarpments
D	Erosion spots
J	Erosion spots on slope / solifluction
V	Gullies / water erosion
K	Landslides
O	Brown soil remnants
M	Gravel
S	Sand and pumice
SM	Sandy gravel
SH	Sandy lava
C	Scree
H	Lava

Waterways

A	River or creek – running water all year
K1	Major dry waterway
K2	Other dry waterways
F	Flood plain

Appendix 3 Amount of erosion material collected in dust traps

Table A-1.
Sand and dust collected in dust traps during sampling periods when erosion events occurred. Red numbers show minimal values as these dust traps filled up during the erosion event.

	2008			2009			2008			2009			2008			2009			2008			2009		
	3/6 – 7/6	20/6 – 5/7	5/7 – 30/8	16/5 - 30/6	24/7 - 30/7	30/7– 24/8	3/6 – 7/6	20/6 – 5/7	5/7 – 30/8	16/5 - 30/6	24/7 - 30/7	30/7– 24/8	3/6 – 7/6	20/6 – 5/7	5/7 – 30/8	16/5 - 30/6	24/7 - 30/7	30/7– 24/8	3/6 – 7/6	20/6 – 5/7	5/7 – 30/8	16/5 - 30/6	24/7 - 30/7	30/7– 24/8
Nr of location	dust traps at 15 cm height - total sand collected in g						dust traps at 30 cm height - total sand collected in g						dust traps at 60 cm height - total sand collected in g						dust traps at 100 cm height - total sand collected in g					
1	-	-	-	-	-	-	1	2	0	0	0	4	-	-	-	-	-	-	-	-	-	-	-	-
2	-	-	-	-	-	-	15	45	3	4	1	1	-	-	-	-	-	-	-	-	-	-	-	-
3	-	-	-	-	-	-	-	-	2	0	0	1	-	-	-	-	-	-	-	-	-	-	-	-
4	-	-	-	-	-	-	-	-	1	0	0	1	-	-	-	-	-	-	-	-	-	-	-	-
5	-	-	-	-	-	-	-	-	1	1	0	3	-	-	-	-	-	-	-	-	-	-	-	-
6	-	126	>846	>1092	-	-	7	67	448	>636	416	>843	-	33	198	192	-	-	-	15	70	59	-	-
7	-	-	-	-	-	-	4	3	4	7	5	21	-	-	-	-	-	-	-	-	-	-	-	-
8	-	-	-	-	-	-	2	2	1	3	3	5	-	-	-	-	-	-	-	-	-	-	-	-
9	-	-	-	-	-	-	25	14	97	19	2	112	-	-	-	-	-	-	-	-	-	-	-	-
10	459	-	-	-	-	-	200	320	-	-	-	-	77	-	8	34	18	130	33	-	-	-	-	-
11	-	-	-	173	667	>1225	>479	>539	-	89	328	>738	-	-	5	56	82	245	-	-	-	38	35	100
12	-	-	-	-	-	-	-	-	-	-	-	-	-	-	7	56	26	218	-	-	-	-	-	-
13	-	>470	26	371	-	-	125	224	11	195	70	361	-	73	4	71	-	-	-	39	2	40	-	-
14	-	-	-	-	-	-	-	-	-	-	-	-	-	-	2	32	27	62	-	-	-	-	-	-
15	-	-	-	-	-	-	-	-	-	-	-	-	-	-	-	111	52	489	-	-	-	-	-	-
16	-	-	-	-	-	-	612	>674	-	-	-	-	-	-	278	36	58	549	-	-	-	-	-	-
17	-	-	-	-	155	>1487	>1485	>739	-	-	66	>1213	-	-	413	50	17	643	-	-	-	-	4	182
18	-	-	-	-	-	-	9	2	0	0	1	4	-	-	-	-	-	-	-	-	-	-	-	-
19	6	-	-	-	-	-	3	2	0	1	1	4	2	-	-	-	-	-	1	-	-	-	-	-
20	-	-	-	-	-	-	2	5	0	2	1	7	-	-	-	-	-	-	-	-	-	-	-	-
21	161	82	179	11	14	62	101	44	127	4	7	31	30	15	50	1	2	11	12	6	20	0	1	6
22	-	-	-	-	173	>529	-	-	-	-	121	361	-	-	-	10	52	151	-	-	-	-	17	63
23	-	-	-	-	-	-	2	0	13	0	0	43	-	-	-	-	-	-	-	-	-	-	-	-
24	-	-	-	-	-	-	0	1	0	0	0	1	-	-	-	-	-	-	-	-	-	-	-	-
25	-	-	-	-	-	-	2	1	11	0	0	9	-	-	-	-	-	-	-	-	-	-	-	-
26	-	-	-	-	-	-	162	84	533	5	27	404	-	-	-	-	-	-	-	-	-	-	-	-
27	27	-	-	-	-	-	14	14	433	2	14	174	8	-	-	-	-	-	3	-	-	-	-	-
28	-	-	-	-	-	-	32	>517	50	7	23	106	-	-	-	-	-	-	-	-	-	-	-	-
29	-	5	33	-	-	-	22	2	22	34	5	49	-	1	9	-	-	-	-	0	4	-	-	-
30	-	-	-	-	-	-	29	2	20	7	2	13	-	-	-	-	-	-	-	-	-	-	-	-
31	-	-	-	-	-	-	23	1	53	-	-	-	-	-	-	-	-	-	-	-	-	-	-	-
32	-	-	-	-	-	-	0	0	1	-	-	-	-	-	-	-	-	-	-	-	-	-	-	-

Appendix 4 Calculations of estimated sand transport

Table A-2. Calculated sand transport (kg m^{-1}), at location no1, for six sampling periods.

height range	coefficient	2008			2009		
cm	(at 30 cm)	- - - - - - - - - - kg m^{-1} - - - - - - - - - -					
0 - 10	2.03	0	0	0	0	0	1
10 - 20	2.03	0	0	0	0	0	1
20 - 30	1.24	0	0	0	0	0	1
30 - 40	0.82	0	0	0	0	0	0
40 - 50	0.57	0	0	0	0	0	0
50 - 60	0.40	0	0	0	0	0	0
60 - 80	0.27	0	0	0	0	0	0
80 - 100	0.18	0	0	0	0	0	0
100 - 140	0.07	0	0	0	0	0	0
	Total	***1***	***2***	***0***	***0***	***0***	***4***

Table A-3. Calculated sand transport (kg m^{-1}), at location no 2, for six sampling periods.

height range	coefficient	2008			2009		
cm	(at 30 cm)	- - - - - - - - - - kg m^{-1} - - - - - - - - - -					
0 - 10	2.03	3	10	1	1	0	0
10 - 20	2.03	3	10	1	1	0	0
20 - 30	1.24	2	6	0	1	0	0
30 - 40	0.82	1	4	0	0	0	0
40 - 50	0.57	1	3	0	0	0	0
50 - 60	0.40	1	2	0	0	0	0
60 - 80	0.27	1	3	0	0	0	0
80 - 100	0.18	1	2	0	0	0	0
100 - 140	0.07	0	1	0	0	0	0
	Total	***14***	***41***	***3***	***4***	***1***	***1***

Table A-4. Calculated sand transport (kg m^{-1}), at location no 3, for four sampling periods.

height range	coefficient	2008			2009		
cm	(at 30 cm)	- - - - - - - - - - kg m^{-1} - - - - - - - - - -					
0 - 10	2.03	-	-	0	0	0	0
10 - 20	2.03	-	-	0	0	0	0
20 - 30	1.24	-	-	0	0	0	0
30 - 40	0.82	-	-	0	0	0	0
40 - 50	0.57	-	-	0	0	0	0
50 - 60	0.40	-	-	0	0	0	0
60 - 80	0.27	-	-	0	0	0	0
80 - 100	0.18	-	-	0	0	0	0
100 - 140	0.07	-	-	0	0	0	0
	Total			***2***	***0***	***0***	***1***

Table A-5. Calculated sand transport (kg m^{-1}), at location no 4, for four sampling periods.

height range	coefficient	2008			2009		
cm	(at 30 cm)	- - - - - - - - - -		kg m^{-1}	- - - - - - - - - -		
0 - 10	2.03	-	-	0	0	0	0
10 - 20	2.03	-	-	0	0	0	0
20 - 30	1.24	-	-	0	0	0	0
30 - 40	0.82	-	-	0	0	0	0
40 - 50	0.57	-	-	0	0	0	0
50 - 60	0.40	-	-	0	0	0	0
60 - 80	0.27	-	-	0	0	0	0
80 - 100	0.18	-	-	0	0	0	0
100 - 140	0.07	-	-	0	0	0	0
	Total			***1***	***0***	***0***	***1***

Table A-6. Calculated sand transport (kg m^{-1}), at location no 5, for four sampling periods.

height range	coefficient	2008			2009		
cm	(at 30 cm)	- - - - - - - - - -		kg m^{-1}	- - - - - - - - - -		
0 - 10	2.03	-	-	0	0	0	1
10 - 20	2.03	-	-	0	0	0	1
20 - 30	1.24	-	-	0	0	0	0
30 - 40	0.82	-	-	0	0	0	0
40 - 50	0.57	-	-	0	0	0	0
50 - 60	0.40	-	-	0	0	0	0
60 - 80	0.27	-	-	0	0	0	0
80 - 100	0.18	-	-	0	0	0	0
100 - 140	0.07	-	-	0	0	0	0
	Total			***1***	***1***	***0***	***3***

Table A-7. Calculated sand transport (kg m^{-1}), at location no 6, for six sampling periods.

height range	coefficient	2008			2009		
cm	(at 30 cm)	- - - - - - - - - -		kg m^{-1}	- - - - - - - - - -		
0 - 10	1.79	1	13	87	>124	81	>164
10 - 20	1.79	1	13	87	>124	81	>164
20 - 30	1.20	1	9	59	>83	54	>110
30 - 40	0.86	1	6	42	>60	39	>79
40 - 50	0.65	0	5	32	>45	29	>60
50 - 60	0.50	0	4	24	>35	23	>46
60 - 80	0.36	1	5	35	>50	32	>66
80 - 100	0.24	0	3	23	>33	22	>44
100 - 140	0.09	0	3	18	>25	16	>33
	Total	***6***	***61***	***407***	***>578***	***378***	***>767***

Table A-8. Calculated sand transport (kg m^{-1}), at location no 7, for six sampling periods.

height range	coefficient	2008			2009		
cm	(at 30 cm)			kg m^{-1}			
0 - 10	1.79	1	1	1	1	1	4
10 - 20	1.79	1	1	1	1	1	4
20 - 30	1.20	1	0	1	1	1	3
30 - 40	0.86	0	0	0	1	0	2
40 - 50	0.65	0	0	0	0	0	1
50 - 60	0.50	0	0	0	0	0	1
60 - 80	0.36	0	0	0	1	0	2
80 - 100	0.24	0	0	0	0	0	1
100 - 140	0.09	0	0	0	0	0	1
	Total	***4***	***3***	***4***	***6***	***4***	***19***

Table A-9. Calculated sand mass flux (kg m^{-1}), at location no 8, for six sampling periods.

height range	coefficient	2008			2009		
cm	(at 30 cm)			kg m^{-1}			
0 - 10	1.79	0	0	0	1	1	1
10 - 20	1.79	0	0	0	1	1	1
20 - 30	1.20	0	0	0	0	0	1
30 - 40	0.86	0	0	0	0	0	0
40 - 50	0.65	0	0	0	0	0	0
50 - 60	0.50	0	0	0	0	0	0
60 - 80	0.36	0	0	0	0	0	0
80 - 100	0.24	0	0	0	0	0	0
100 - 140	0.09	0	0	0	0	0	0
	Total	***2***	***2***	***1***	***3***	***3***	***5***

Table A-10. Calculated sand transport (kg m^{-1}), at location no 9, for six sampling periods.

height range	coefficient	2008			2009		
cm	(at 30 cm)			kg m^{-1}			
0 - 10	2.03	5	3	21	4	0	24
10 - 20	2.03	5	3	21	4	0	24
20 - 30	1.24	3	2	13	2	0	15
30 - 40	0.82	2	1	8	2	0	10
40 - 50	0.57	2	1	6	1	0	7
50 - 60	0.40	1	1	4	1	0	5
60 - 80	0.27	1	1	6	1	0	6
80 - 100	0.18	1	1	4	1	0	4
100 - 140	0.07	1	0	3	1	0	3
	Total	***22***	***12***	***85***	***17***	***2***	***98***

Table A-11. Calculated sand transport (kg m^{-1}), at location no 10, for six sampling periods.

height range	coefficient	coefficient	2008			2009		
cm	(at 30 cm)	(at 60 cm)	- - - - - - - - - -	kg m^{-1}		- - - - - - - - - -		
0 - 10	2.03	6.15	45	72	5	23	12	89
10 - 20	2.03	6.15	45	72	5	23	12	89
20 - 30	1.24	3.76	28	44	3	14	8	54
30 - 40	0.82	2.48	18	29	2	9	5	36
40 - 50	0.57	1.71	13	20	2	6	3	25
50 - 60	0.40	1.20	9	14	1	5	2	17
60 - 80	0.27	0.78	12	19	1	6	3	23
80 - 100	0.18	0.54	8	13	1	4	2	16
100 - 140	0.07	0.21	6	10	1	3	2	12
		Total	***184***	***294***	***22***	***94***	***50***	***360***

Table A-12. Calculated sand transport (kg m^{-1}), at location no 11, for six sampling periods.

Height range	coefficient	coefficient	2008			2009		
cm	(at 30 cm)	(at 60 cm)	- - - - - - - - - -	kg m^{-1}		- - - - - - - - - -		
0 - 10	2.03	6.15	>103	>116	3	19	71	>159
10 - 20	2.03	6.15	>103	>116	3	19	71	>159
20 - 30	1.24	3.76	>63	>71	2	12	43	>97
30 - 40	0.82	2.48	>42	>47	1	8	29	>64
40 - 50	0.57	1.71	>29	>33	1	5	20	>45
50 - 60	0.40	1.20	>20	>23	1	4	14	>31
60 - 80	0.27	0,78	>27	>31	1	5	19	>42
80 - 100	0.18	0.54	>18	>21	1	3	13	>28
100 - 140	0.07	0.21	>14	>16	0	3	10	>22
		Total	***>420***	***>472***	***13***	***78***	***288***	***>647***

Table A-13. Calculated sand transport (kg m^{-1}), at location no 12, for four sampling periods.

height range	coefficient	2008			2009		
cm	(at 60 cm)	- - - - - - - - - -	kg m^{-1}		- - - - - - - - - -		
0 - 10	6.15	-	-	4	35	16	135
10 - 20	6.15	-	-	4	35	16	135
20 - 30	3.76	-	-	3	21	10	83
30 - 40	2.48	-	-	2	14	7	55
40 - 50	1.71	-	-	1	10	4	38
50 - 60	1.20	-	-	1	7	3	26
60 - 80	0.78	-	-	1	9	4	35
80 - 100	0.54	-	-	1	6	3	24
100 - 140	0.21	-	-	1	5	2	19
	Total			***18***	***141***	***66***	***549***

Table A-14. Calculated sand transport (kg m^{-1}), at location no 13, for six sampling periods.

height range	coefficient	2008			2009		
cm	(at 30 cm)			kg m^{-1}			
0 - 10	2.03	26	46	2	40	14	74
10 - 20	2.03	26	46	2	40	14	74
20 - 30	1.24	16	28	1	24	9	45
30 - 40	0.82	10	19	1	16	6	30
40 - 50	0.57	7	13	1	11	4	21
50 - 60	0.40	5	9	0	8	3	15
60 - 80	0.27	7	12	1	11	4	20
80 - 100	0.18	5	8	0	7	3	13
100 - 140	0.07	4	6	0	6	2	10
	Total	***104***	***187***	***9***	***163***	***59***	***302***

Table A-15. Calculated sand transport (kg m^{-1}), at location no 14, for four sampling periods.

height range	coefficient	2008			2009		
cm	(at 60 cm)			kg m^{-1}			
0 - 10	6.15	-	-	1	20	17	39
10 - 20	6.15	-	-	1	20	17	39
20 - 30	3.76	-	-	1	12	10	24
30 - 40	2.48	-	-	1	8	7	16
40 - 50	1.71	-	-	0	6	5	11
50 - 60	1.20	-	-	0	4	3	8
60 - 80	0.78	-	-	0	5	4	10
80 - 100	0.54	-	-	0	4	3	7
100 - 140	0.21	-	-	0	3	2	5
	Total			***5***	***81***	***68***	***156***

Table A-16. Calculated sand transport (kg m^{-1}), at location no 15, for three sampling periods.

Height range	coefficient	2008			2009		
cm	(at 60 cm)			kg m^{-1}			
0 - 10	6.15	-	-	-	76	35	334
10 - 20	6.15	-	-	-	76	35	334
20 - 30	3.76	-	-	-	46	22	204
30 - 40	2.48	-	-	-	31	14	135
40 - 50	1.71	-	-	-	21	10	93
50 - 60	1.20	-	-	-	15	7	65
60 - 80	0.78	-	-	-	19	9	85
80 - 100	0.54	-	-	-	13	6	59
100 - 140	0.21	-	-	-	10	5	46
	Total				***307***	***144***	***1353***

Table A-17. Calculated sand transport (kg m^{-1}), at location no 16, for six sampling periods.

height range	coefficient	coefficient	2008			2009		
cm	(at 30 cm)	(at 60 cm)	- - - - - - - - - - kg m^{-1} - - - - - - - - - -					
0 - 10	2.03	6.15	135	>149	186	24	39	368
10 - 20	2.03	6.15	135	>149	186	24	39	368
20 - 30	1.24	3.76	83	>91	114	15	24	225
30 - 40	0.82	2.48	55	>60	75	10	16	148
40 - 50	0.57	1.71	38	>42	52	7	11	102
50 - 60	0.40	1.20	27	>29	36	5	8	72
60 - 80	0.27	0.78	36	>39	47	6	10	93
80 - 100	0.18	0.54	24	>26	33	4	7	64
100 - 140	0.07	0.21	19	>21	25	3	5	50
		Total	***551***	***>607***	***755***	***98***	***158***	***1491***

Table A-18. Calculated sand transport (kg m^{-1}), at location no 17, for six sampling periods.

height range	coefficient	coefficient	2008			2009		
cm	(at 30 cm)	(at 60 cm)	- - - - - - - - - - kg m^{-1} - - - - - - - - - -					
0 - 10	2.03	6.15	>314	>156	264	32	12	441
10 - 20	2.03	6.15	>314	>156	264	32	12	441
20 - 30	1.24	3.76	>192	>95	161	20	7	270
30 - 40	0.82	2.48	>127	>63	107	13	5	178
40 - 50	0.57	1.71	>88	>44	73	9	3	123
50 - 60	0.40	1.20	>62	>31	52	6	2	86
60 - 80	0.27	0.78	>83	>41	67	8	3	111
80 - 100	0.18	0.54	>55	>28	46	6	2	77
100 - 140	0.07	0.21	>43	>21	36	4	2	60
		Total	***>1276***	***>635***	***1070***	***130***	***47***	***1788***

Table A-19. Calculated sand transport (kg m^{-1}), at location no 18, for six sampling periods.

height range	coefficient	2008			2009		
cm	(at 30 cm)	- - - - - - - - - - kg m^{-1} - - - - - - - - - -					
0 - 10	2.03	2	0	0	0	0	1
10 - 20	2.03	2	0	0	0	0	1
20 - 30	1.24	1	0	0	0	0	1
30 - 40	0.82	1	0	0	0	0	0
40 - 50	0.57	1	0	0	0	0	0
50 - 60	0.40	0	0	0	0	0	0
60 - 80	0.27	1	0	0	0	0	0
80 - 100	0.18	0	0	0	0	0	0
100 - 140	0.07	0	0	0	0	0	0
	Total	***8***	***2***	***0***	***0***	***1***	***4***

Table A-20. Calculated sand transport (kg m^{-1}), at location no 19, for six sampling periods.

height range	coefficient	2008			2009		
cm	(at 30 cm)	- - - - - - - - - - kg m^{-1} - - - - - - - - - -					
0 - 10	2.03	1	0	0	0	0	1
10 - 20	2.03	1	0	0	0	0	1
20 - 30	124	0	0	0	0	0	1
30 - 40	0.82	0	0	0	0	0	0
40 - 50	0.57	0	0	0	0	0	0
50 - 60	0.40	0	0	0	0	0	0
60 - 80	0.27	0	0	0	0	0	0
80 - 100	0.18	0	0	0	0	0	0
100 - 140	0.07	0	0	0	0	0	0
	Total	***3***	***2***	***0***	***1***	***1***	***4***

Table A-21. Calculated sand transport (kg m^{-1}), at location no 20, for six sampling periods.

height range	coefficient	2008			2009		
cm	(at 30 cm)	- - - - - - - - - - kg m^{-1} - - - - - - - - - -					
0 - 10	1.53	0	1	0	0	0	1
10 - 20	1.53	0	1	0	0	0	1
20 - 30	1.15	0	1	0	0	0	1
30 - 40	0.88	0	0	0	0	0	1
40 - 50	0.67	0	0	0	0	0	1
50 - 60	0.50	0	0	0	0	0	0
60 - 80	0.35	0	0	0	0	0	1
80 - 100	0.23	0	0	0	0	0	0
100 - 140	0.08	0	0	0	0	0	0
	Total	***2***	***4***	***0***	***2***	***1***	***6***

Table A-22. Calculated sand transport (kg m^{-1}), at location no 21, for six sampling periods.

height range	coefficient	2008			2009		
cm	(at 30 cm)	- - - - - - - - - - kg m^{-1} - - - - - - - - - -					
0 - 10	2.03	22	9	27	1	2	7
10 - 20	2.03	22	9	27	1	2	7
20 - 30	1.24	13	6	17	1	1	4
30 - 40	0.82	9	4	11	0	1	3
40 - 50	0.57	6	3	8	0	0	2
50 - 60	0.40	4	2	5	0	0	1
60 - 80	0.27	6	3	7	0	0	2
80 - 100	0.18	4	2	5	0	0	1
100 - 140	0.07	3	1	4	0	0	1
	Total	**89**	**39**	**111**	**4**	**6**	**27**

Table A-23. Calculated sand transport (kg m^{-1}), at location no 22, for three sampling periods.

height range	coefficient	coefficient	2008			2009		
cm	(at 30 cm)	(at 60 cm)	- - - - - - - - - -			kg m^{-1}	- - - - - - - - - -	
0 - 10	1.53	3.50	-	-	-	4	20	60
10 - 20	1.53	3.50	-	-	-	4	20	60
20 - 30	1.15	2.68	-	-	-	3	15	45
30 - 40	0.88	2.04	-	-	-	2	12	35
40 - 50	0.67	1.55	-	-	-	2	9	26
50 - 60	0.50	1.15	-	-	-	1	7	20
60 - 80	0.35	0.80	-	-	-	2	9	27
80 - 100	0.23	0.52	-	-	-	1	6	18
100 - 140	0.08	0.25	-	-	-	1	4	13
		Total				***20***	***102***	***304***

Table A-24. Calculated sand transport (kg m^{-1}), at location no 23, for six sampling periods.

height range	coefficient	2008			2009		
cm	(at 30 cm)	- - - - - - - - - -			kg m^{-1}	- - - - - - - - - -	
0 - 10	1.53	0	0	2	0	0	7
10 - 20	1.53	0	0	2	0	0	7
20 - 30	1.15	0	0	2	0	0	5
30 - 40	0.88	0	0	1	0	0	4
40 - 50	0.67	0	0	1	0	0	3
50 - 60	0.50	0	0	1	0	0	2
60 - 80	0.35	0	0	1	0	0	3
80 - 100	0.23	0	0	1	0	0	2
100 - 140	0.08	0	0	0	0	0	1
	Total	***2***	***0***	***11***	***0***	***0***	***36***

Table A-25. Calculated sand transport (kg m^{-1}), at location no 24, for six sampling periods.

height range	coefficient	2008			2009		
cm	(at 30 cm)	- - - - - - - - - -			kg m^{-1}	- - - - - - - - - -	
0 - 10	1.53	0	0	0	0	0	0
10 - 20	1.53	0	0	0	0	0	0
20 - 30	1.15	0	0	0	0	0	0
30 - 40	0.88	0	0	0	0	0	0
40 - 50	0.67	0	0	0	0	0	0
50 - 60	0.50	0	0	0	0	0	0
60 - 80	0.35	0	0	0	0	0	0
80 - 100	0.23	0	0	0	0	0	0
100 - 140	0.08	0	0	0	0	0	0
	Total	***0***	***1***	***0***	***0***	***0***	***1***

Table A-26. Calculated sand transport (kg m^{-1}), at location no 25, for six sampling periods.

height range	coefficient	2008			2009		
cm	(at 30 cm)			kg m^{-1}			
0 - 10	1.53	0	0	2	0	0	1
10 - 20	1.53	0	0	2	0	0	1
20 - 30	1.15	0	0	1	0	0	1
30 - 40	0.88	0	0	1	0	0	1
40 - 50	0.67	0	0	1	0	0	1
50 - 60	0.50	0	0	1	0	0	0
60 - 80	0.35	0	0	1	0	0	1
80 - 100	0.23	0	0	1	0	0	0
100 - 140	0.08	0	0	0	0	0	0
	Total	***2***	***1***	***9***	***0***	***0***	***7***

Table A-27. Calculated sand transport (kg m^{-1}), at location no 26, for six sampling periods.

height range	coefficient	2008			2009		
cm	(at 30 cm)			kg m^{-1}			
0 - 10	1.53	26	13	85	1	4	64
10 - 20	1.53	26	13	85	1	4	64
20 - 30	1.15	19	10	64	1	3	48
30 - 40	0.88	15	8	49	0	2	37
40 - 50	0.67	11	6	37	0	2	28
50 - 60	0.50	8	4	28	0	1	21
60 - 80	0.35	12	6	39	0	2	29
80 - 100	0.23	8	4	25	0	1	19
100 - 140	0.08	5	3	18	0	1	13
	Total	***130***	***68***	***429***	***4***	***22***	***325***

Table A-28. Calculated sand transport (kg m^{-1}), at location no 27, for six sampling periods.

height range	coefficient	2008			2009		
cm	(at 30 cm)			kg m^{-1}			
0 - 10	1.53	3	3	78	0	3	31
10 - 20	1.53	3	3	78	0	3	31
20 - 30	1.15	2	2	58	0	2	23
30 - 40	0.88	1	1	45	0	1	18
40 - 50	0.67	1	1	34	0	1	14
50 - 60	0.50	1	1	25	0	1	10
60 - 80	0.35	1	1	35	0	1	14
80 - 100	0.23	1	1	23	0	1	9
100 - 140	0.08	1	1	16	0	1	7
	Total	***13***	***13***	***392***	***2***	***13***	***158***

Table A-29. Calculated sand transport (kg m^{-1}), at location no 28, for six sampling periods.

height range	coefficient	2008			2009		
cm	(at 30 cm)		- - - - - - - - - - kg m^{-1} - - - - - - - - - -				
0 - 10	1.53	5	>82	8	1	4	17
10 - 20	1.53	5	>82	8	1	4	17
20 - 30	1.15	4	>62	6	1	3	13
30 - 40	0.88	3	>47	5	1	2	10
40 - 50	0.67	2	>36	3	0	2	7
50 - 60	0.50	2	>27	3	0	1	6
60 - 80	0.35	2	>37	4	1	2	8
80 - 100	0.23	2	>25	2	0	1	5
100 - 140	0.08	1	>17	2	0	1	4
	Total	***26***	***>416***	***40***	***6***	***18***	***85***

Table A-30. Calculated sand transport (kg m^{-1}), at location no 29, for six sampling periods.

height range	coefficient	2008			2009		
cm	(at 30 cm)		- - - - - - - - - - kg m^{-1} - - - - - - - - - -				
0 - 10	1.53	4	0	4	6	1	8
10 - 20	1.53	4	0	4	6	1	8
20 - 30	1.15	3	0	3	4	1	6
30 - 40	0.88	2	0	2	3	0	5
40 - 50	0.67	2	0	2	2	0	4
50 - 60	0.50	1	0	1	2	0	3
60 - 80	0.35	2	0	2	3	0	4
80 - 100	0.23	1	0	1	2	0	2
100 - 140	0.08	1	0	1	1	0	2
	Total	***19***	***2***	***19***	***29***	***4***	***41***

Table A-31. Calculated sand transport (kg m^{-1}), at location no 30, for six sampling periods.

height range	coefficient	2008			2009		
cm	(at 30 cm)		- - - - - - - - - - kg m^{-1} - - - - - - - - - -				
0 - 10	1.53	5	0	3	1	0	2
10 - 20	1.53	5	0	3	1	0	2
20 - 30	1.15	4	0	3	1	0	2
30 - 40	0.88	3	0	2	1	0	1
40 - 50	0.67	2	0	1	1	0	1
50 - 60	0.50	2	0	1	0	0	1
60 - 80	0.35	2	0	2	1	0	1
80 - 100	0.23	1	0	1	0	0	1
100 - 140	0.08	1	0	1	0	0	0
	Total	***24***	***2***	***17***	***6***	***2***	***11***

Table A-32. Calculated sand transport (kg m^{-1}), at location no 31, for three sampling periods.

height range	coefficient	2008			2009		
cm	(at 30 cm)		- - - - - - - - - -	kg m^{-1}	- - - - - - - - - -		
0 - 10	1.53	4	0	9	-	-	-
10 - 20	1.53	4	0	9	-	-	-
20 - 30	1.15	3	0	7	-	-	-
30 - 40	0.88	2	0	5	-	-	-
40 - 50	0.67	2	0	4	-	-	-
50 - 60	0.50	1	0	3	-	-	-
60 - 80	0.35	2	0	4	-	-	-
80 - 100	0.23	1	0	3	-	-	-
100 - 140	0.08	1	0	2	-	-	-
	Total	***20***	***1***	***46***			

Table A-33. Calculated sand transport (kg m^{-1}), at location no 32, for three sampling periods.

height range	coefficient	2008			2009		
cm	(at 30 cm)		- - - - - - - - - -	kg m^{-1}	- - - - - - - - - -		
0 - 10	1.53	0	0	0	-	-	-
10 - 20	1.53	0	0	0	-	-	-
20 - 30	1.15	0	0	0	-	-	-
30 - 40	0.88	0	0	0	-	-	-
40 - 50	0.67	0	0	0	-	-	-
50 - 60	0.50	0	0	0	-	-	-
60 - 80	0.35	0	0	0	-	-	-
80 - 100	0.23	0	0	0	-	-	-
100 - 140	0.08	0	0	0	-	-	-
	Total	***0***	***0***	***1***			

Appendix 5 Calculated sand transport in erosion events

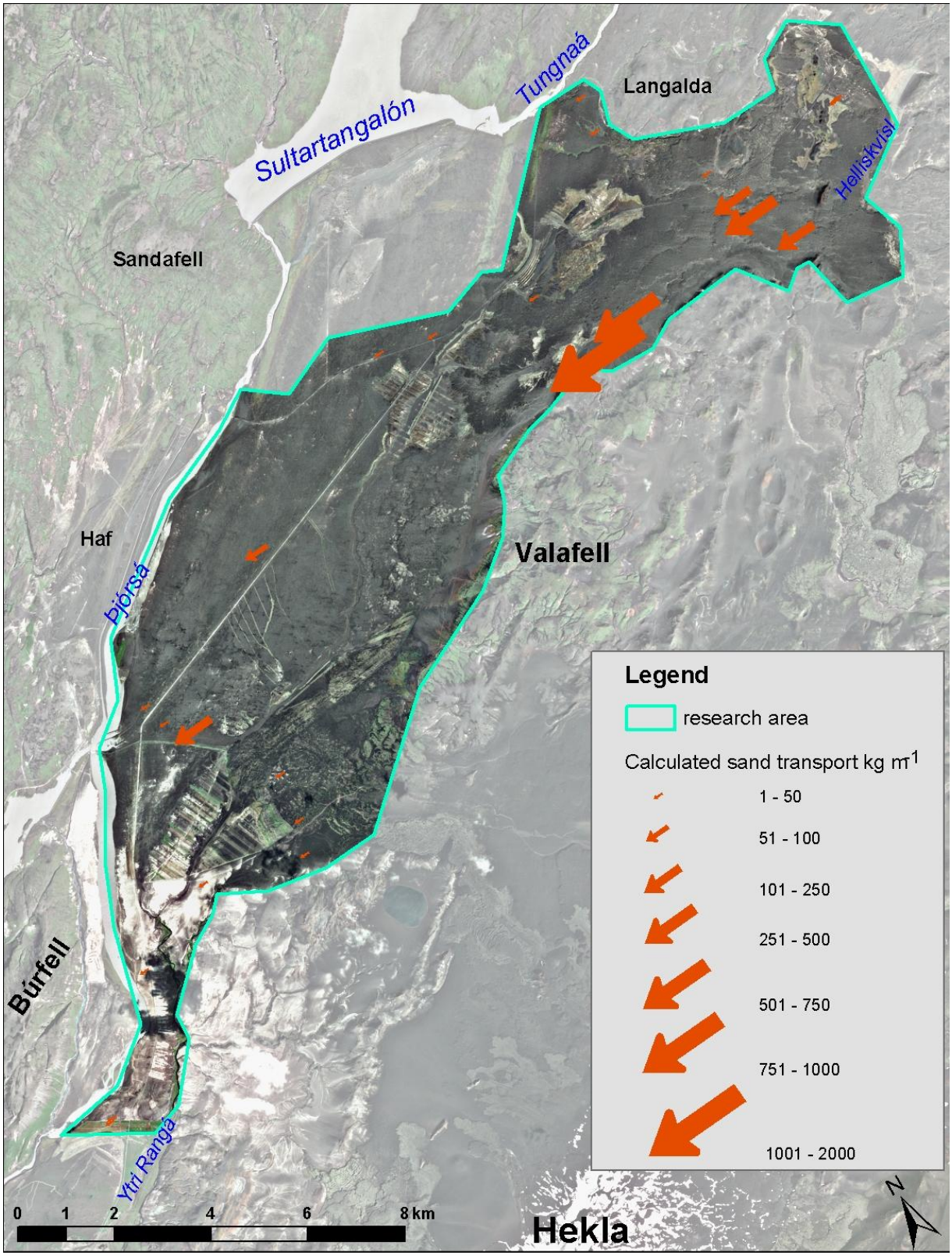

Fig. A-32. Calculated sand transport during sampling period A, June 3rd – June 7th 2008.

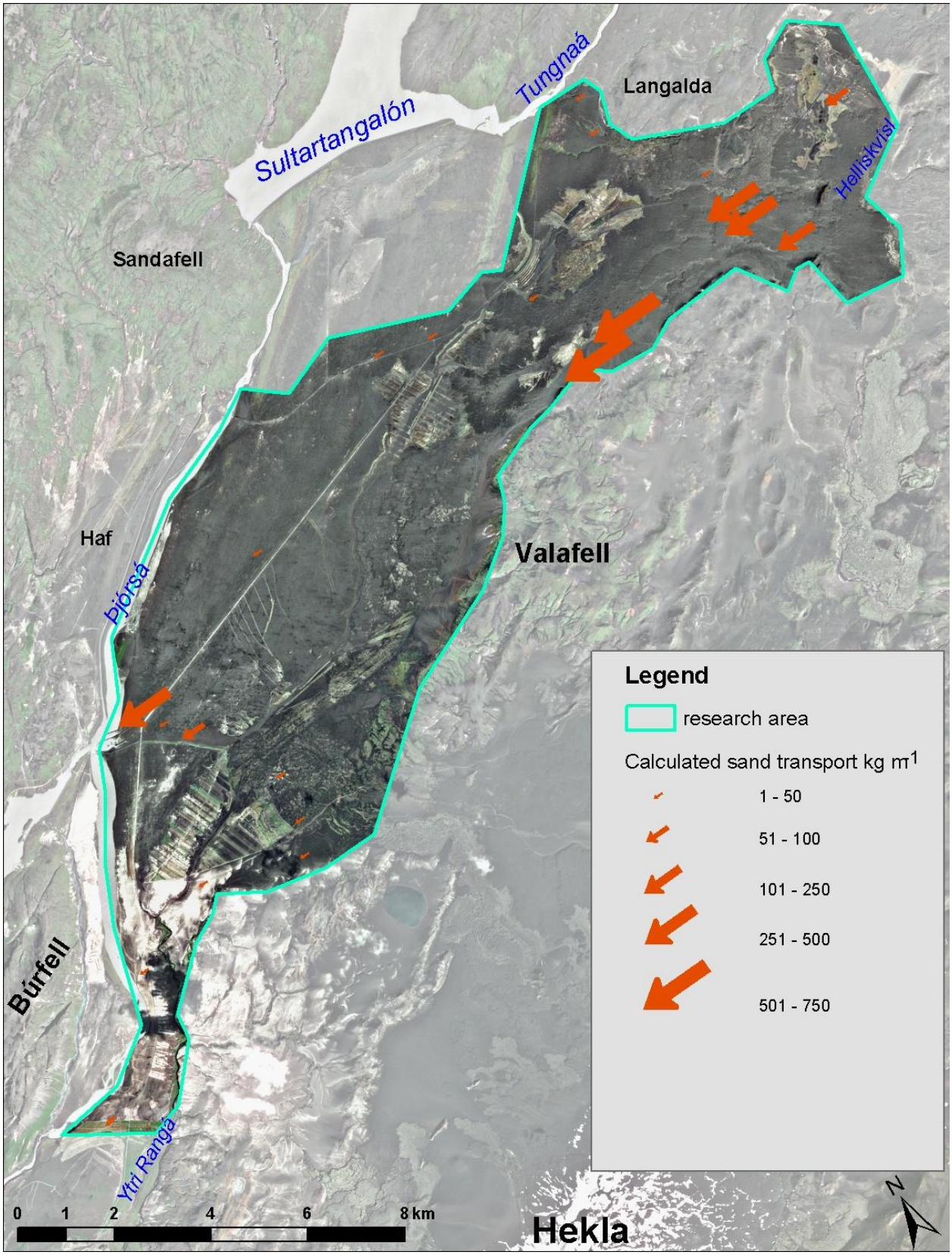

Fig. A-33. Calculated sand transport during sampling period B, June 20th – July 5th 2008.

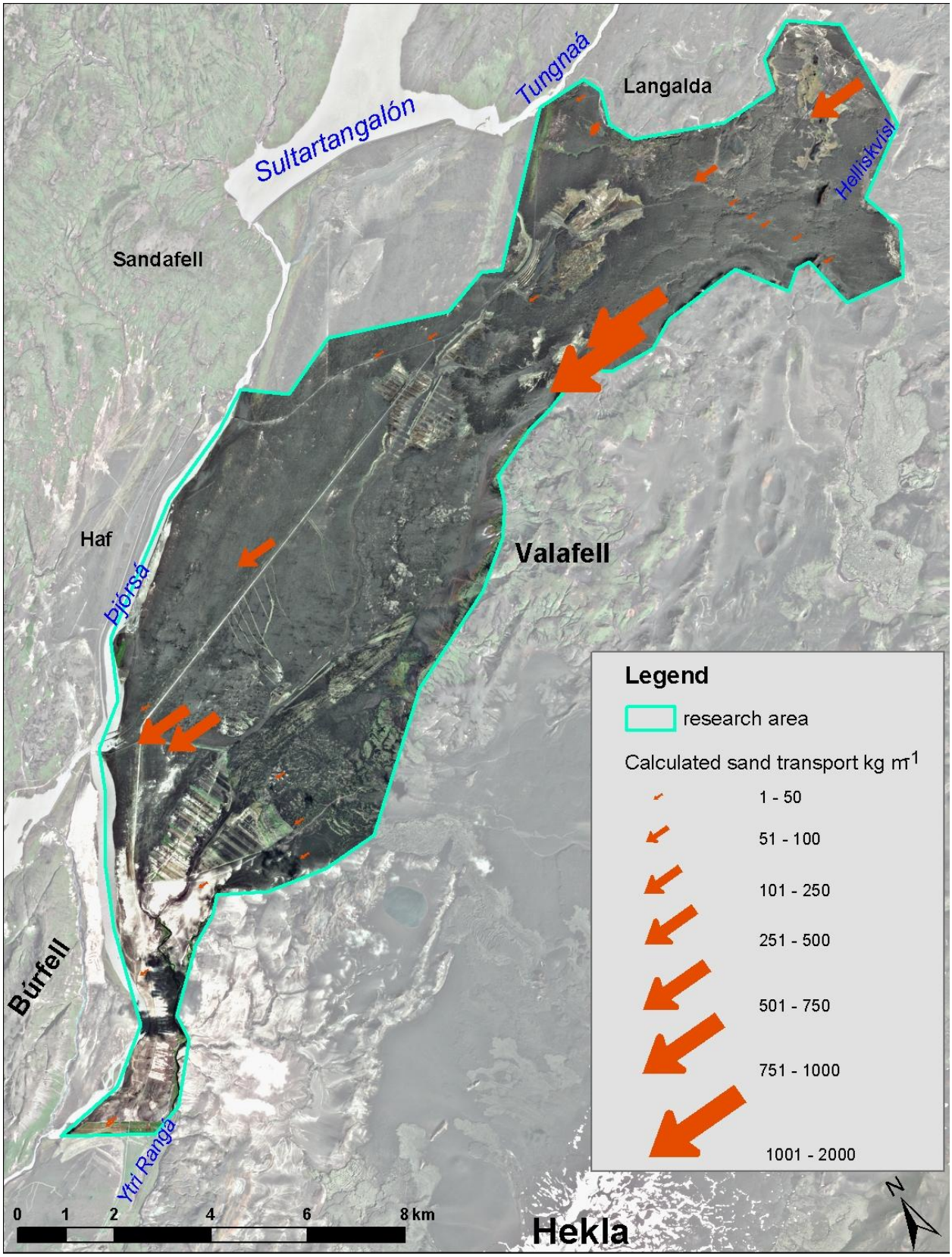

Fig. A-34. Calculated sand transport during sampling period C, July 5th – August 30th 2008.

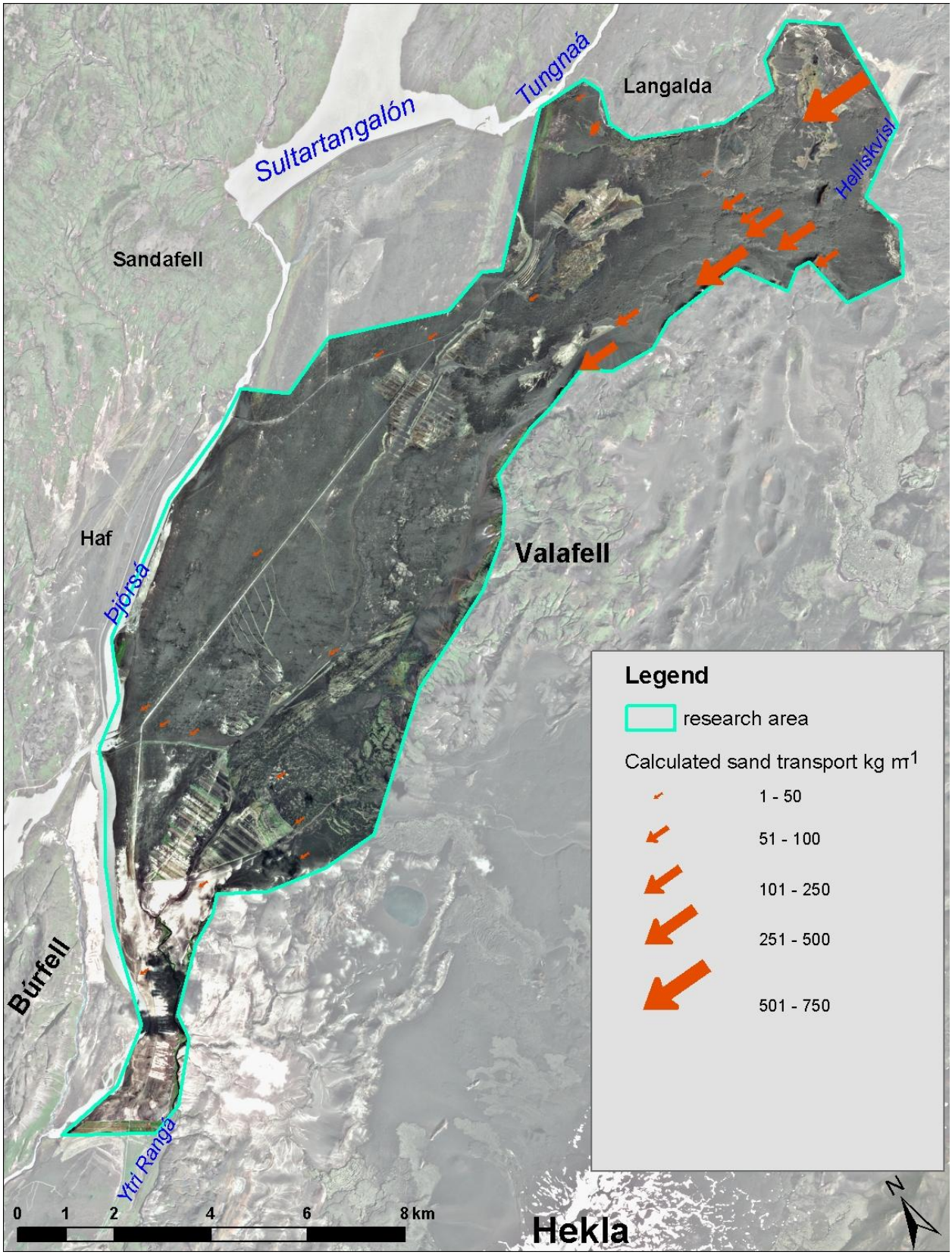

Fig. A-35. Calculated sand transport during sampling period D, May 16th – June 30th 2009.

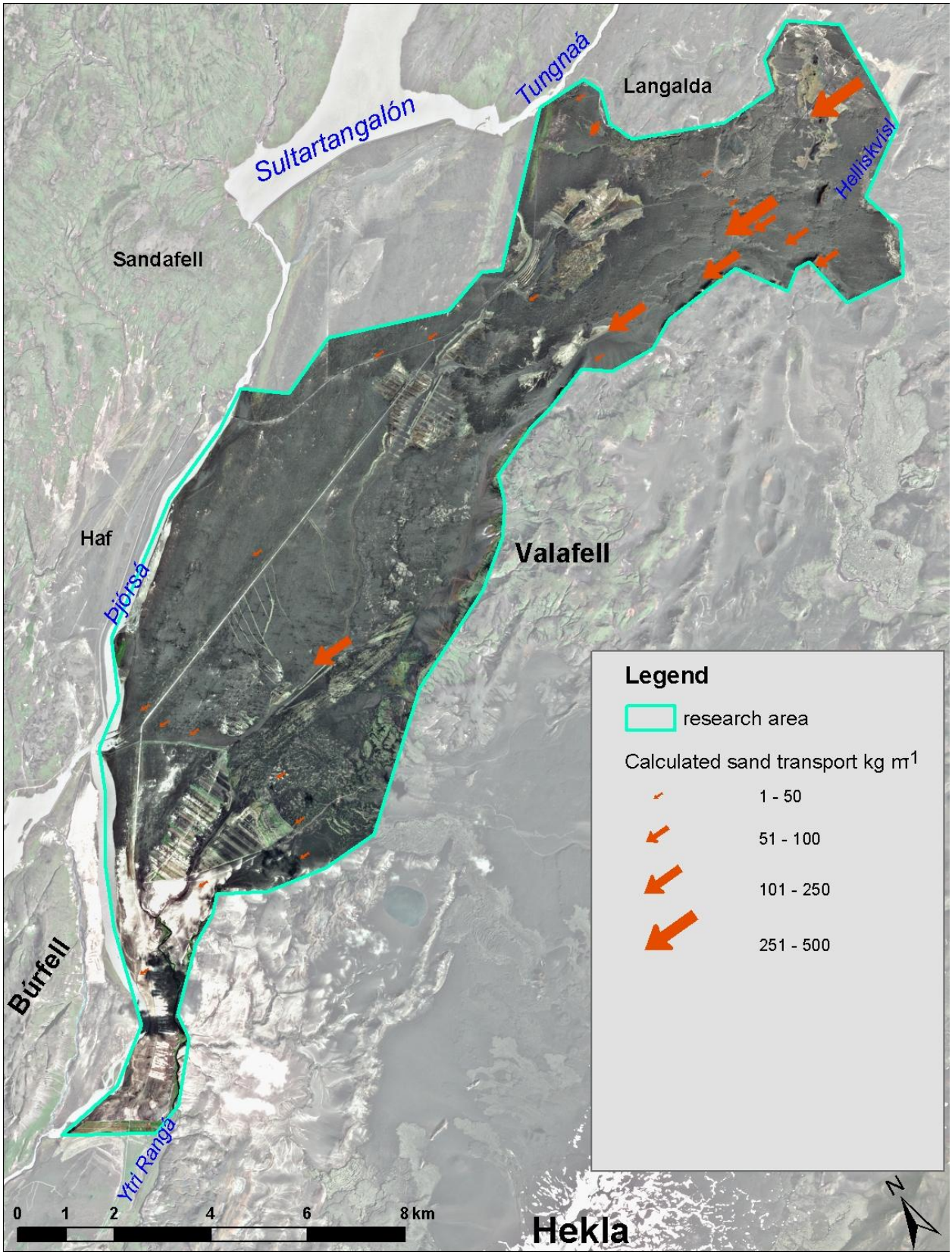

Fig. A-36. Calculated sand transport during sampling period E, July 24th – July 30th 2009.

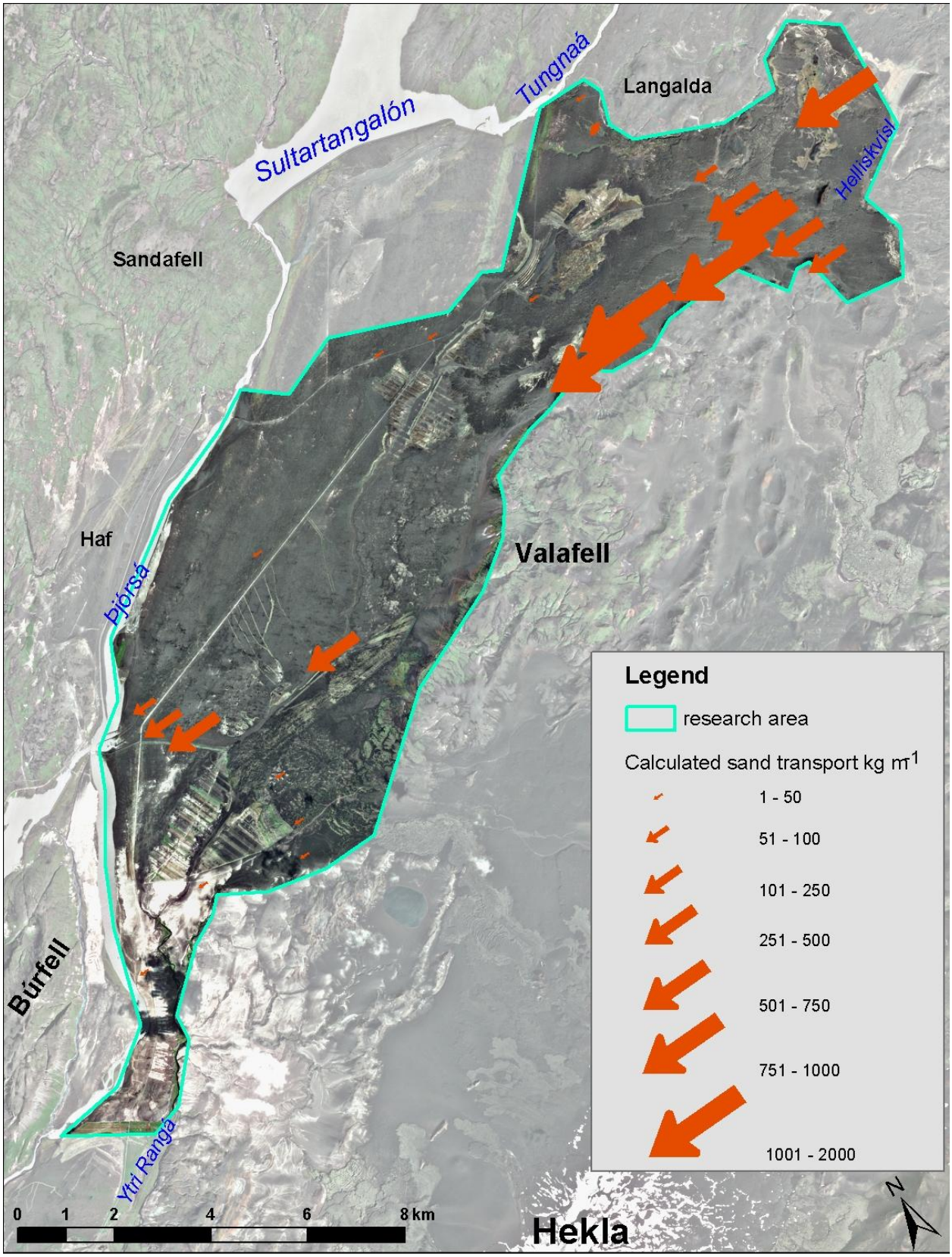

Fig. A-37. Calculated sand transport during sampling period F, July 30th – August 24th 2009.